DISCLAIMER

This report was prepared as an account of work sponsored by an agency of the United States Government. Neither the United States Government nor any agency thereof, nor any of their employees, makes any warranty, express or implied, or assumes any legal liability or responsibility for the accuracy, completeness, or usefulness of any information, apparatus, product, or process disclosed, or represents that its use would not infringe privately owned rights. Reference herein to any specific commercial product, process, or service by trade name, trademark, manufacturer, or otherwise does not necessarily constitute or imply its endorsement, recommendation, or favoring by the United States Government or any agency thereof. The views and opinions of authors expressed herein do not necessarily state or reflect those of the United States Government or any agency thereof. Reference herein to any social initiative (including but not limited to Diversity, Equity, and Inclusion (DEI); Community Benefits Plans (CBP); Justice 40; etc.) is made by the Author independent of any current requirement by the United States Government and does not constitute or imply endorsement, recommendation, or support by the United States Government or any agency thereof.

Technology Case Study: Techno-Economic and Life Cycle Analysis for Microalgae Conversion Pathways to Fuels and Products

Matthew Wiatrowski,[1] Bruno Klein,[1] Thai Ngan Do,[2] Longwen Ou,[2] Hao Cai,[2] Nicholas Carlson,[1] and Ryan Davis[1]

1 National Renewable Energy Laboratory
2 Argonne National Laboratory

NREL is a national laboratory of the U.S. Department of Energy
Office of Energy Efficiency & Renewable Energy
Operated by the Alliance for Sustainable Energy, LLC

This report is available at no cost from the National Renewable Energy Laboratory (NREL) at www.nrel.gov/publications.

Contract No. DE-AC36-08GO28308

Technical Report
NREL/TP-5100-91854
January 2025

Technology Case Study: Techno-Economic and Life Cycle Analysis for Microalgae Conversion Pathways to Fuels and Products

Matthew Wiatrowski,[1] Bruno Klein,[1] Thai Ngan Do,[2] Longwen Ou,[2] Hao Cai,[2] Nicholas Carlson,[1] and Ryan Davis[1]

1 National Renewable Energy Laboratory
2 Argonne National Laboratory

Suggested Citation
Wiatrowski, Matthew, Bruno Klein, Thai Ngan Do, Longwen Ou, Hao Cai, Nicholas Carlson, and Ryan Davis. 2025. *Technology Case Study: Techno-Economic and Life Cycle Analysis for Microalgae Conversion Pathways to Fuels and Products*. Golden, CO: National Renewable Energy Laboratory. NREL/TP-5100-91854. https://www.nrel.gov/docs/fy25osti/91854.pdf.

NREL is a national laboratory of the U.S. Department of Energy
Office of Energy Efficiency & Renewable Energy
Operated by the Alliance for Sustainable Energy, LLC

This report is available at no cost from the National Renewable Energy Laboratory (NREL) at www.nrel.gov/publications.

Contract No. DE-AC36-08GO28308

Technical Report
NREL/TP-5100-91854
January 2025

National Renewable Energy Laboratory
15013 Denver West Parkway
Golden, CO 80401
303-275-3000 • www.nrel.gov

NOTICE

This work was authored in part by the National Renewable Energy Laboratory, operated by Alliance for Sustainable Energy, LLC, for the U.S. Department of Energy (DOE) under Contract No. DE-AC36-08GO28308. Funding provided by the U.S. Department of Energy Office of Energy Efficiency and Renewable Energy Bioenergy Technologies Office. The views expressed herein do not necessarily represent the views of the DOE or the U.S. Government.

Cover Photos by Dennis Schroeder: (clockwise, left to right) NREL 51934, NREL 45897, NREL 42160, NREL 45891, NREL 48097, NREL 46526.

List of Acronyms

AD	anaerobic digestion
AFDW	ash-free dry weight
BEV	break-even value
CAP	combined algae processing
CH_4	methane
CI	carbon intensity
CO_2	carbon dioxide
CO_2e	carbon dioxide equivalent
EVA	ethylene vinyl acetate
FAME	fatty acid methyl ester
FFA	free fatty acid
GGE	gasoline gallon equivalent
GHG	greenhouse gas
H_2O_2	hydrogen peroxide
HDO	hydrodeoxygenation
HI	hydroisomerization
HL	high-lipid
HP	high-protein
IRR	internal rate of return
LCA	life cycle analysis
LCFS	Low Carbon Fuel Standard
MAC	marginal abatement cost
MFSP	minimum fuel selling price
NIPU	non-isocyanate polyurethane
NREL	National Renewable Energy Laboratory
PU	polyurethane
PUFA	polyunsaturated fatty acid
RIN	renewable identification number
SAF	sustainable aviation fuel
SOT	state of technology
TAG	triacylglycerides
TEA	techno-economic analysis
WTI	West Texas Intermediate

Executive Summary

The U.S. Department of Energy has launched numerous programs in recent years to accelerate net greenhouse gas (GHG) emissions reductions from carbon-based fuels and products, including the Clean Fuels & Products Shot™ and the Sustainable Aviation Fuel (SAF) Grand Challenge. Both programs lay out ambitious GHG reduction goals that will require the deployment of a wide variety of feedstock and fuel technologies. This technology case study details the cost and sustainability prospects for an emerging feedstock—microalgae—converted to fuels and products via a fractionation and upgrading approach termed combined algae processing (CAP). This study represents an update incorporating new opportunities and other learnings gained since publication of a design report on the CAP concept 10 years prior.

To assess these prospects, detailed techno-economic analysis (TEA) and life cycle analysis (LCA) are conducted for the conversion of farmed algae biomass, with two primary scenarios considering the conversion of either high-compositional-quality biomass enriched in lipids (high-lipid [HL]) or lower-quality biomass enriched in protein (high-protein [HP]). Each scenario employs a different biorefinery configuration tailored towards extracting the maximum value from the given biomass composition, with the conversion strategies selected from an expansive set of technologies which have been investigated through R&D and TEA/LCA analysis. A rigorous process model of each scenario is developed to aid in estimating the cost and life cycle inventory associated with constructing and operating the biorefinery. Both scenarios generally entail pretreatment and extraction of the biomass to isolate lipids, which are subsequently purified and upgraded to fuels. The HL case also diverts a portion of lipids for producing rigid non-isocyanate polyurethane (NIPU) foam coproduct, a novel bio-based product that may enable displacing conventional polyurethane (PU) without the use of toxic isocyanate inputs. Residual biomass in the HL case is subjected to anaerobic digestion (AD) to recover energy in the form of biogas and supplement process heat and power requirements. In the HP scenario, all lipids are used for fuel production, and the residual solids are dried and used for production of a partially bio-based thermoplastic capable of displacing petroleum-based ethylene vinyl acetate (EVA).

The results for the HL scenario were particularly promising, with a minimum fuel selling price (MFSP) of $3.68 per gasoline gallon equivalent (GGE) and fuel GHG emissions translating to 54%–76% reduction compared to petroleum fuels depending on the coproduct handling method used. These results are driven by the production of the high-value NIPU coproduct while simultaneously achieving high fuel yields (121 GGE/ton ash-free dry weight [AFDW], 63% of which is SAF). High fuel yields can also be extrapolated to a highly promising national-scale potential based on the sites in the continental United States which presently meet criteria for establishing an algae farm, with the potential to support up to 14.1 billion GGE per year (including 8.3 billion gallons of SAF per year, more than 20% of the projected national demand in 2050). Incorporating current policy incentives for producing sustainable fuels enhances the economic viability further, with the potential to reduce MFSP to as low as $0.45/GGE and demonstrate an internal rate of return (IRR) of 26% if fuels were alternatively sold at market prices. When viewing the system strictly from a cost of decarbonization perspective, the HL base case could achieve a marginal cost of GHG abatement of $169/tonne carbon dioxide equivalent (CO_2e), representing the incremental cost for reducing GHG emissions across all products compared to business as usual. This compares favorably with alternative technologies such as direct air capture at near-term benchmark costs of $600/tonne CO_2e or greater. Additionally, a

fuel-centric HL scenario suggests that positive economic outcomes and reduced fuel carbon intensity (CI) could be achieved without relying on the NIPU coproduct, with GHG reductions exceeding 50% compared to petroleum fuels, and MFSP values approaching market viability ($6.60/GGE, or $3.90/GGE with policy incentives).

In contrast, the HP scenario faced more challenges in producing biofuels economically, projecting an MFSP of $7.92/GGE despite significant revenues from the residual algae solids due to lower fuel yields (38 GGE/ton AFDW, 60% of which is SAF; reflecting a national-scale potential of 5.4 billion GGE/year or 3.1 billion gallons of SAF per year). LCA results for the HP case reflected a 24% reduction potential in biorefinery-level GHG emissions. When viewed holistically from an overall biorefinery output perspective, this scenario also could demonstrate a favorable marginal GHG abatement cost of $221/tonne CO_2e. However, these GHG reductions were primarily associated with the thermoplastic coproduct, which accounted for 93% of all biorefinery outputs by mass. In this case, the LCA displacement method was not used, because it could significantly distort the fuel CI when the fuel may more arguably be viewed as the coproduct. Alternative allocation-based coproduct handling methods led to much less favorable results, with a net *increase* in fuel GHG emissions versus petroleum fuels, disqualifying the HP scenario from most policy incentives and further highlighting the reliance of this scenario on the thermoplastic coproduct. A *theoretical* scenario that considered applying policy incentives based on biorefinery-level reductions indicated potential for the HP case to achieve similar economics to the HL case with incentives. However, this is not reflective of how incentives are applied at present day and would require a major shift in broadening GHG reduction policies to include bioproduct decarbonization alongside biofuels.

Key cost and sustainability drivers for each scenario were identified to highlight important areas for future research focus. Success for the HL scenario depends on demonstrating a biomass composition sufficiently high in lipids and, more specifically, polyunsaturated fatty acids (PUFAs) for NIPU production, while the HP scenario requires that residual solids meet the minimum compositional requirements to justify the high value associated with use as a feedstock in the bioplastic production process. In either case, the cost of the algae feedstock remains a key TEA driver in keeping with prior algae conversion analyses, in turn primarily a function of upstream cultivation productivity and farm size.

The contrasting results of the HL and HP scenarios suggest that research on dedicated algae cultivation should focus on achieving compositions elevated in lipids (and preferably PUFAs) while continuing ongoing efforts to improve biomass productivity. Continued R&D on NIPU technology can also help drive algal biofuels and products to become a reality. Favorable results in the HP scenario would depend heavily on revenues and GHG reductions from the solid coproduct, in keeping with similar results observed for other conversion approaches beyond CAP when processing HP compositions. Thus, future research on HP biomass conversion could be more optimally suited to forgo fuels and pursue products-only pathways, or otherwise prioritize lower-cost sources of HP microalgae (e.g., algal biomass utilized for wastewater treatment). Future opportunities also exist to further evaluate algal proteins for food/feed applications to meet growing global needs in this space, though this must be considered across a combination of requisite high values, lower CI than alternative protein sources, and large market volumes that would be needed to support such an option if the vast national-scale resource potential for algal biomass were to be realized.

Table of Contents

List of Figures

List of Tables

1 Introduction

In 2014, the National Renewable Energy Laboratory (NREL) published a "design report" outlining a plausible path to achieving biofuel costs from microalgae below $5 per gallon gasoline equivalent (GGE) in the future through NREL's combined algae processing (CAP) concept [1]. Consistent with other historical NREL design reports [2,3], the 2014 design case provided an in-depth analysis focused primarily on process, design, and economic details for a hypothetical integrated biorefinery pathway supporting the conversion of (microalgal) biomass to fuels, focused at the time on renewable diesel and ethanol fuel products. Also consistent with historical NREL analysis efforts, the design case utilized techno-economic analysis (TEA) as a means to quantify future cost reduction potential via minimum fuel selling price (MFSP) projections as the primary focus, in turn used as a guide to compare against demonstrated performance via annual state-of-technology (SOT) benchmarking updates [4–6].

Broadly, the CAP approach follows biochemical conversion practices, making use of a moderately low-temperature pretreatment step to fractionate the harvested biomass feedstock into its compositional constituent categories, followed by subsequent operations to selectively convert key constituents (i.e., lipids, carbohydrates, and proteins) into fuels or products. The initial 2014 CAP conversion pathway utilized a fairly straightforward process consisting of dilute acid pretreatment, fermentation of liberated sugars to fuel-grade ethanol, extraction and upgrading (hydrotreating) of lipids to renewable diesel, and processing of the residual material (primarily protein) via anaerobic digestion (AD) to biogas to supply heat and power to the biorefinery [1]. Since the original 2014 design report, CAP has undergone numerous iterations to focus on different fuel/product slates and associated research directions under NREL's experimental algae conversion efforts, including alternative routes to upgrade carbohydrates to succinic acid, muconic/adipic acid, butyric acid and 2,3-butanediol (both as intermediates for fuel upgrading), and yeast lipids; as well as conversion of algal lipids to various fuel products and value-added chemical coproducts including polyols, polyurethanes (PUs), and surfactants (from sterols) [7,8]. Conversion of algal protein has also been investigated through various CAP configurations, including fermentation to fusel alcohols and valorization to food/feed or bioplastics, in addition to AD [9]. Alternative approaches have also been investigated to thermochemically convert multiple components of the biomass via mild oxidative treatment [9,10]. Additionally, the economic potential of the CAP approach has been assessed for alternative sources of microalgae biomass, such as that generated from wastewater treatment, collected from harmful algae blooms, or left over from commercial lipid extraction operations [11].

While many of the CAP configuration scenarios noted above have been shown to offer promising potential, the large range of options and their integration with widely varying algal biomass compositions can complicate the picture regarding which CAP approach may be optimal for a given composition (e.g., degree of nutrient depletion during harvest versus cultivation productivity and cost). Moreover, the U.S. Department of Energy's Bioenergy Technologies Office program priorities are evolving relative to the priorities that dictated the context for the 2014 design report, pivoting away from specific MFSP goals in favor of deep decarbonization of fuels and products, including sustainable aviation fuel (SAF) products and processes achieving at least 50%—and more optimally at least 70%—greenhouse gas (GHG) reductions compared to

conventional benchmarks [12,13]. Economic and deployment practicality at scale also remain important considerations, while recognizing external market factors that can confound designing a system around a specific MFSP target (e.g., petroleum prices, economic conditions, price swings of input materials and output products/coproducts, policy incentives). Given the uncertainty in these external factors, along with unpredictability of future advancements in algae cultivation and conversion strategies, it is not possible to define a true optimal singular conversion approach. However, our past work has elucidated which pathways and products are likely to enable economical and sustainable algal biofuels, as well as those which present greater challenges. As such, the present report presents a more comprehensive analysis covering both TEA and life cycle analysis (LCA) metrics for leading strategies as a case study to achieve new Bioenergy Technologies Office priorities through selected example CAP conversion pathways. We consider one CAP configuration tailored to accommodate high-lipid (HL)/low-protein algae and a second configuration for low-lipid/high-protein (HP) algae. Key outputs are reported in consideration of priorities for deep decarbonization, economic viability, and process simplification/near-term deployability.

2 Design Basis and Conventions

2.1 Algae Cultivation Facility

Algae cultivation was modeled using a modified version of the NREL Algae Farm Model [14], as developed for a recently-published algae harmonization study [15] and shown in Figure 1. CO_2 is assumed to be sourced through capture from current industrial processes, such as electricity generation, petroleum refineries, and chemical production plants. The price point of $46/tonne is consistent with the average CO_2 capture cost for 137 individual sites in Southeastern US (Florida and Georgia) [15]. Urea and diammonium phosphate are sourced from the fertilizers market, being generally obtained through conventional production pathways. The main refinements relative to prior NREL designs include (1) use of a basket filter for the removal of insoluble ash (assumed to account for 50% of the total ash content) prior to dewatering using membrane filtration; (2) consideration of a washing step prior to centrifugation to reduce the salinity of the outlet stream to 15 ppt; and (3) employment of a forward osmosis unit to generate freshwater for the washing step from the saline water blowdown removed from the ponds and for reducing the volume of saline water sent to underground disposal [16,17]. Additional granularity was also included in the sizing of other pieces of equipment, such as capital and operating expenses for the saline groundwater well and for deep well injection of the concentrated brine obtained as a byproduct of the forward osmosis unit. Specific algae cultivation and general farm parameters were derived from data considered in the algae harmonization study, as detailed in Table 1. When not otherwise specified, other parameters follow those in [7]. A facility size of 3,900 acres was chosen, consistent with the average farm size in the harmonization study [15], though noting this is significantly higher compared to the median farm size from the same dataset (2,145 acres). The economic implications of farm size are explored in detail in Section 6.2.4.

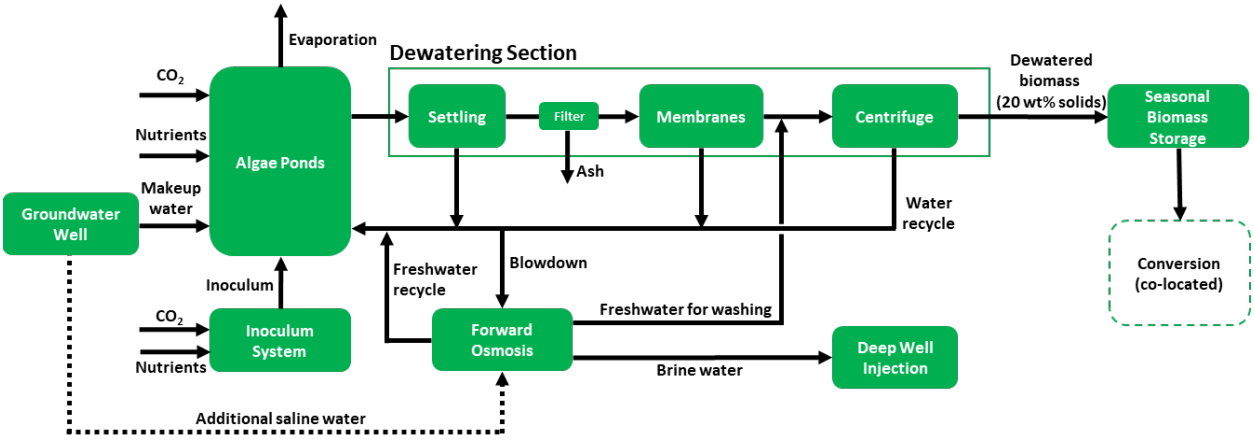

Figure 1. General structure of the algae farm model employed in this study

Table 1. Main Parameters Employed in the Simulation of Large-Scale Algae Farm Cultivations

Parameter	Value	Rational
Facility size	3,900 acres	Considerations in the 2022 algae harmonization study [15]
Carbon dioxide (CO_2) uptake efficiency	75%	
Nutrient source	Urea, diammonium phosphate	
Salt tolerance of algae strain	50,000 mg/L (50 ppt [a])	Average for the individual sites in the Southeastern United States (Florida and Georgia) assessed in [15]
Salt content in water makeup	5,551 mg/L (5.55 ppt)	
Evaporation rate	0.44 cm/day	
CO_2 price	$46/metric ton	
Depth of deep well for brine injection	274 m	
Capital expenses of well for saline water sourcing	$710,000	
Power requirement for saline water pumping	2,062 kW	

[a] ppt: parts per thousand (or g/kg)

Assumed seasonal productivity ratios were held consistent with future target values presented in NREL's SOT reports [16–19], but values were modified to match the specified annual average productivity scenarios discussed below. A target cultivation productivity of 25 g/m^2/day was assigned to the HP compositional case, subsequently reduced to 20 g/m^2/day in shifting to the HL composition, recognizing reductions in biomass productivity commonly observed moving from HP (replete) to HL (deplete) conditions [20]. It is noteworthy that, based on the data presented in the algae harmonization report [15], the Southeastern U.S. region (considered as the basis for several of the algae farm parameters) may be able to support algae biomass productivities above the 25 g/m^2/day target defined for HP microalgae biomass (potentially up to an average of 30 g/m^2/day, as reflected in the above-cited harmonization study). The modeled biomass compositions for each case are shown in Table 2 along with the modeled biomass and lipid productivities. The minimum biomass selling prices for each case were quite close ($691/ton for HL and $688/ton for HP), with cost reductions from higher biomass productivity in the HP case nearly offset by increased nutrient costs demanded by nutrient-replete harvesting conditions, though noting this is before inclusion of nutrient recycles which are credited in the CAP model downstream to reduce fuel costs.

2.2 Feedstock Composition

2.2.1.1 Algae Composition

The composition of algae biomass can vary significantly depending on the strain used, the nutrient loadings applied during cultivation, and the stage of growth in which the biomass is harvested (biomass accumulation versus lipid induction). Biomass harvested under nutrient-replete conditions often reflects a composition relatively elevated in proteins and deficient in lipids, whereas biomass in a nutrient-deplete environment contains relatively higher lipid and lower protein levels. While more lipids and less protein are preferable from a fuels-centric

conversion standpoint given the potential for much higher fuel yields and/or more flexibility to incorporate value-added coproducts [1,4,15,21], this typically comes at the expense of a slowdown in cultivation productivity and resultant increase in biomass cost [22,23]. Recognizing these trade-offs, two representative algae compositional profiles were considered in this analysis, containing an elevated level of either lipid or protein. These were based on biomass compositions demonstrated experimentally by NREL collaborations under the Development of Integrated Screening, Cultivar Optimization, and Verification Research (DISCOVR) consortium (in the case of HP) and by industrial partners (in the case of HL algae); these compositions are detailed in Table 2.

The HL composition reflects biomass produced in a "simulated pond" environment by industry partner Viridos (San Diego, CA). The Viridos simulated ponds are small vessels (approximately 2 m^2) that operate on the same mechanical basis as a raceway pond, but which are subject to artificial light and temperature controls that are programmed and controlled to simulate specific location- and season-specific outdoor cultivation conditions. Additional details regarding the simulated ponds and the validation of the related production data relative to outdoor cultivation comparators can be found in NREL's algae farm 2023 SOT report [18]. The assumed target productivity (20 g/m^2/day) is consistent with the productivity observed in the simulated pond environment, though would be reduced to approximately 13 g/m^2/day when seasonal variability reductions are applied (recognizing this study represents future aspirational productivities for both the HP and HL cases). In the original data, compositional values for lipid impurities (e.g., phospholipids, sterols) were not measured; here, we have adjusted the compositional data to include these components assumed in proportion with the measured fatty acid methyl ester (FAME) lipid content extrapolated from an HL biomass composition assessed previously [10]. This approximation results in low (1.2%) phospholipid content, which is consistent with published data for a separate source of biomass from Viridos indicating no quantifiable phospholipids [24]. To maintain 100% compositional closure, the "cell mass" content (a mixture of chlorophyll, nucleic acids, and other unidentified components that are not assumed to contribute to fuel or product yields, generally employed to close analytical mass balances) was reduced by an equivalent amount. The HP composition is reflective of the average biomass composition demonstrated by the DISCOVR consortium in the 2022 SOT report [19] (maintained consistently in the 2023 SOT report [18]). The HP case also reflects a slightly lower ash content as the underlying 2022 SOT included several months of cultivation data on a seasonally rotated *Monoraphidium* strain grown in lower-salinity conditions (5 ppt). Elemental compositions are unadjusted from the original reported data.

Table 2. Modeled Elemental and Biochemical Biomass Compositions for Each Strain, Along With Assumed Productivity and Key Outputs From Cultivation Model

	HL	HP
Elemental Composition		
C	63.5	50.6
H	12.1	7.5
O	19.9	30.6
N	2.1	9.9
S	2.3	0.2
P	0.2	1.2
Total	100	100
Biochemical Composition		
Ash	23.8	18.7
Fermentable carbohydrates	8.3	6.4
Non-fermentable carbohydrates	0.8	1.3
Protein	7.5	38.5
Lipids (measured as FAME) [a]	47.4	8.0
Non-FAME lipid impurities	1.2	4.3
Sterol	1.3	4.6
Cell mass [b]	9.8	18.2
Total	100	100
Productivity		
Biomass productivity (g/m^2/day ash-free dry weight [AFDW])	20	25
Lipid productivity (g/m^2/day FAME lipids)	9.5	2.0
Minimum biomass selling price ($/ton AFDW)	$691	$688

[a] Lipids were originally characterized as triglycerides and adjusted within the model to 50% triglycerides and 50% free fatty acid (FFA) plus glycerol (assumed basis fixed constant in all cases).

[b] Refers to a mixture of chlorophyll, nucleic acids, and other unidentified components not assumed to contribute to fuel or product yields, generally employed to close analytical mass balances.

2.2.1.2 Lipid Profile and Considerations for Biorefinery Conversion

In addition to the total lipid content, the characterization of the specific fatty acids present (i.e., carbon chain length and degree of unsaturation) can also influence process economics to varying degrees depending on the configuration of the conversion process. In the context of fuel production, the fatty acid profile can impact the hydrogen requirement during fuel upgrading, as more unsaturated fatty acids require higher hydrogen consumption to produce saturated alkanes. In the context of chemical coproducts such as PUs as a key focus for the HL compositional case in this study, the fatty acid profile is an even more critical factor, because the unsaturation sites serve as the reaction point for the linkage chemistry of the final polymer, directly influencing yields and product properties.

PU coproduction from algal lipids has become a central element of NREL research focus over recent years, owing to a favorable combination of high market values and market volumes [10,25]. Likewise, NREL's TEA work has showcased the ability for algae-based PUs to reduce MFSPs by more than $4/GGE by diverting a fraction of lipids away from fuel production, as highlighted in prior SOT benchmarking updates [4]. In recent years, NREL TEA models have been built and subsequently refined for lipid upgrading to PU, initially reflecting conventional chemistries through reaction of lipid-derived polyols with isocyanates [7] to yield PU foams. This largely reflects commercial technology that has also been applied to other bio-based lipid feedstocks [26], and while more technologically mature, suffers a key drawback due to the use of highly toxic isocyanates, derived from the toxic and environmentally deleterious precursor phosgene. As such, isocyanate-based PU manufacturing is facing increasingly strict regulatory pressures [27–29]. Given these and other considerations (e.g., high GHG intensity for isocyanate production), NREL researchers have pioneered an emerging technology for the production of non-isocyanate polyurethane (NIPU), replacing isocyanate with diamine as the cross-linker (discussed in more detail in Section 3.4) [21,30–32]. Accordingly, this study focuses on lipid upgrading to NIPU coproducts in light of promising economic, sustainability, and potential future market regulatory advantages.

The required degree of lipid unsaturation for PU or NIPU production depends on the lipid feedstock being used and the chemistry of the process. Our previous work focused on assessing the production of PU [4,10] and NIPU [21] initially from triacylglycerides (TAG). In these cases, because there are multiple fatty acids present per TAG molecule, there is a lower unsaturation requirement per fatty acid compared to the use of FFAs or FAME for PU/NIPU upgrading. For example, in the case of producing NIPUs, experimental work has suggested the ideal product may be produced from lipids containing 6.3 double bonds per TAG (2.1 double bonds per fatty acid) [21]. TAG feedstocks with lower degrees of unsaturation (e.g., soybean oil) exhibited poor tensile performance, whereas feedstocks with more double bonds (e.g., algae oil enriched in PUFAs) were too viscous to process at full carbonation, though showed more promising results at partial carbonation [21]. The double bond requirement assumed in prior work for producing conventional PU is even lower (2.9 double bonds per TAG, or 0.9 double bonds per fatty acid) [10].

However, one challenge with using TAG for PU/NIPU production is that the fatty acids constituting the TAG molecule are not easily tunable. While the fatty acids may be hydrolyzed from the TAG and then separated based on degree of unsaturation, complete conversion back to TAG is challenging, with significant amounts diglycerides and monoglycerides produced [33]. Thus, even if a given fatty acid profile is highly enriched in polyunsaturated fatty acids (PUFAs), the presence of saturated fatty acids may incur challenges in using the lipids for PU production.

More recent experimental work has also investigated the suitability of FAME as a feedstock for NIPU and has found that a minimum of 3 double bonds per FAME are required to produce a suitable product; feedstocks with lower unsaturation generally exhibit poor tensile strength, while higher amounts of double bonds are associated with a polymer which is too brittle [32]. While this higher requirement means that less of the algal lipids may be suitable for PU production compared to TAG as a feedstock, this approach allows for hydrolysis of all algal lipids to FFAs, conversion of FFAs to FAME, and isolation of the preferred PUFA-based FAME fraction, thus allowing more controlled tuning of the fatty acid profile used to produce PU. We

focus on this approach for the HL scenario of the present study, necessitating that the algae biomass feedstock is sufficiently enriched in PUFAs. A secondary effect of using FAME instead of TAG is that the ratio of TAG to FFA in the biomass lipids becomes less important. This ratio can vary significantly by biomass strain and harvest stage, which has a direct impact on PU/NIPU yields *if using TAG-based chemistry* [10]. However, in the process design approach used here, all TAGs are hydrolyzed and the NIPU yield is instead directly related to the PUFA content (whether originating from TAG or FFA). We maintain an assumption from our previous analyses [4,9,10] of a 1:1 TAG:FFA ratio here, though emphasize that this assumption has limited impact on process yields beyond slight variations in chemical consumption during lipid cleanup and transesterification.

Given the direct relationship between the PUFA content and NIPU yield, it is important to understand the factors which influence the fatty acid profile. The fatty acid profile of microalgae can vary significantly by species and harvest stage [34,35]. Some strains of microalgae can demonstrate very high levels of PUFAs, especially when harvested in nutrient-replete (HP) conditions; for example, *Nannochloropsis* has shown the potential to exceed levels of 50% eicosapentaenoic acid (C20:5) [36]. Relatively high PUFA content has also been observed in *Scenedesmus* sp. (>20% C18:3) [24] and *Chlorella* sp. (>30% C18:3) [37]. Other strains (*N. apropphilia, R. Salina,* and *Nitzschia* sp.) have demonstrated eicosapentaenoic acid levels ranging from 15-25% in autotrophic conditions [38], and eicosapentaenoic acid levels of 25-30% have been reportedly been produced in an outdoor pond setting [39]. However, other strains, including the HL biomass used as the basis for the modeled HL scenario, have produced lower amounts of fatty acids with at least 2 degrees of unsaturation (double bonds) [24,40]. Higher PUFA fractions of algal lipids generally correlate to nitrogen-replete environments and concomitant lower overall lipid levels [34,36], creating a challenge for achieving HL biomass while still maintaining high PUFA content.

In the HL case, we assume that 15% of the fatty acids are present as C18:3 (linolenic acid) as a representative PUFA component, with this fraction isolated from the remainder of the fatty acids containing lower unsaturation and used for NIPU production. While much higher PUFA levels have been observed in some cases, this value does represent a challenge for nutrient-deplete (HL) algae harvesting and could require concerted efforts in strain selection, harvest condition optimization, and/or genetic engineering to achieve as an aspirational goal. It should also be noted that this assumption is maintained year-round, while recognizing that maximizing year-round productivity may require seasonally rotating strains, each with their own variation in PUFA content – in practice this may be more challenging to achieve particularly for winter strain cultivation, in order to maintain consistent lipid/PUFA content and thus downstream NIPU production output. Despite these challenges, we view this as a reasonable target PUFA content for HL algae. However, given such dynamic variables that can influence this parameter, we also present the implications of varying PUFA content in Section 6.2.2.

In the HP case, all lipids are diverted to fuel production to maximize fuel outputs from a lower-fuel-yielding biomass basis; thus, the PUFA content of the lipids is less impactful. As is consistent with our previous analyses [6,10], hydrogen use and hydrotreating yields for fuel upgrading are based on experimental conversion data (originally based on lipids extracted from *Scenedesmus* sp.), rather than calculated based on a specified fatty acid profile. The hydrogen requirement for fuel upgrading and its relation to PUFA content are explored in Section 6.3.

3 Process Design and Cost Estimation Details

In the envisioned biorefinery approach, the algae farm described above is co-located with a conversion facility. The biomass from the algae farm following harvesting and dewatering to 20 wt % AFDW is delivered to the conversion facility. The CAP conversion schematic varies depending on the algae composition; the approach for converting HL algae is shown in Figure 2, while the approach for HP algae is shown in Figure 3. In both cases, biomass to the conversion process is maintained at a constant throughput despite seasonal variability in upstream cultivation by sending biomass to wet anaerobic storage during peak seasons and adding supplemental biomass from storage during seasons with low productivity. Biomass is subjected to a dilute acid pretreatment step followed by solvent extraction. In the HL case, lipids are treated via degumming and transesterification with methanol, followed by saturated versus unsaturated FAME separation via low-temperature crystallization, exploiting differences in melting points. FAMEs with a high degree of unsaturation (3 double bonds or more) are diverted to NIPU production to generate coproduct revenue, while the remaining FAMEs are sent to hydrotreating for fuel production. In the HP case, extracted lipids undergo saponification to remove polar lipid impurities (more prevalent in HP biomass) followed by esterification to FAME lipids, all of which are hydrotreated to maximize fuel yields from a much lower-lipid fuel precursor. Given the relatively low carbohydrate content for either compositional scenario (and in keeping with an emphasis on process simplification), the CAP configurations in this study do not include a dedicated carbohydrate conversion operation. Residual biomass is either sent to AD to recover energy in the form of biogas (in the HL case) or dried and sold for thermoplastic production as the necessary value-added coproduct (in the HP case) in the absence of the NIPU processing train, with the AD effluent (HL case) or extraction raffinate liquor phase (HP case) returned to the production ponds for nutrient recycle. Each case also includes combined heat and power to meet the heating and electricity requirements of the process, with excess electricity sold to the grid. CO_2 from combined heat and power is also recycled to the ponds.

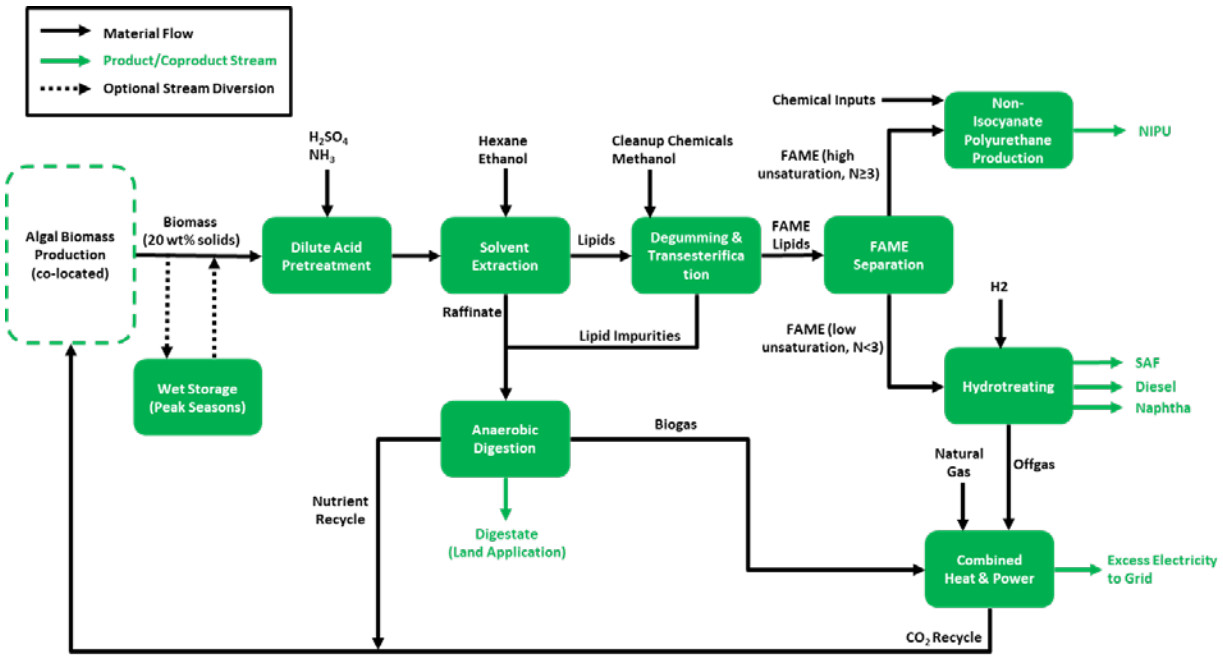

Figure 2. Process flow diagram for the conversion of HL biomass

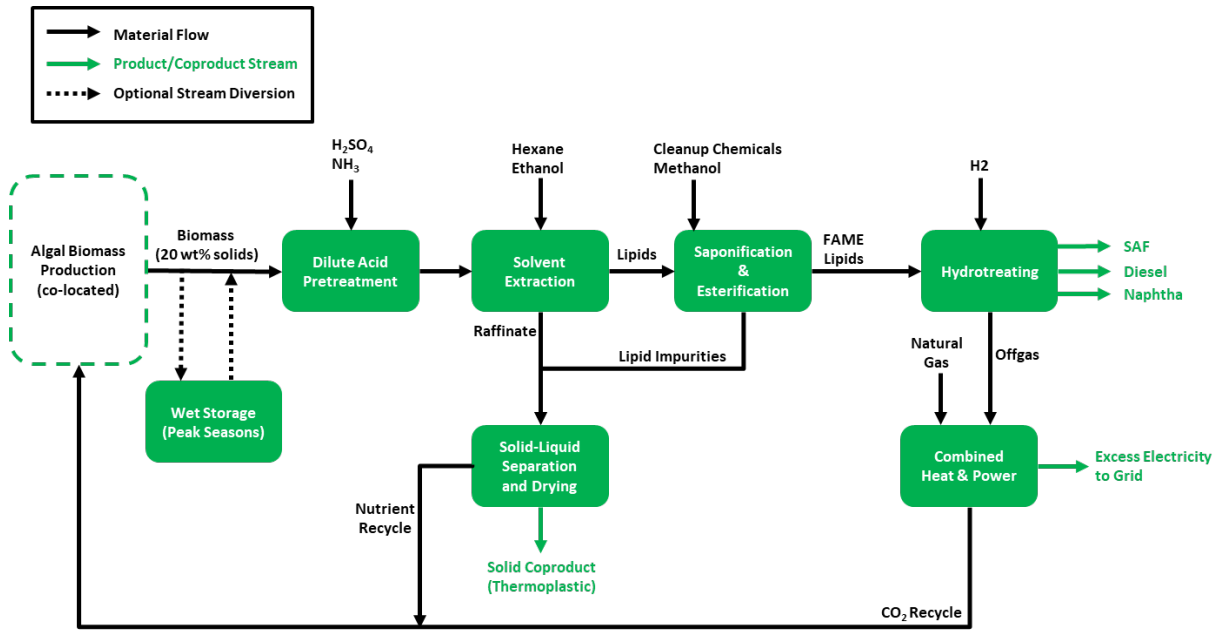

Figure 3. Process flow diagram for the conversion of HP biomass

3.1 Storage and Pretreatment

CAP conversion for either compositional scenario begins with seasonal storage to mitigate fluctuations in feed rate through the facility tied to upstream cultivation productivity swings. This step has been described in prior analyses based on research conducted by Idaho National Laboratory [41] and will not be repeated in detail here. In summary, peak seasonal flows from the algae farm in excess of the annual average are diverted to wet anaerobic storage as a method of biomass ensilage, to be blended with algae farm biomass produced during low-productivity seasons. This allows for a low-cost method of feeding biomass through the CAP biorefinery at a constant rate near the annual average output from the farm, albeit at a slightly lower rate equating to biomass degradation losses incurred during storage. All design/cost and processing details for seasonal storage are maintained consistent with NREL's latest SOT analyses [6]—namely the use of a lined and covered in-ground pit at a cost of $0.15 per gallon of storage volume, incurring 13% storage degradation losses of whole biomass to CO_2 and organic acids. However, at the 2.6:1 maximum seasonal variability assumed in this study, only 16% of total annual biomass production is subjected to seasonal storage, translating to 2.1% degradation loss of total annual biomass from cultivation. Storage incurs minor compositional shifts, generally sacrificing carbohydrates while adding to lipids based on previous data from Idaho National Laboratory. The fatty acid profile is assumed to be consistent between raw and stored algae, though there is some evidence that PUFA content may decrease in stored algae [42,43]; in this case, any PUFA degradation would similarly be limited to 16% of the total annual production. Key details pertaining to the seasonal storage operation are summarized in Table 3.

Table 3. Summary of Key Parameters for Seasonal Biomass Storage

	Raw Algae	Wet Storage Algae
Key Biochemical Composition Changes		
Ash	Base	+0%
Fermentable carbohydrates	Base	−5.9%
Non-fermentable carbohydrates	Base	−4.9%
Protein	Base	+0.3%
Lipids (measured as FAME)	Base	+3.2%
CAP Biorefinery Inputs		
Whole biomass intact after storage (kg)	1.0	0.87
Degradation to organic acids (kg) [a]	0	0.10
HL scenario seasonal biomass flow rates (tonnes/day AFDW):	**From farm:**	**To conversion:**
Spring	373	317
Summer	465	317
Fall	277	317
Winter	181	317
Annual average	324	317
HP scenario seasonal biomass flow rates (tonnes/day AFDW):	**From farm:**	**To conversion:**
Spring	460	396
Summer	564	396
Fall	373	396
Winter	217	396
Annual average	403	396

[a] Primarily succinic and lactic acids.

The biomass slurry is then routed to dilute acid pretreatment, again largely maintaining similar design/processing assumptions as in prior studies [1,6]. Pretreatment has been shown to be a crucial step in CAP, as a means of fractionating the algal biomass compositional constituents to enable effective downstream recoveries/conversion of those constituents. The 2014 design case and other historical TEA efforts for CAP had placed an emphasis on producing and converting high levels of algal carbohydrates separately from lipids and protein, given the ability of some strains such as *Scenedesmus* to reach high carbohydrate levels of approximately 50 wt % during early nutrient depletion before shifting to high lipids [37]. In such cases, dilute acid pretreatment is also key in liberating carbohydrates as monomeric sugars for downstream upgrading [44]. However, the present analysis de-emphasizes focusing on carbohydrates given the priority in this work to simplify processing/cost complexity for more near-term deployment, and given numerous other terrestrial biomass options for sourcing carbohydrates. Nonetheless, dilute acid pretreatment remains a reliable option to also enable high downstream lipid extraction efficacy, experimentally achieving more than 95% lipid recovery for *Scenedesmus* sp. biomass containing up to 27 wt % FAME lipid content [6]. An alternative pretreatment option has also been considered in prior work, namely flash hydrolysis [10]. This option may enable lower capital costs but at the expense of higher temperatures, and thus generally more detrimental impacts to LCA given higher energy demands. Given renewed priorities to maximize decarbonization

potential under relaxed cost constraints as well as more extensive experimental history, dilute acid pretreatment is maintained as the focus for this work.

Table 4 summarizes key parameters for dilute acid pretreatment processing. In summary, the operation is performed at 20 wt % solids AFDW and 150°C for a 5-minute residence time using 1 wt % acid loading versus feed liquor (i.e., on the mass basis of the slurry), largely consistent with recent SOT conditions [6]. The pretreated hydrolysate is then flashed to 0.5 atm and neutralized with a stoichiometric amount of ammonium hydroxide. Although monomeric sugar release is not specifically targeted, the latest SOT performance of 83% fermentable sugar solubilization is maintained. One key update for this step, in contrast to original design/costing assumptions employed in the 2014 design case, is the assertion that dilute acid pretreatment can be performed in an agitated pressure vessel, rather than requiring the complex presteamer and horizontal acid treatment reactor design typically utilized for processing milled terrestrial biomass such as corn stover. This results in a roughly 60% capital cost savings for the storage and pretreatment area, although still requiring Incoloy 825 cladding metallurgy at the given acid loading conditions.

Table 4. Summary of Key Parameters for Dilute Acid Pretreatment

Temperature	150°C
Pressure	4.6 atm
Total solids loading (AFDW)	20 wt %
Residence time	5 min
Acid loading (wt % of feed liquor rate)	1%
Carbohydrate conversion to sugars	83%
Carbohydrates conversion to furfurals	0.3%

3.2 Lipid Extraction and Cleanup

3.2.1 Lipid Extraction

Subsequent to the 2014 NREL design report [1], the lipid extraction step was updated to reflect a lower-cost and more scalable approach. The new approach as demonstrated experimentally and reflected in recent SOT updates [6] eliminates the single-solvent system utilizing a costly reciprocating Karr liquid-liquid extraction column, now replaced with a dual-solvent approach utilizing a nonpolar (hexane) solvent with a polar (ethanol) co-solvent. The new approach offers a more optimal design that mitigates formation of emulsions (a common challenge with wet hexane lipid extraction) owing to the added secondary ethanol solvent, while also reducing solvent carryover losses into the raffinate (primarily hexane losses into the aqueous phase, which are then recovered through an added ethanol distillation column for ethanol solvent recovery). This also utilizes simpler equipment largely consisting of agitated vessels and phase separation centrifuges, though at a similar overall capital cost versus the prior extraction column design.

As depicted in Figure 4, the updated design utilizes a series of three agitated vessels each followed by a centrifuge to separate the organic and aqueous phases, with the organic phase from each step routed to a hexane recovery distillation column and the aqueous phase sent to the next extraction stage along with makeup hexane. Following the final stage, the aqueous phase is routed to a distillation column to recover ethanol and any residual hexane, resulting in near-

complete recovery of both solvents. Experimental work with this approach has achieved up to 96% FAME lipid extraction yields based on algal biomass up to 27 wt % FAME lipid content. However, we note that new data utilizing higher-lipid biomass has suggested the possibility of more challenging phase separation when processing HL biomass due to lower density of the lipids and thus the solid biomass, which may in turn partially report to the organic rather than aqueous phase following initial centrifugation. This issue is not assumed to pose an insurmountable challenge in the present study, but requires further investigation and quantitative characterization moving forward. Key parameters for the lipid extraction step are summarized in Table 5.

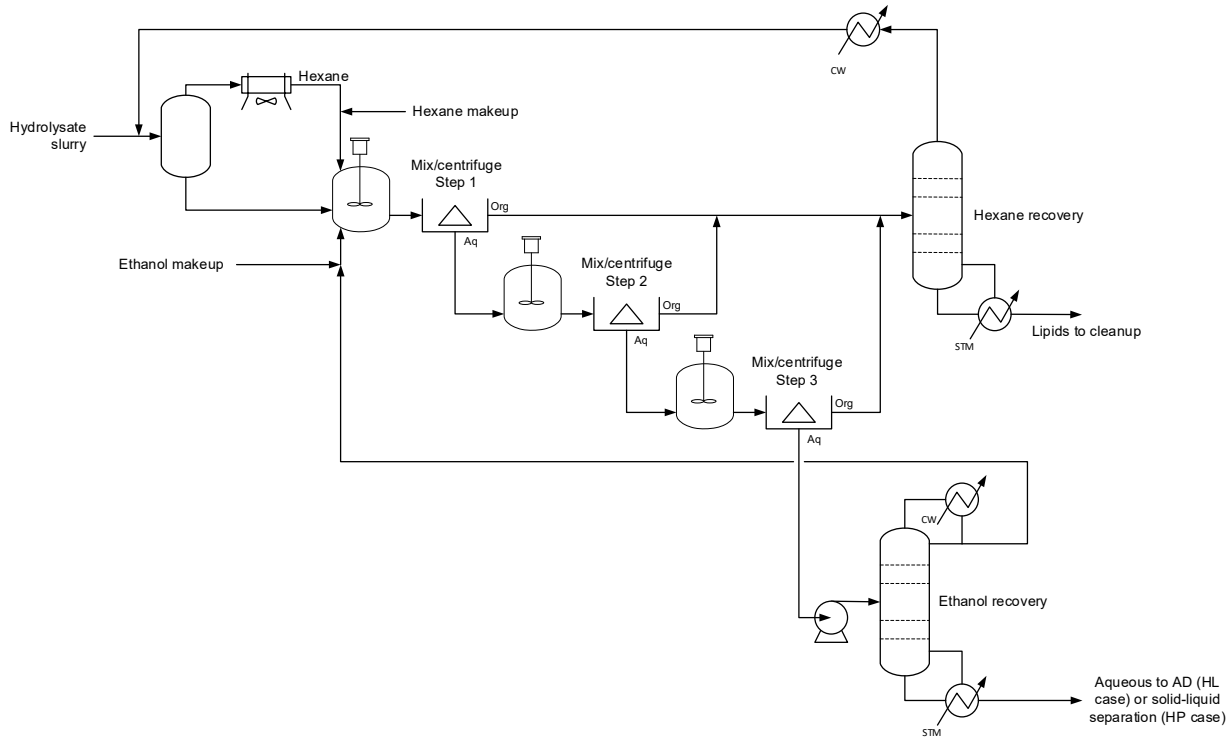

Figure 4. Schematic diagram of three-stage lipid extraction process

Table 5. Summary of Key Parameters for Lipid Extraction

Solvent loading (hexane: ethanol: dry biomass ratio, wt)	2.7 : 1.1 : 1.0
Extraction method	Three-stage agitation/two solvents
Insoluble solids to extraction (wt %)	20 wt %
FAME lipid extraction yield (%)	96.0%
Lipid impurity partition to extract	11.5%
Sterol partition to extract	96.0%
Hexane/ethanol solvent losses	Ethanol: 1.2% of recycle flow Hexane: 0.14% of recycle flow

3.2.2 Saponification and Esterification (HP Only)

HP biomass is known to contain higher amounts of polar lipid impurities relative to FFA, requiring a saponification step to isolate FFAs prior to upgrading. In the HP case, the extracted lipids are cooled to 70°C and saponified with sodium hydroxide (NaOH), producing sodium-based fatty acid salts (soap). The mixture then proceeds to the esterification reaction, where it is reacted with methanol (30 mole/mole FFA) in the presence of sulfuric acid (5 mole/mole FFA) to produce FAME and water [45]. Esterification of FFA soaps proceeds to 99% conversion [45]. Following esterification, FAME lipids are separated from the aqueous phase and proceed to fuel upgrading. The aqueous phase, containing acid, methanol, glycerol, and polar lipid impurities, is recycled back to the esterification reactor. A purge rate of approximately 20% is maintained to prevent the water content in the esterification reactor feed from exceeding 5 wt % [46]. Key details relating to the saponification and esterification operations can be found in Table 6.

Table 6. Summary of Key Parameters for Saponification and Esterification.

These operations apply only in the HP scenario.

Saponification	
Temperature	70°C
NaOH loading (mole per mole TAG)	1.0
Esterification	
Methanol loading (methanol: fatty acid mole ratio)	30:1
Sulfuric acid loading (H_2SO_4: fatty acid mole ratio)	5:1
Conversion	99%
Residence time	30 minutes

3.2.3 Lipid Cleanup and Transesterification (HL Only)

In the HL case, extracted lipids are subjected to a less severe cleanup operation consisting of degumming, demetallization, and bleaching, described in our previous work [1,10]. Degumming includes a dilute treatment with phosphoric acid followed by a water wash and centrifugation to remove polar lipid impurities. Next, lipids are demetallized and bleached using silica and clay, respectively, producing a mixture of clean lipids. While metals/inorganics measurements were not available for the extracted lipids from these two compositional cases, prior data as reported in the 2014 design case indicated metals content above 35 ppm in extracted lipids from *Scenedesmus*, consisting primarily of sodium, iron, copper, phosphorus, and calcium [1]. However, the 2014 design case also reflected fresh/brackish water strains, thus the presence of other inorganics such as chlorides imparted from high-salinity cultivation as reflected in this study have not been extensively investigated (though this study also includes upstream washing to reduce salinity down to 15,000 mg/L as noted above).

The clean lipids (consisting of 50% FFA and 50% TAG) then proceed to transesterification, where they are reacted with methanol (6 mole/mole FFA) in the presence of sulfuric acid (1.5 mole/mole FFA) to produce FAME, water, and glycerol [47]. Conversion of TAG and FFA proceed to 92% conversion [46]. Following transesterification, FAME lipids are separated from the aqueous phase and proceed to low-temperature crystallization for fractionation to NIPU and fuel production. The aqueous phase, containing acid, methanol, glycerol, and polar lipid impurities, is recycled back to the transesterification reactor. A purge rate of approximately 20%

is maintained to prevent the water content in the esterification reactor feed from exceeding 5 wt % [46]. Key details relating to the lipid cleanup and transesterification operations can be found in Table 7.

Table 7. Summary of Key Parameters for Lipid Cleanup and Transesterification.

These operations apply only in the HL scenario.

Lipid Cleanup	
Temperature	110°C
Degumming: Phosphoric acid loading (wt % of feed)	0.19%
Degumming: Water wash (wt % of feed)	10%
Demetallization: Silica loading (wt % of feed)	0.1%
Bleaching: Clay loading (wt % of feed)	0.2%
Transesterification	
Temperature	80°C
Methanol loading (methanol: fatty acid mole ratio)	6:1
Sulfuric acid loading (H_2SO_4: fatty acid mole ratio)	1.5:1
Conversion	92%
Residence time	6 hours

3.2.4 Low-Temperature Crystallization (HL Only)

In the HL case, the clean FAME lipids are separated to a PUFA-enriched fraction (suitable for producing rigid NIPU foams) and a fraction containing lower amounts of unsaturation (more ideal for fuel upgrading). This separation is accomplished through five sequential low-temperature crystallization steps at progressively lower temperatures to exploit the lower melting points of more unsaturated fatty acids, with the liquid phase from each crystallization containing increasingly elevated levels of PUFA. The details associated with this operation are consistent with those reported in our previous work [9], though applied here to FAME lipids as opposed to FFA lipids in the referenced study.

It is important to note that this process has not yet been implemented at a commercial scale for PUFA enrichment. While initial experimental results are promising, they do not achieve perfect separation. To represent a future target scenario, the model assumes that the PUFA-enriched fraction has an average of 3 double bonds per FAME, which is consistent with the minimum requirement for producing NIPUs with satisfactory properties [32]. The presence of FAME with fewer double bounds in the PUFA-enriched fraction could affect the final properties of the NIPU. Conversely, achieving a pure PUFA phase, but with significant losses to the saturated fatty acid fraction, would negatively impact NIPU yields. In the model, recovery of a pure PUFA phase is assumed with no losses. Losses to the saturated fatty acid fraction would result in lower diversion of PUFAs to NIPU, which is examined in detail in Section 6.2.2. Key details relating to low-temperature crystallization can be found in Table 8.

Table 8. Summary of Key Parameters for the Low-Temperature Crystallization Unit Operation

Number of stages	5
Stage temperatures	35°C; 30°C; 25°C; 20°C; 9°C
Average double bonds per FAME in PUFA-enriched fraction	3.0
PUFA-enriched fraction (% of feed)	15%

3.3 Fuel Upgrading

Both the HL and HP cases include an identical hydrotreating operation for upgrading lipids to liquid hydrocarbon fuels. Details regarding the fuel upgrading operation are generally consistent with those reflected in the 2022 conversion SOT [6] and include a combined one-step catalytic hydrodeoxygenation (HDO) and hydroisomerization (HI) reaction, followed by phase separation and steam fractionation into naphtha, jet, and diesel cuts. However, one key difference is a shift from a TAG- and FFA-based lipid feedstock to a FAME (biodiesel) feedstock. This new approach addresses metallurgy concerns associated with hydrotreating lipids containing appreciable amounts of FFAs, which contribute to a total acid number that may be too high for conventional metallurgies, increasing the risk of reactor failures [48,49]. Converting all lipids to FAMEs reduces their total acid number, enabling the use of conventional carbon steel metallurgy in a coprocessing scenario. This results in lower-cost upgrading equipment and enhances the suitability of the lipids for coprocessing in a standard refinery. A total acid number of 0.5–0.6 mg KOH/g is a typical industry-accepted limit before requiring upgraded metallurgy [49]. Biodiesel typically has a total acid number value in the range of 1–3 mg KOH/g [50], so would be somewhat limited by blending constraints, but would be a marked improvement compared to FFAs, which can have total acid number values on the order of 200 mg KOH/g.

One complication associated with moving to a FAME-based lipid feedstock is that the one-step catalytic hydrodeoxygenation (HDO) and hydroisomerization (HI) operation is optimized for oil containing a mixture of TAG and FFA. Promising results have been demonstrated for one-step HDO/HI of TAG and FFA over a Pt/SAPO-11 catalyst, resulting in a liquid fuel yield of up to 84% in prior studies [4–6]. These assumptions are maintained here from fatty acids, with additional hydrogen consumption included for converting the FAME methyl groups to methane (CH_4). Hydrotreating yields from fatty acids are based on adjusting original experimental data to maintain mass and elemental balance of carbon, hydrogen, and oxygen, resulting in slightly different fuel yields for each case. A yield of 75.6% (63% SAF) is targeted in the HL case, and a yield of 80.1% (60% SAF) is targeted in the HP case. However, it should be noted that alternate catalysts or reaction approaches may be required in the future to meet the asserted yields with a FAME feedstock (e.g., a two-stage fixed bed with catalysts optimized for HDO and subsequent hydrocracking/HI). Due to the somewhat aspirational nature of the asserted yields from FAME lipids, we consider the sensitivity of economics to the liquid fuel yield in Section 6.3. Key details relating to fuel upgrading can be found in Table 9.

Table 9. Summary of Key Parameters for Fuel Upgrading

	HL	HP
Temperature (°C)	375°C	375°C
Pressure (psig)	435 psig	435 psig
Catalyst	1% Pt/SAPO-11	1% Pt/SAPO-11
Catalyst weight hourly space velocity (h^{-1})	1	1
Hydrogen loading (scf/bbl oil feed)	5,900	5,900
Hydrogen consumption (wt % of oil feed)	3.1%	3.1%
Fuel yield (wt % of oil feed)	75.6%	80.1%
Diesel	20.2%	20.5%
SAF	47.7%	48.5%
Naphtha	7.6%	11.1%

3.4 NIPU Production

In the HL case, the PUFA-enriched fraction of FAME lipids is used as a feedstock for NIPU production. In our prior study [21], we developed a preliminary TEA model for producing NIPUs from generic TAG lipids. More recently, we engaged an engineering subcontractor (KBR) to refine the process design and equipment costing assumptions included in the NIPU model. This work incorporates the revised modeling and costing basis for NIPU production, broadly consisting of epoxidation of PUFA-enriched algae oil, carbonation of epoxides with CO_2, and polymerization of the carbonated oil with a diamine cross-linker to produce a rigid foam, depicted in Figure 5 and described in more detail below.

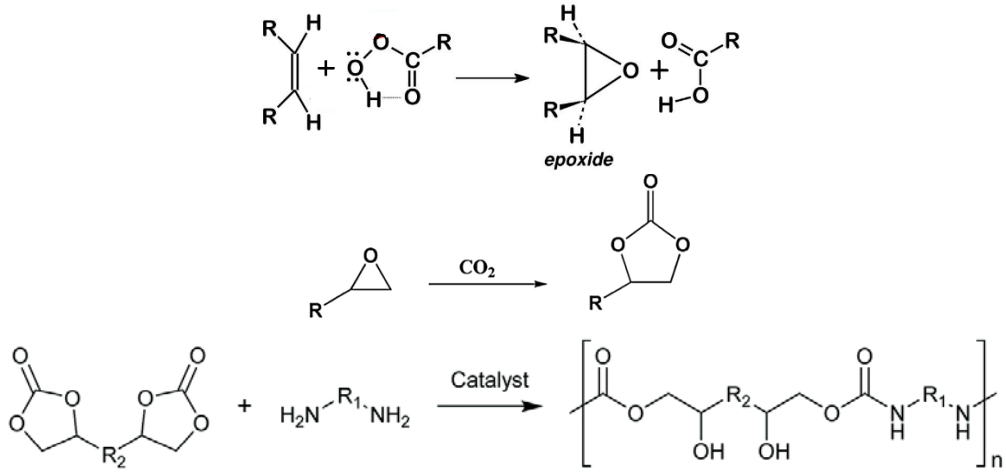

Figure 5. Chemistry underlying the epoxidation (top), carbonation (middle), and polymerization (bottom) reactions

3.4.1 Epoxidation

PUFA-enriched FAME lipids with an average double bond number of 3 are sent to a holdup tank along with acetic acid and toluene. The effluent from the holdup is combined with hydrogen

peroxide (H_2O_2), heated to 65°C, and pumped to a series of fixed-bed reactors loaded with solid ion-exchange resin catalyst. Three reactors are included in the process, with two reactors online and one in standby. This configuration allows for filtration of the catalyst in post-reaction processing and avoids the need for slurry handling and stirring during reaction. A catalyst recovery of 90% per batch is assumed. Complete conversion of double bonds to epoxides is assumed, a simplification that is relatively consistent with demonstrated experimental results showing 96% conversion [21]. Following reaction, the crude epoxide product is combined with additional toluene to allow for mixing at reduced temperatures and washed with water in a mixer settler tank. The aqueous phase from the mixer settler, containing water and acetic acid, is sent to AD, while the organic phase proceeds to a short-path evaporator to recover toluene (recycled to the mixer settler and holdup tank). The epoxide intermediate then proceeds to carbonation. A process flow diagram of the epoxidation step is shown in Figure 6, with key parameters provided in Table 10.

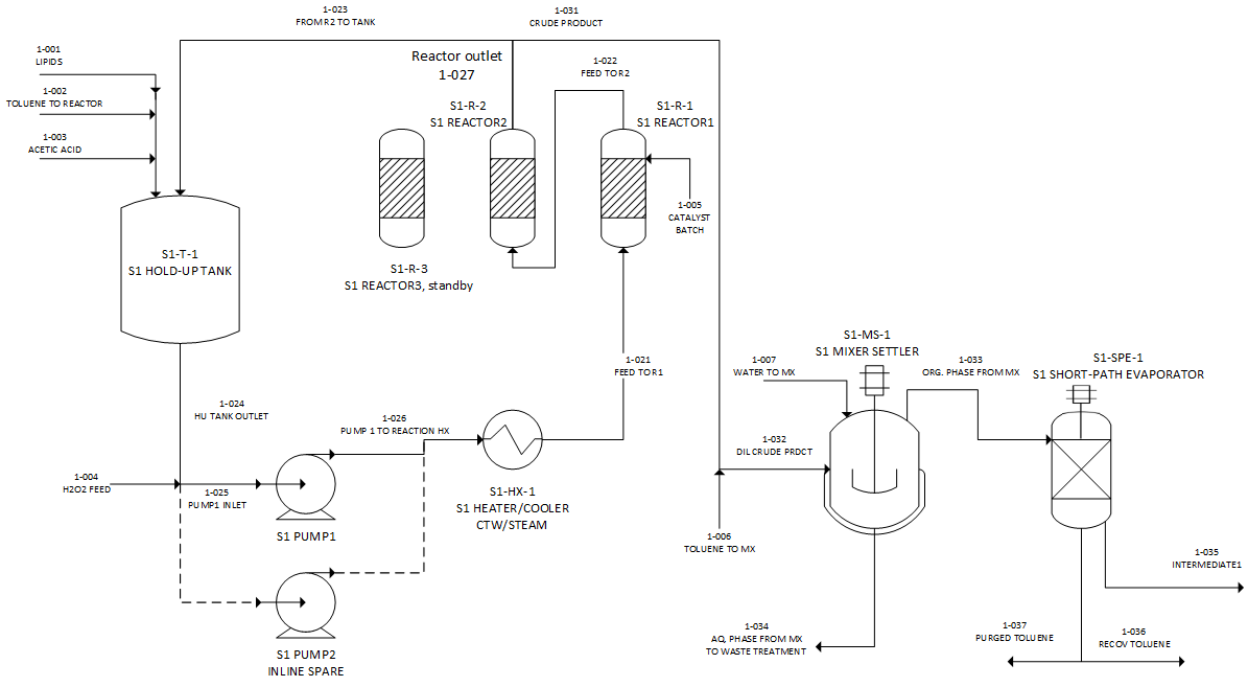

Figure 6. Process flow diagram for the epoxidation step of NIPU production

Table 10. Summary of Key Parameters for Epoxidation

Feedstock	
Lipid form	FAME lipids
Average double bonds per mole of feedstock	3.0
Epoxidation	
Reactor configuration	Batch, three fixed beds (two online, one standby)
Temperature	65°C
Pressure	1 atm
H_2O_2 loading (mol/mol double bond)	1.5 (50% excess)
Acetic acid loading (mol/mol double bond)	0.5
Catalyst	Ion-exchange resin
Catalyst loading (wt % lipid feed)	25%
Catalyst recovery per batch	90%
Toluene loading to reactor (wt % lipid feed)	50%
Toluene loading to mixer settler (wt % lipid feed)	150%
Toluene recovery	90%
Water wash ratio (water: acetic acid, w/w)	3.0
Conversion of double bonds	100%
Residence time	9 hours

3.4.2 Carbonation

In the carbonation step, epoxidized lipids are reacted with CO_2 in the presence of a heterogeneous tetrabutylammonium bromide catalyst. The CO_2 is assumed to be sourced from the same power plant flue gas as is used as an input to the algae farm, allowing for additional carbon sequestration. This reaction takes place in a batch continuous stirred-tank reactor equipped with a steam jacket and gas dispersing impeller (140°C, 500 psig). A batch time of 24 hours is assumed, which includes reaction time as well as allowance for transfer time and any cleaning required; two reactors operate at a staggered schedule 12 hours apart. Complete conversion of epoxides is assumed, again relatively consistent with demonstrated results of 96% conversion [21]. Following reaction, the carbonated oil is combined with toluene (again, to allow for mixing at reduced temperatures) and washed with water in a mixer settler tank. The aqueous phase from the mixer settler, containing water and dissolved tetrabutylammonium bromide catalyst, is sent to AD, while the organic phase is sent to another short-path evaporator to recover toluene. Tetrabutylammonium bromide has been shown to have inhibitory effects in anaerobic digestion; however, the concentration is significantly diluted to levels below 1 g/L, below the levels indicated to be inhibitory in literature [51]. If found to be necessary, this stream could also be treated prior to anaerobic digestion by various means such as use of activated carbon, membrane separation, or chemical oxidation [52], though this is not considered here. The carbonated oil then proceeds to polymerization. A process flow diagram of the carbonation step is shown in Figure 7, with key parameters provided in Table 11.

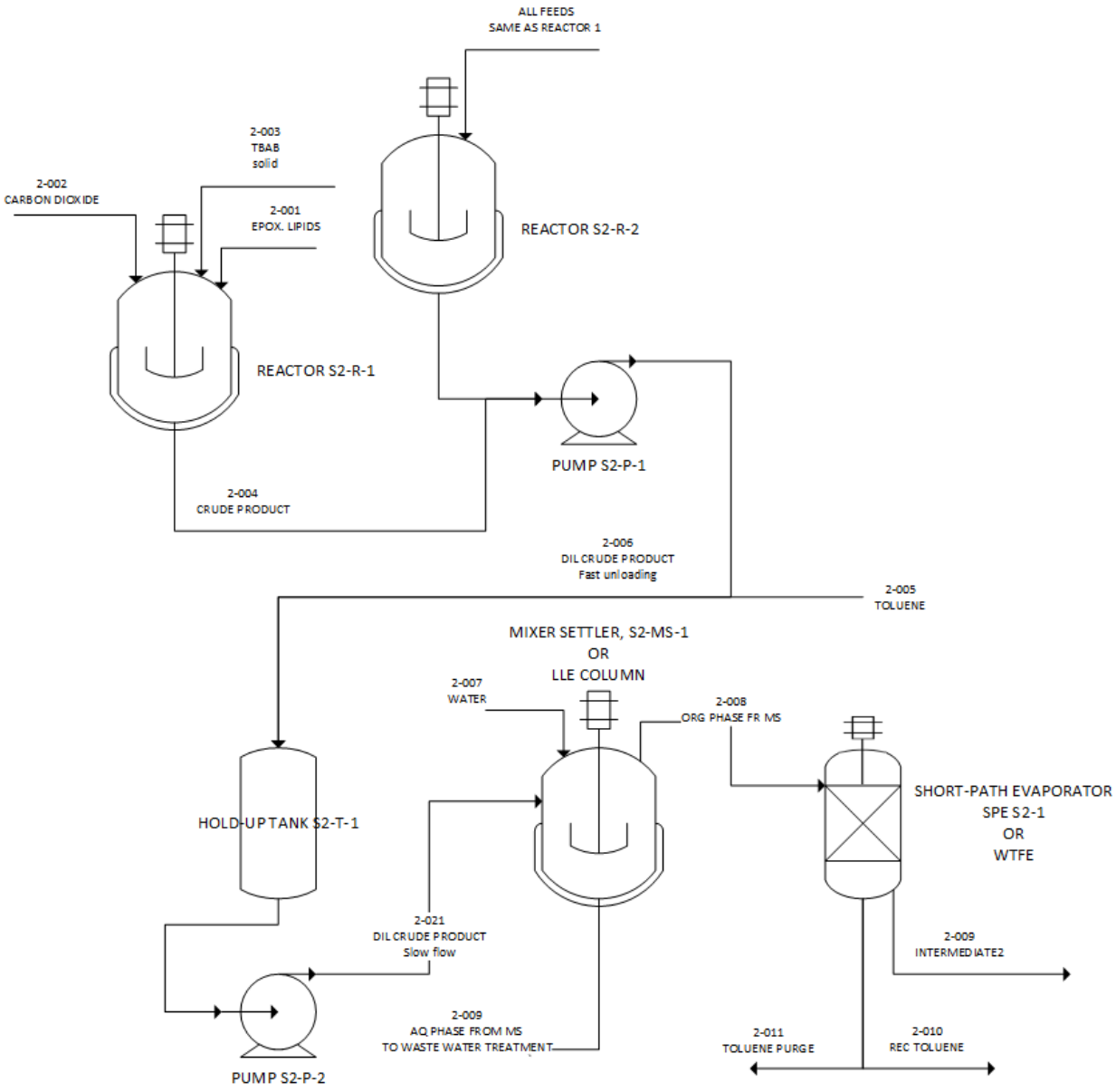

Figure 7. Process flow diagram for the carbonation step of NIPU production

Table 11. Summary of Key Parameters for Carbonation

Reactor configuration	Batch, continuous stirred-tank reactor with steam jacket and gas dispersing impellers
Temperature	140°C
Pressure	500 psig
CO_2 loading (mol/mol epoxide group)	1.1 (10% excess)
Catalyst	Tetrabutylammonium bromide
Catalyst loading (mol/mol epoxide)	0.03
Toluene loading to mixer settler (wt % lipid feed)	200%
Toluene recovery	90%
Water wash ratio (water: organic phase)	2.0
Conversion of epoxides	100%
Batch cycle time	24 hours

3.4.3 Polymerization

In the polymerization step, the carbonated oil is polymerized with ethylene diamine carbamate, which serves as a bifunctional blowing agent (this is a novel foaming method compared to what was modeled previously, which used acid and bicarbonate as a blowing agent and hexamethylene diamine as the cross-linker [21]). Ethylene diamine carbamate is produced in a separate continuous stirred-tank reactor with a gas dispersing impeller, whereby CO_2 reacts spontaneously with ethylene diamine to form the carbamate. The ethylene diamine carbamate and carbonated oil are dosed into the foam slab manufacturing line along with a catalyst (triazabicyclodecene) and surfactant. CO_2 is again assumed to be sourced from power plant flue gas, though in this case the CO_2 is outgassed during foaming and thus does not contribute to any sequestration. The foam slab manufacturing line differs from traditional PU in that it occurs at elevated temperatures (110°C) and requires a longer residence time (30 min, as opposed to 5–8 min) for curing. Accordingly, custom foam slab manufacturing equipment would have to be developed for this process. To estimate the cost of this equipment, we used the cost for a conventional foam slab line ($5,000,000 for automated equipment capable of processing 3 m/s of foam) and added a 5× cost factor. Given the significant uncertainty associated with this assumption, economic sensitivity to the foam production cost factor is considered in Section 6.3. The rigid NIPU foam is assumed to be suitable for replacing conventional PU foam and is sold at a value of $2.69/lb, consistent with a 5-year average selling price (2017–2021) of rigid PU obtained from industrial databases (converted from a value of $0.45/board foot, assuming a density of 2 lb/ft^3). A 4% loss to scrap is assumed during the foam slab formation and cutting process; scrap material is sold at half value ($1.35/lb). A process flow diagram of the polymerization step is shown in Figure 8, with key parameters provided in Table 12. Key details related to the NIPU product, as predicted by the process model, are also provided in Table 13.

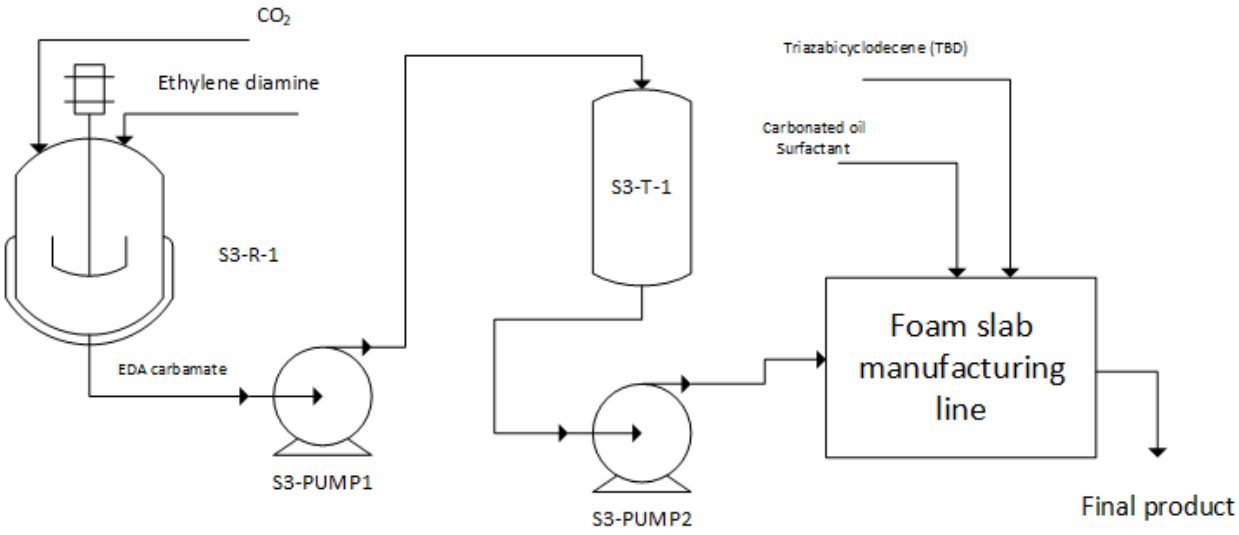

Figure 8. Process flow diagram for the polymerization step of NIPU production

Table 12. Summary of Key Parameters for Carbamate Formation and NIPU Polymerization

Carbamate Formation	
Reactor configuration	Batch, continuous stirred-tank reactor with gas dispersing impeller
Temperature	25°C
Pressure	1 atm
CO_2 absorption (w/w ethylene diamine)	0.3
Polymerization	
Reactor configuration	Automated foam slab manufacturing equipment
Temperature	110°C
Pressure	1 atm
Residence time	30 min
Diamine loading (mol/mol carbonate group)	0.5 (0% excess)
Triazabicyclodecene loading (w/w carbonated oil)	0.004125
Surfactant loading (w/w carbonated oil)	0.006305
Electricity requirement (kWh/kg product)	4.0
Foaming equipment cost factor	5.0

Table 13. NIPU Product Details, Calculated as an Output of the Process Model

	Value	Units
NIPU yield	1.80	w/w FAME
	0.14	w/w biomass (AFDW)
Contributions to polymer		
Carbonated algae oil	90.6%	wt %
FAME	61.4%	wt % of carbonated algae oil
CO_2	28.3%	wt % of carbonated algae oil
Oxygen from H_2O_2	10.3%	wt % of carbonated algae oil
Ethylene diamine	8.8%	wt %
Surfactant	0.4%	wt %
Triazabicyclodecene	0.3%	wt %
Carbon content	55.2%	wt %
Biogenic (from algae oil)	76.4%	% of carbon
Carbon from CO_2	12.4%	% of carbon
From methanol (via FAME)	4.2%	% of carbon
Carbon from other chemicals [a]	7.0%	% of carbon

[a] Ethylene diamine, triazabicyclodecene, and surfactant

3.5 Solid Coproduct

3.5.1 Solid-Liquid Separation and Drying

In the HP case, the raffinate from lipid extraction is routed to solid-liquid separation and drying. The solids are washed with water to remove residual soluble components such as sugars and salts, which can cause issues in the downstream bioplastic product process, before being dewatered to 36% solids using a vacuum belt filter press. The solids are then dried in a double-drum dryer to <10% moisture content, yielding a dry solid coproduct suitable for use in the bioplastic production process. These solids may also be suitable for use in food (i.e., human consumption) or feed (i.e., animal/aquaculture applications) applications, though the value which the solids would command in these instances vary broadly. In applications where the quality of the solids are assumed to be used for feed, the value has been assessed to be on the order of $500/ton or less [53–55]. In scenarios where a protein product is of a higher quality or purity, such as protein concentrate applications, higher values on the order of $1000-$2000/ton may be warranted [15]; however, these protein concentrates do not necessarily correspond to the extracted solids produced in this process, and further justification would be required to make these assertions.

3.5.2 Bioplastic Production

Details regarding ethylene vinyl acetate (EVA) bioplastic production were provided by industry collaborator BLOOM Materials; however, detailed information such as raw material and energy consumption were deemed confidential and were not provided. Instead, BLOOM Materials provided guidance on the value of the residual algae solids in the context of the bioplastic production process (ranging from $800 to $1,000/dry tonne [$727 to $909/dry ton], with a value of $900/dry tonne [$818/dry ton] used in the analysis). Guidance was also provided on key compositional specifications, shown in Table 14 along with the composition of the residual solids predicted by the process model. Residual algal biomass must contain sufficient protein

(>35 wt %) while limiting the content of undesirable components that interfere with the bioplastic production process, including ash, carbohydrates, lipids, sugars, salts, and moisture. Additionally, to allow for quantification of LCA results, BLOOM Materials provided an LCA of the bioplastic production process conducted by a third party. GHG emissions associated with the overall bioplastic production process, not including the carbon intensity (CI) of the residual algal solids, were provided as 1.65 kg carbon dioxide equivalent (CO_2e) per kilogram of masterbatch plastic. Approximately 0.45 kg of residual algae solids are consumed per kilogram of masterbatch plastic. The biogenic carbon content of the residual solids was estimated to be 34% based on the biochemical composition predicted by process model, resulting in a biogenic carbon content of 15% for the masterbatch plastic. This carbon content may be higher if there is significant carbon content in the ash fraction of the biomass (e.g., as $CaCO_3$); however, this is not considered here.

Table 14. Residual Solid Composition (Calculated as an Output of the Process Model) Compared to the Feedstock Specifications for the BLOOM Bioplastic Process

	Value (wt %)	Specification (wt %)
Protein	34.6%	>30%
Ash	32.7%	<35%
Carbohydrates	1.7%	<20%
Lipids	0.3%	<10%
Sugars	1.1%	Low
Salts	NQ	Low
Moisture	0.5%	<10%

In the BLOOM process, algal biomass is milled to break up cell structures and make proteins and other macromolecules in the biomass processable, and then the algal biomass is thermomechanically mixed with conventional polymers. This mixing not only denatures protein, allowing them to conform to the rheological conditions of the plastic they are being blended with and enhancing compatibility, but it also drives out moisture and allows for the establishment of polymer-to-algae intermolecular forces to develop. The thermomechanical mixing is supplemented with venting and vacuum assistance to help with moisture removal, as well as the removal of volatile constituents that might otherwise contribute to poor composite smell characteristics. After adequate mixing, the plastic melt is cut, cooled, and dried through a die face cut underwater pelletizing process to form a ready-to-use masterbatch plastic pellet that can be applied to a number of applications (assumed to displace EVA in this assessment).

Table 15. Summary of Key Parameters for the Solid-Liquid Separation, Drying, and Bioplastic Production Operations

Solid-Liquid Separation	
Solid-liquid separation equipment	Vacuum belt filter press
Flocculant loading (g/kg solids)	10
Wash ratio (L water: kg solids)	5.0
Solids content of filter cake	36 wt %
Retention of soluble components in filter cake	5%
Drying	
Drying equipment	Double-drum dryer
Heat source	Low-pressure steam
Bioplastic Production	
Residual algae solid consumption (kg/kg masterbatch plastic)	0.45
Residual algae solid selling price	$818/dry ton
Displaced product	EVA

3.6 Ancillary Operations

3.6.1 Anaerobic Digestion

In contrast to the HP compositional scenario pursuing higher-value uses of the elevated protein fraction (discussed above), the HL case maintains the use of AD to process the lipid-extracted residual biomass. Design/cost and processing details for the AD unit remain largely consistent with the detailed discussion presented in the 2014 design report [1]. In summary, raffinate from the HL lipid extraction step is combined with lipid impurities removed during downstream degumming/lipid cleanup, as well as wastewater from NIPU production, in total constituting 13.8% volatile solids (19.5% total solids) and fed to AD after cooling to 35°C. AD is operated at a hydraulic retention time (AD volume divided by volumetric throughput rate) of 20 days, translating to a volatile solids loading rate of 5.0 g/L/day. Total AD volume and cost is calculated based on a maximum size of 27 million gallons per single AD unit and scaled from a purchased cost of $6.5 million per unit as originally quoted (2012 $).

The AD unit serves to both treat wastewater generated in the CAP conversion process, as well as to support LCA benefits through combined heat and power generation and nutrient recycle. AD biogas is generated based on a fixed value of 48% volatile carbon destruction to biogas composed of 67 mol % CH_4 and the balance CO_2 (0.22 L CH_4/g volatile solids), subsequently routed to combined heat and power. AD digestate is routed to a centrifuge, with the clarified effluent recycled to upstream cultivation enabling a net 81% nitrogen and 100% phosphate recycle relative to total nitrogen/phosphate nutrient demands in the algae farm (100% phosphate recovery is achieved due to phosphoric addition in the degumming operation). In the HP case, this is reduced to 40% and 88% recycle for nitrogen and phosphate, respectively, based only on protein hydrolysis that occurs during dilute acid pretreatment and subsequent soluble component

recovery into the liquor from solid/liquid separation (no phosphoric acid is used in the HP case). Of the remaining 15% nitrogen partitioning to the AD solids sludge product after centrifugation, 40% is assumed to be bioavailable as fertilizer and sold as such for a marginal coproduct credit of $561/ton bioavailable nitrogen. Table 16 summarizes key parameters for the AD step.

Table 16. Summary of Key Parameters for AD (HL Case Only)

Temperature	35°C
Hydraulic retention time	20 days
Volatile (total) solids in AD feed (wt %)	13.8% (19.5%)
Volatile solids loading rate	5.0 g/L/day
AD heat demand	0.22 KWh/kg total solids (thermal)
AD power demand	0.085 KWh/kg total solids
Methane yield in biogas	0.22 L/g volatile solids (48% carbon destruction)
Biogas composition (mol %)	67% CH_4/33% CO_2
Nitrogen recycle in effluent	81% net (85% with 5% volatilization loss)
Phosphate recycle in effluent	100%
Bioavailable nitrogen in digestate solids	40%

3.6.2 Combined Heat and Power

Combined heat and power is employed for both the HL and HP compositional scenarios, utilizing a gas turbine coupled with heat recovery steam generator exchangers on the turbine flue gas. In the HL case, AD biogas is combined with hydrotreating off-gases, though also requiring supplemental natural gas to satisfy all biorefinery heat demands. This natural gas requirement increases in the HP case given additional heat requirements for drying along with the exclusion of AD, leaving only the hydrotreater off-gas stream. Again, the gas turbine design details are maintained consistently with those described in the 2014 design case and will not be repeated in detail here [1]. Generally, the combined gas feed stream is mixed with injection air to maintain a turbine temperature near 1,155°C prior to expansion, subsequently let down to 7 psig (1.5 atm) to allow for sufficient hydraulic pressure losses across downstream heat recovery steam generator heat exchangers and subsequent flue gas recycle/injection to the upstream cultivation ponds. Final exhaust conditions for the flue gas are maintained above 140°C. In turn, superheated steam (268°C) is raised to supply the dilute acid pretreatment stage, as well as high- and low-pressure saturated steam (260°C and 130°C) generated to meet utility steam heating requirements for lipid extraction and solvent recovery, hydrotreating, AD heating for the HL case, and NIPU upgrading or solids drying for the HL/HP cases, respectively. A steam heating efficiency of 85% is assumed for both high- and low-pressure steam. Both cases of combined heat and power result in a net power coproduct exported to the grid (equating to 4.2 and 10.7 MW for the HL and HP scenarios, respectively, after accounting for facility power demands), but require supplemental natural gas imports in order to satisfy facility steam/heat demands.

3.6.3 Storage and Utilities

Also in keeping with prior design cases, storage tanks for fuel products are included ensuring at least 7 days of product storage capacity, as well as water for fire suppression scaled from a 600,000-gallon basis according to algal feed rates. NIPU product is cured and stored in a separate warehouse capable of storing 5 days of production capacity; storage for other process inputs/outputs was costed based on a 20% balance-of-plant factor.

On-site utilities are also accounted for, including a cooling tower system to supply cooling water (i.e., for condensers and feed/product coolers), chilled water, and steam headers from the gas turbine heat recovery steam generator exchangers, as well as other minor utilities such as plant/instrument air and clean-in-place systems. A full accounting of process water balances will not be repeated in this study, as the underlying methodology to ensure water balance closures remains unchanged from prior reports. In both compositional scenarios, supplemental natural gas inputs are varied to satisfy steam/heat demands throughout the facility after optimizing heat integration via process cross-exchange; thus, excess heat availability is minimal. For power balances, in the HL case roughly 47% of the electricity generated in the gas turbine is used throughout the conversion facility to power pumps, compressors, agitators, etc. This reduces to 27% in the HP case. A breakdown of annual average power balances relative to total power generated is provided in Figure 9 for the two compositional scenarios. Additionally, a detailed breakdown of utility requirements by process by area is provided in Table A-3 and Table A-4.

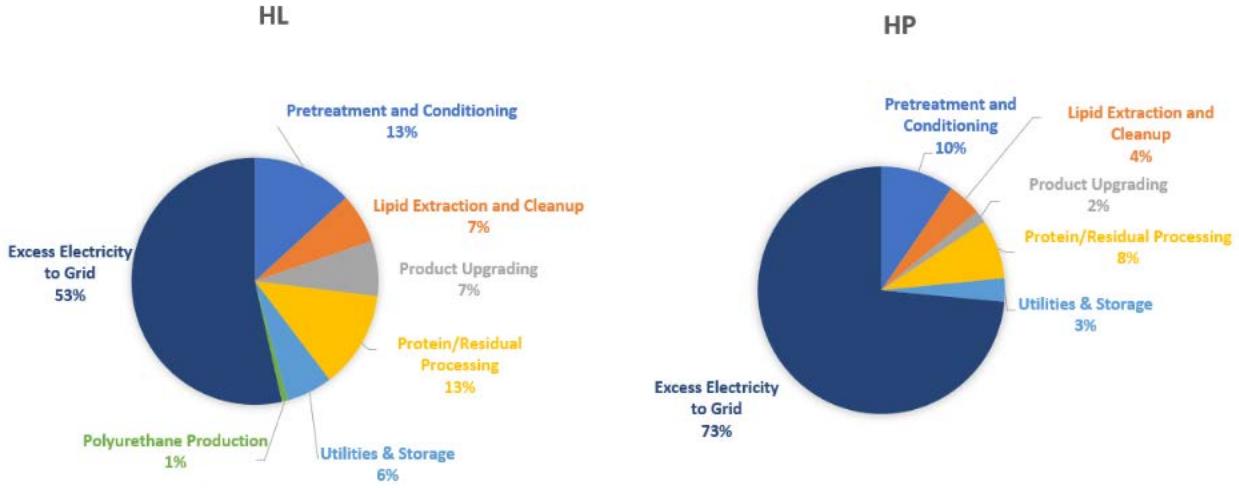

Figure 9. Average annual distribution of plant electricity utilization by process area

Total power generation for HL and HP cases is 9,076 kW and 14,538 kW, respectively.

4 Life Cycle Analysis

Argonne National Laboratory conducted the LCA to estimate the life cycle GHG emissions associated with hydrocarbon fuels processed in CAP using Argonne National Laboratory's R&D Greenhouse gases, Regulated Emissions, and Energy use in Technologies (R&D GREET) model [56]. This analysis focuses on the 100-year global warming potential, measuring estimated emissions in CO_2e through the feedstock-to-fuel supply chain. Emissions of CO_2, CH_4, and N_2O were estimated with 100-year global warming potential factors of 1, 29.8, and 273, respectively, based on guidelines from the Intergovernmental Panel on Climate Change's Sixth Assessment Report [57].

Within the CAP system, the effects of coproducts such as NIPU for the HL case and thermoplastic EVA for the HP case were addressed using several coproduct handling methods: process-level allocation (mass-based, market value/dollar-based, and energy-based), the displacement method, and the biorefinery-level method [58]. The functional unit for GHG emissions of fuels is grams of CO_2e per megajoule of fuel output, while the biorefinery-level GHG emissions were estimated in kilograms of CO_2e per tonne AFDW algal biomass that is fed to the biorefinery.

1. The process-level allocation method distributes emissions based on the mass, market value, or energy content of the fuel and non-fuel products. In this analysis, the market values are \$0.02/MJ for fuels [59], \$5.93/kg for NIPU, and \$2.30/kg for EVA. The energy contents of these products are 43.9, 31.5 [60], and 38.9 MJ/kg [61], respectively [62]. Table 17 summarizes the energy and material consumption, specifying which values in each unit operation are allocated exclusively to fuels, exclusively to non-fuel products, or allocated to both.
2. The displacement method allocates all supply chain emissions to the fuel product but provides a credit to the biofuel for the emissions avoided by producing coproducts using conventional technologies, referred to as the "*displacement credit*." It is assumed that the biomass-derived coproducts displace the fossil-derived counterparts one for one by mass.

   Note that the displacement method essentially includes the emissions reduction credit of the non-fuel coproduct. As discussed in Cai et al. [58], the fuel CI with the displacement method when the coproduct is significant may distort the fuel CI. This is especially true for the HP case because of its outsized EVA production relative to the fuel output (>90% of products by mass or energy); accordingly, displacement results are not presented for the HP case.
3. The biorefinery-level approach calculates the overall emissions from the production of both the biofuel and its coproducts, while also considering the reduction in emissions achieved by replacing conventional fuels and products with these bio-based alternatives. A biorefinery-level emissions reduction potential is estimated by comparing the biorefinery-level total emissions against those from producing the same quantities of the incumbent products.

Table 17. Overall Energy and Material Inputs and Outputs in the HL and HP Cases.

Yellow inputs contribute to fuel production only, green inputs contribute to the NIPU only, pink inputs contribute to the EVA only, and blue inputs and outputs are shared by both the fuel and biochemical products.

	HL	HP	
Products		**Production Rate**	
Hydrocarbon Fuels			
SAF	3,175	1,169	kg/h
Diesel	1,346	496	kg/h
Naphtha	508	268	kg/h
Coproducts			
Thermoplastic EVA		25,534	kg/h
PU	1,914		kg/h
Electricity export to grid	4,856	10,687	kW
Resource Consumption		**Flow Rate (kg/h)**	
Feedstock (AFDW basis)	13,502	16,805	
Pretreatment and Conditioning			
Sulfuric acid (as pure)	552	687	
Ammonia	192	239	
Lipid Extraction and Cleanup			
Hexane	146	151	
Ethanol	166	198	
Caustic		106	
Phosphoric acid	148	0	
Silica	8		
Clay	16		
Methanol	1,614	607	
Sulfuric acid (as pure)	512	354	
Product Upgrading			
Hydrogen	228	81	
Catalyst (1% Pt/SAPO-11)	0.4	0.2	
Protein/Residual Processing			
Flocculant		115	
Thermoplastic: Algae milling		25,534	
Thermoplastic: EVA		25,534	
Thermoplastic: Compounding		25,534	
Thermoplastic: Water		25,534	
Thermoplastic: Wastewater		25,534	
Thermoplastic: Scrap		25,534	
PU Production			
Toluene	127		
Acetic acid	335		
H_2O_2	569		
Ion-exchange resin	27		
CO_2 (carbonation)	540		
Tetrabutylammonium bromide catalyst	54		
Toluene	63		
CO_2 (foaming)	50		
Ethylene diamine	168		
Triazabicyclodecene	5		

	HL	HP	
Surfactant	8		
Other Resource Consumption			
Process water (total)	33,103	85,898	kg/h
Natural gas (total)	29	229	MMBtu/h
Common operations	13	65	MMBtu/h
Fuel and PU	13	74	MMBtu/h
Fuel only	2	3	MMBtu/h
PU only	2		MMBtu/h
Solid coproduct only		86	MMBtu/h
Output Streams	**Flow Rate (kg/h)**		
Digestate (bioavailable nitrogen)	63		
Ammonia	243	571	
Diammonium phosphate	96	758	
Recycle water	33,738	124,035	
CO_2 Recycle			
CO_2 (biogenic)	6,381	118	
CO_2 (fossil)	3,715	12,975	

5 Process Economics

5.1 Total Capital Investment

All details regarding TEA methodologies for applying capital and operating expenses to solve for MFSP remain unchanged from prior NREL reports and will not be repeated here [1,2]. Purchased and installed capital costs reflect design/costing guidance recently furnished from KBR for NIPU upgrading as noted above, while costs for the rest of the processing steps were scaled from prior estimates documented previously [1,6,7], using a standard cost scaling expression as a function of size (typically dictated by throughput) and scaling exponent *n*:

$$New\ Cost = (Base\ Cost) \times (New\ Size/Base\ Size)^n$$

Costs for residual protein valorization to bioplastics were estimated based on inputs from BLOOM Materials. After obtaining scaled installed costs for pertinent equipment items, additional direct and indirect costs are added based on consistent cost factors as in prior analyses, with exception of NIPU warehouse storage, which was costed separately given that this is a unique product requiring a dedicated space for curing and incurring substantial volume swell from the foaming operation. NIPU storage costs were added based on a correlation with NIPU hourly production rate, based on a prior engineering subcontract with Nexant. Key assumptions factored into the correlation include sizing for 5 days of storage, a warehouse cost of \$110/ft^2, standard-sized rigid NIPU panels (4 ft × 8 ft × 2 in) with a density of 2 lb/ft^3, and a cure time of 18 hours. Total installed equipment costs are roughly 40% higher for the HL case, although with added NIPU storage costs the resulting total capital investment becomes roughly 45% higher in the HL case compared to HP biomass. However, given significantly higher fuel yields achievable from HL biomass, total capital investment per annual GGE fuel output is nearly half that of the HP basis.

Table 18. Capital Cost Summary for Each Scenario

Area	HL (317 tonne/day AFDW feed)	HP (396 tonne/day AFDW feed)
A100: Pretreatment and Conditioning	$8,423,000	$9,882,000
A300: Lipid Extraction and Cleanup	$32,208,000	$16,977,000
A400: Product Upgrading	$11,395,000	$5,430,000
A500: Protein/Residual Processing	$4,891,000	$28,711,000
A600: Combined Heat and Power	$6,031,000	$9,042,000
A700: Utilities & Storage	$3,774,000	$3,191,000
A800: Polyurethane Production	$35,879,000	$0
Total Installed Equipment Cost	**$102,601,000**	**$73,233,000**
Warehouse (excluding NIPU)	4% of inside battery limits [a]	
Warehouse (NIPU)	$2,548 × NIPU [b]	N/A
Site development	9% of inside battery limits	
Additional piping	5% of inside battery limits	
Total Direct Costs	**$122,282,000**	**$83,907,000**
Proratable expenses	10% of total direct costs	
Field expenses	10% of total direct costs	
Home office and construction fee	20% of total direct costs	
Project contingency	10% of total direct costs	
Other costs (e.g., startup, permits)	10% of total direct costs	
Total Indirect Costs	**$73,369,000**	**$50,344,000**
Fixed Capital Investment	**$195,651,000**	**$134,252,000**
Land	$140,000	$140,000
Working capital	5% of fixed capital investment	
Total Capital Investment	**$205,573,000**	**$141,105,000**
Installed equipment cost/annual GGE	$7.18	$13.32
Total capital investment/annual GGE	$14.38	$25.67

[a] A100, A300, A400, A500, and A800.

[b] Costed at a rate of $2,548 × kg/h NIPU production rate, based on inputs from engineering subcontractor (Nexant).

5.2 Variable Operating Costs

5.2.1 Raw Materials and Waste/Product Outputs

Also consistent with prior reports, all methodologies regarding variable operating costs are applied consistently in the present study. This includes handling variable operating costs on a seasonal basis, although costs remain relatively steady given the use of upstream wet storage to eliminate seasonal flow fluctuations (only imparting some differences due to compositional degradation in storage). All input/output unit costs and their resulting contributions to MFSP are summarized in Table 19.

Table 19. Modeling Assumptions for Raw Material Costs, Recycle Credit Values, and Product Values

Raw Material	Cost (2020 $)	Unit	MFSP Contribution ($/GGE) HL	MFSP Contribution ($/GGE) HP
Feedstock				
Biomass from algae farm (HL/HP)	$691/$688	$/ton AFDW	$5.70	$18.37
Pretreatment				
Sulfuric acid	$116	$/ton	$0.04	$0.14
Ammonia	$885	$/ton	$0.10	$0.34
Lipid Extraction/Cleanup + HDO/HI				
Hexane	$1,251	$/ton	$0.11	$0.30
Ethanol	$2.53	$/gal	$0.08	$0.24
Caustic	$516	$/ton	N/A	$0.09
Phosphoric acid	$825	$/ton	$0.07	N/A
Silica	$2,293	$/ton	$0.01	N/A
Clay	$688	$/ton	$0.01	N/A
Methanol	$272	$/ton	$0.27	$0.26
Sulfuric acid	$116	$/ton	$0.04	$0.07
Hydrogen	$1,537	$/ton	$0.21	$0.20
HDO/HI catalyst	$720,897	$/ton	$0.13	$0.12
Solid/Liquid Separation				
Flocculant	$2,293	$/ton	N/A	$0.42
Utilities/Combined Heat and Power				
Natural gas	$4.10	$/MMBtu	$0.07	$1.35
Process water	$0.33	$/ton	$0.01	$0.05
NIPU Upgrading				
Toluene	$715	$/ton	$0.08	N/A
Acetic acid	$592	$/ton	$0.12	N/A
H_2O_2	$974	$/ton	$0.34	N/A
Ion-exchange resin	$6,575	$/ton	$0.11	N/A
CO_2	$42	$/ton	$0.01	N/A
Tetrabutylammonium bromide catalyst	$3,288	$/ton	$0.11	N/A
Ethylene diamine	$2,531	$/ton	$0.26	N/A
Triazabicyclodecene catalyst	$491	$/ton	$0.001	N/A
Surfactant	$393	$/ton	$0.002	N/A
Recycle Credits	**Value**	**Unit**		
Nitrogen (as ammonia)	$885	$/ton NH_3	−$0.13	−$0.80
Phosphorus (as diammonium phosphate)	$722	$/ton diammonium phosphate	−$0.04	−$0.87
CO_2	$42	$/ton	−$0.26	−$0.86
Product	**Value**	**Unit**		
Diesel-range fuel	$3.41	$/gal [a]	N/A	N/A
Jet-range fuel	$1.87	$/gal [a]	N/A	N/A
Naphtha-range fuel	$2.98	$/gal [a]	N/A	N/A
Electricity to grid	$0.0572	$/kWh	−$0.15	−$0.88
AD sludge	$561	$/ton bioavailable nitrogen	−$0.02	N/A
PU	$5,380	$/ton	−$6.16	N/A
Solid coproduct (thermoplastic co-feed)	$818	$/ton	N/A	−$14.92

[a] U.S. Energy Information Administration 2018–2022 [59]. Fuel market values are not used in calculating MFSPs (MFSP is solved for on a total $/GGE combined fuel basis), but are considered in calculation of (1) internal rate of return (IRR) metrics as an alternative to MFSP, (2) LCA metrics with market-based allocations, and (3) marginal cost of GHG abatement.

5.2.2 Policy Incentives

In addition to MFSP estimates for the process concepts in isolation, economic implications with the inclusion of renewable fuel policy credits were also considered. The policy incentive landscape in the United States is continually changing; some policy incentives, such as tax credits for biodiesel blending, have expired, lapsed, and been renewed (in some cases retroactively) numerous times. Several policies are set to expire at the end of 2025, including blenders tax credits for gasoline, diesel, and SAF (26 U.S. Code § 40, 40A, and 40B) as well as the second-generation biofuel producer credit (26 U.S. Code § 40), after which they will be replaced by the Clean Fuel Production Credit (26 U.S. Code § 45Z). However, it is impossible to speculate if some or all of these credits will be renewed again in the future. To simplify the policy incentives considered in this analysis, we have excluded policy incentives expiring in 2025 and included the 45Z Clean Fuel Production Credit. Other policy incentives considered include D4 and D5 renewable identification number (RIN) credits and 45Q credits (administered at the federal level) and Low Carbon Fuel Standard (LCFS) credits (administered at a local level, with credit values and rules assumed to be consistent with the California LCFS). There are no known limitations on double counting any of these credits. A summary of the policy credits considered is shown in Table 20.

Each of the policy incentives considered has its own rules on qualification and valuation of credits. For D4 and D5 RIN credits, a minimum GHG reduction of 50% must be demonstrated relative to the petroleum baseline to qualify for credits. LCFS credits are earned for any fuel demonstrating a reduction compared to the petroleum baseline, and generation is proportional to the demonstrated GHG reduction compared to petroleum fuels, with no set limit for negative CI values; thus, there are increased financial incentives for demonstrating increasingly low fuel CI values. In contrast, RIN credits are generated at a flat rate based on the volume of fuel produced. The Clean Fuel Production Credit value will vary based on the fuel produced, as well as the fuel CI demonstrated; a credit of $1.75/gal for SAF or $1.00/gal for other transportation fuels can be earned for a 100% CI reduction (0 g CO_2e/MJ or less). These values decrease linearly until a CI of 50 kg CO_2e/MMBtu (47.4 g CO_2e/MJ, roughly equivalent to a 50% GHG reduction), after which no credits are earned. There are no minimum GHG reduction requirements for 45Q carbon sequestration credits, which are earned based on the sequestration of CO_2 from industrial and power generation facilities of a sufficient size (producing >12,500 tonnes of CO_2/year, surpassed in all modeled cases). The value of the 45Q credits is assumed to be $60/tonne CO_2, credited for carbon which is captured and subsequently utilized in products (which in these cases includes fuels, NIPU, and/or thermoplastics).

The duration for which each credit is active also varies. LCFS and RIN credits have no set expiration date, while 45Q credits are specified to be active for 12 years. The duration of the Clean Fuel Production Credit is less clear. As written, the credit is set to expire after 3 years; however, the fuel credits that it is set to replace have been in place for much longer time periods (e.g., the biodiesel blenders tax credit has been active since 2005 and has been renewed at least 7 times). Here, we assume a duration of 3 years for the Clean Fuel Production Credit and examine variations of this duration in Section 6.3.

It should also be noted that although many of the policy incentives are specified as a “tax credit,” certain provisions may exist that allow for a direct payment in the event that the credits exceed the tax liability of the fuel producer. Alternatively, for larger commercial entities, tax liability

from related ventures may be leveraged to earn the tax credit if sufficient tax liability is not generated directly from the biorefinery. For simplicity, this analysis assumes all policy credits take the form of direct revenue, while tax liability is calculated separately.

Table 20. Modeled Policy Credit Values and Length of Duration for the Base Case, as Well as Required GHG Reduction Threshold at Which the Policy Becomes Applicable

Policy Incentive	Base Value	Duration (years)	Minimum GHG Reduction	Reference
LCFS credits	\$132/tonne CO_2 reduction	Life of plant	None [a]	California LCFS; 5-year average (2019–2023)
D4 RIN credits	\$1.08/gal ethanol equivalent (applies to diesel and SAF)	Life of plant	50% [b]	Renewable Fuel Standard; D4 5-year average (2019–2023)
D5 RIN credits	\$1.08/gal ethanol equivalent (applies to naphtha only)	Life of plant	50% [b]	Renewable Fuel Standard; D5 5-year average (2019–2023)
45Q credits	\$60/tonne CO_2 captured from an industrial source and utilized	12	n/a	26 U.S. Code § 45Q
45Z Clean Fuel Production Credit [c]	Up to \$1.75/gal SAF Up to \$1.00/gal non-SAF	5	CI value of 47.4 gCO_2e (~50% reduction)	26 U.S. Code § 45Z

[a] Baseline values for each fuel vary by year and are established by the California Air Resource Board through the year 2030 [63]; values are assumed to continually decrease on the same linear trend for the life of the plant

[b] Baseline values for each fuel are constant and are established by the U.S. Environmental Protection Agency [64]; conventional fuel GHG baselines are 93.1 gCO2e/MJ for gasoline/naphtha and 91.9 gCO2e/MJ for diesel and jet fuel

[c] Varies linearly based on GHG reduction; the full amount is applied at a CI of 0 g CO_2e/MJ or less (100% reduction versus petroleum), decreasing linearly to 0 at a CI of 47.4 g CO_2e/MJ.

5.3 Fixed Operating Costs

Finally, fixed operating cost assumptions are largely maintained consistently with prior reports, but updating as appropriate for the operations included. Table 21 summarizes all fixed operating costs for both compositional scenarios. Labor costs are higher for the HL case owing to more substantial labor requirements for NIPU processing, reflecting multiple reaction steps and labor-intensive logistical operations for foam slab cutting, movement, and storage, following guidance from engineering subcontractors.

Table 21. Fixed Operating Costs and MFSP Contributions for HL/HP Compositional Scenarios

Position	2020 Salary	# Required	2020 Cost	MM$/yr (2020 $)	HL ¢/GGE (2020 $)	HP ¢/GGE (2020 $)
Labor and Supervision						
Plant manager	188,535	1	188,535			
Plant engineer	89,779	2	179,557			
Maintenance supervisor	73,106	1	73,106			
Maintenance technician	51,302	5	256,511			
Lab manager	71,823	1	71,823			
Lab tech	51,302	2	102,604			
Shift supervisor	61,563	2	123,125			
Shift operators	51,302	9	461,719			
Shift supervisor – NIPU	61,563	2 (HL)	123,125 [a]			
Shift operators – NIPU	51,302	12 (HL)	615,626 [a]			
Laborers – NIPU	35,911	30 (HL)	1,077,345 [a]			
Yard employees	35,911	2	71,823			
Clerks and secretaries	46,172	2	92,344			
Total salaries			(HL/HP)	3.44/1.62	24.0	29.5
Labor burden (90%)			(HL/HP)	3.09/1.46	21.6	26.5
Other Overhead			**HL MM$/yr**	**HP MM$/yr**	**HL ¢/GGE**	**HP ¢/GGE**
Maintenance	3.0% of inside battery limits		2.78	1.83	19.5	33.3
Property insurance	0.7% of fixed capital investment		1.37	0.94	9.6	17.1
Total Fixed Operating Costs			**10.68**	**5.85**	**74.7**	**106.4**

[a] Applies to HL case only.

5.4 Discounted Cash Flow Analysis and MFSP

5.4.1 Discount Rate, Equity Financing, and Other Financial Metrics

Also in keeping with capital and operating cost details discussed above, the overall methodology for integrating capital and operating costs into an engineering cash flow analysis remains consistent with prior reports, as do the majority of underlying economic/financial assumptions [1,2], while adding several additional layers of analysis including LCA-based policy incentives and marginal GHG abatement costs. All TEA calculations performed here maintain the basis of n^{th}-plant technology maturity, avoiding cost inflations typically expected to be incurred for pioneer plant facilities related to equipment overdesign/redundancies, operational reliability/on-stream time, labor expenses, financing costs, target rate of return, etc. On the latter, a 10% discount rate is maintained here as the IRR required to achieve zero net present value in order to solve for the required MFSP. While the focus within the fuel product category is on maximizing SAF production, for purposes of calculating MFSPs all fuel products are combined into total

GGE based on their lower heating values, coupled with a standard gasoline reference value of 116,090 Btu/gal [65]. Alternatively, given the substantial influence exerted by coproduct revenues and policy incentives in reducing the MFSPs for both compositional scenarios, we also calculate the facility IRR associated with selling all fuels and products at their respective market values.

The economic analysis maintains a basis of 40% equity/60% debt financing with a 10-year loan at 8% interest rate, 30-year total facility lifetime preceded by 3 years of construction, and 21% federal income tax rate. All costs are adjusted to 2020 dollars using the same methods for cost-year inflation as in prior reports, namely scaling capital costs by the Plant Cost Index published by *Chemical Engineering Magazine*, input/output material costs based on the chemical manufacturing Producer Price Index published by the U.S. Bureau of Labor Statistics, and labor costs based on U.S. Bureau of Labor Statistics labor indices [66–68].

6 Analysis and Discussion

6.1 Base Case Results

6.1.1 LCA Results

Figure 10 shows the supply chain GHG emissions of fuels produced via HL and HP using the process-level allocation method for coproduct handling, along with their key contributing processes, in comparison to the CI benchmark of 89 g CO_2e/MJ for petroleum jet fuels [69]. With the process-level allocation method, fuels produced via the HL approach exhibit GHG emissions ranging from 21.6 to 40.8 g CO_2e/MJ, which represents a reduction of 54%–76% compared to that of petroleum jet fuels. In contrast, fuels in the HP case have a much higher CI of 89.8–96.2 g CO_2e/MJ.

In the HL case, the fuel's CI is 38.6 g CO_2e/MJ when using a mass-based allocation factor, while market-based allocation results in a lower CI of 21.6 g CO_2e/MJ. The energy-based allocation factor for fuels is 79% (i.e. fuels account for 79% of the total outputs based on energy content), leading to the highest CI of 40.8 g CO_2e/MJ among the methods assessed. When the displacement method is applied to address the NIPU coproduct, which accounts for about 28% of the total product slate by mass, all emissions and energy burdens are allocated to the fuels. However, NIPU coproducts subsequently contribute a displacement credit of 42.9 g CO_2e that reduces the CI for the fuels to 21.9 g CO_2e/MJ.

In the HP case, fuels are produced in a much smaller proportion, comprising only 7% of total finished products by mass. Fuels also account for just 2.6% of the market share and 8% based on energy content. The CI of the fuel outputs ranges from 89.8 to 96.2 g CO_2e/MJ with the process-level allocation method, using mass, market value, or energy as the allocation basis.

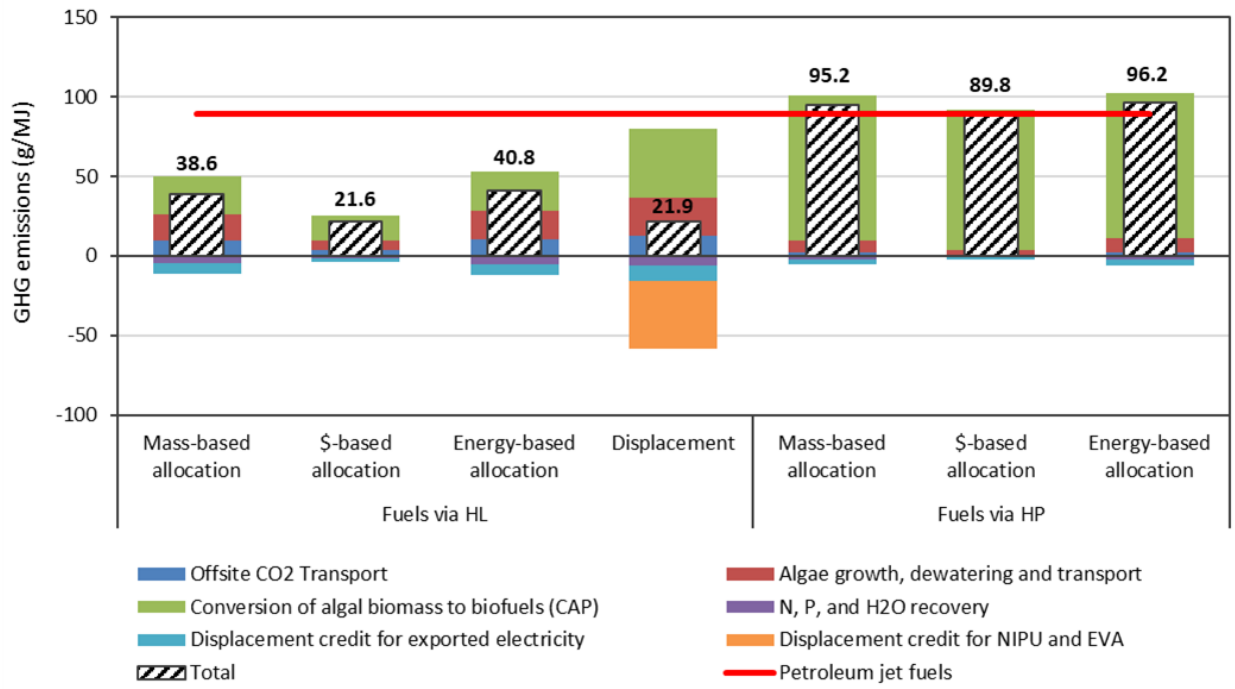

Figure 10. Supply chain GHG emissions of fuels via CAP, using the process-level allocation method, in comparison to 89 g CO_2e/MJ for petroleum jet fuels

The biorefinery-level GHG emissions of CAP via HL and HP are shown in Figure 11(c), in comparison to reference benchmarks for fossil-based fuels, rigid PU foam and EVA. The total emissions associated with the biorefinery are estimated in kilograms CO_2e per tonne AFDW. Additionally, the emissions for "*Conventional*" products were calculated for an equivalent quantity of products produced by the biorefinery, as summarized in Figure 11(a), based on the CIs of conventional counterparts, as shown in Figure 11(b). In addition to the total life cycle GHG emissions associated with all the process energy and materials in the biorefinery, both biorefinery designs produce bioproducts (i.e., NIPU and EVA), which are considered durable bioproducts that could sequester biogenic carbon originating from the algal biomass feedstock, representing a carbon removal credit. Specifically, NIPU from the HL case contains 55 wt % of biogenic carbon and CO_2, representing a sequestration credit equal to 1.79 kg CO_2e per kilogram of NIPU; meanwhile, EVA sequesters an additional 15 wt % of biogenic carbon, or 0.56 kg CO_2e per kilogram of EVA. Overall, the biorefinery-level GHG emissions from HL are71% lower than those from HP, based on net GHG emissions of 955 and 3,349 kg CO_2e/tonne AFDW, respectively. Both process designs demonstrate a significant reduction at the biorefinery level over the conventional production processes, reducing emissions by 1,106 and 1,057 kg CO_2e/tonne AFDW, respectively, for the HL and HP cases compared to conventional fuel and product benchmarks (a reduction by 54% and 24%, respectively).

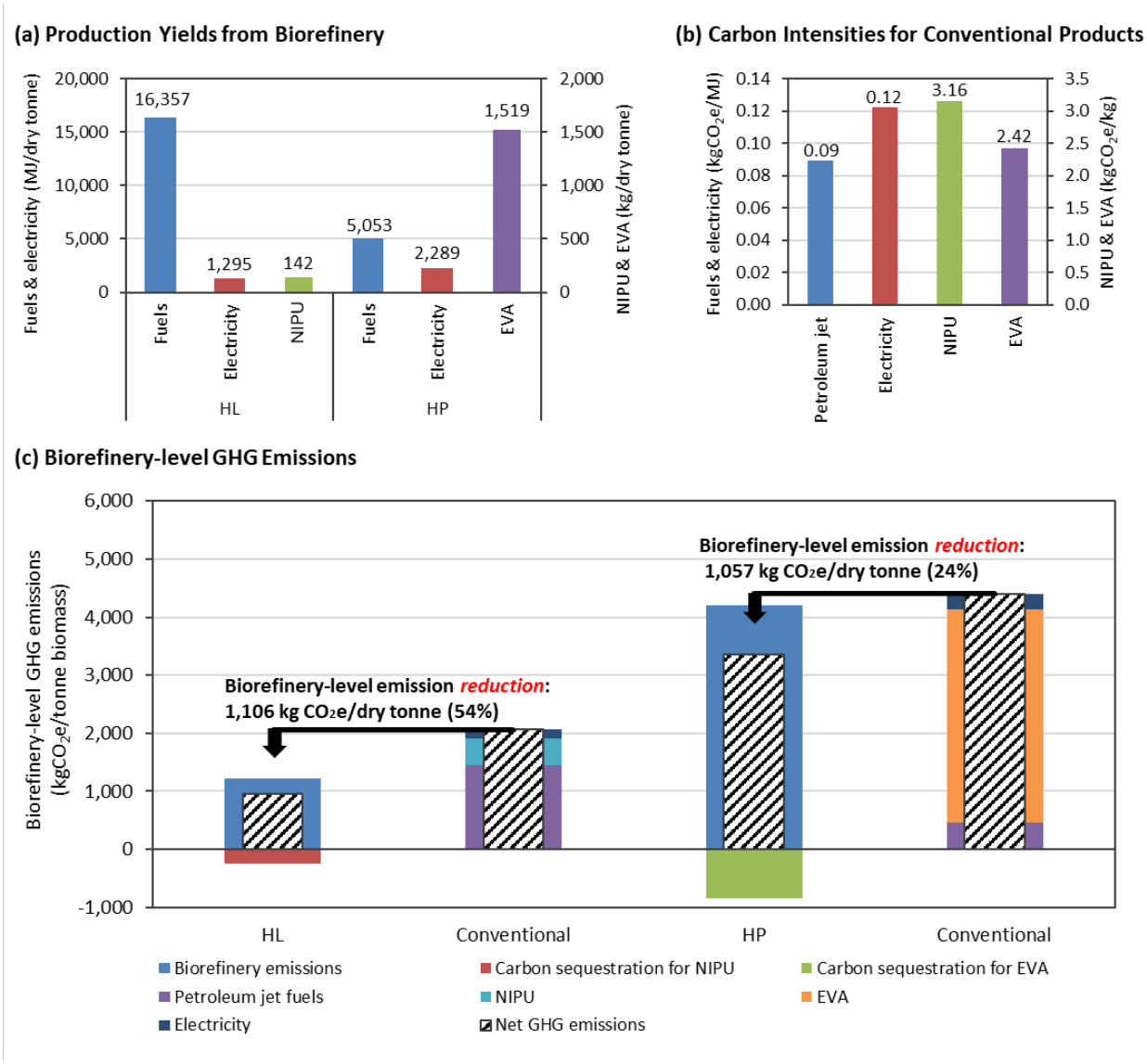

Figure 11. Biorefinery-level GHG emissions reduction (kg CO_2e/ton AFDW; panel c) as influenced by (a) the production yields from the biorefinery and (b) the carbon intensities for conventional products

6.1.2 TEA Results

The base case TEA results are presented in Table 22, alongside corresponding GHG emissions as pertinent to calculating policy incentive credits. The HL case in particular reflects promising economics even without inclusion of policy credits at an MFSP of $3.68/GGE, owing to a very high fuel yield of approximately 121 GGE/ton AFDW biomass from the algae farm after diverting 15% of the lipids to NIPU coproduction. A single HL algae biorefinery at the base case scale produces 14.3 million GGE/year of total fuel, 63% of which is SAF, alongside 27% diesel and 10% naphtha-range fuels. Extending this fuel yield to a national-scale potential (assuming the same total algal biomass potential of 152 million tons/year AFDW as reported in the above-referenced 2022 harmonization report and scaling down to a productivity of 20 g/m^2/day assumed in this study, versus the average projected target productivity of 26.2 g/m^2/day spanning

the collection of farm sites reflected in the harmonization report) [15]) results in a total fuel potential of 14.1 *billion* GGE/year, or 8.3 billion gallons of SAF per year, for the continental United States. This potential compares very favorably to the production goals laid out in the SAF Grand Challenge, which include 3 billion gallons of SAF per year by 2030 and 35 billion gallons per year by 2050. As is typical with HP algae focused on fuel production [15], the HP scenario reflects more challenging economics at an MFSP of $7.92/GGE prior to consideration of policy incentives, driven by roughly threefold lower fuel yields of roughly 38 GGE/ton AFDW. This scenario enables a fuel output of 5.5 million GGE/year with a roughly similar fuel product breakdown as the HL case. Similarly extrapolating this fuel yield to a national level yields a total fuel production potential of 5.4 billion GGE/year (3.1 billion gallons of SAF per year) for the continental United States [15].

In either case, also as typical for algal conversion pathways [1,70], biomass feedstock represents the large majority of MFSP allocations, contributing $5.27/GGE (net, after accounting for nutrient/CO_2 recycle credits) out of $7.91/GGE prior to coproduct/policy reductions in the HL case, or $15.84/GGE out of $20.62/GGE for the same basis in the HP case (Figure 12). Feedstock (and conversion) contributions to MFSP in Figure 12 are so much higher in the HP case due to the lower fuel yield, as the algal biomass costs are nearly identical between HL and HP biomass (higher cultivation productivity for HP biomass is offset by higher nutrient demands at elevated nitrogen/phosphorus content). In both cases, coproduct credits provide substantial revenues to lower net MFSPs, with NIPU production enabling a net $4.23/GGE MFSP reduction in the HL case (including fully burdened costs for the NIPU processing operations), and bioplastics providing a $12.70/GGE reduction in the HP case (including costs for residual solids separation and drying but excluding downstream costs for upgrading to the bioplastic polymer).

Table 22. Key Results for the TEA and GHG Assessment

	Units	HL	HP
MFSP (no policy incentives)	**$/GGE**	**$3.68**	**$7.92**
MFSP (with policy incentives)	**$/GGE**	**$0.45**	**$6.61**
IRR (with policy incentives) [a]	%	26.0%	n/a
Fuel CI			
Displacement	**g CO_2e/MJ**	**21.9**	
Mass	**g CO_2e/MJ**	**38.6**	**95.2**
Market	**g CO_2e/MJ**	**21.6**	**89.8**
Energy	**g CO_2e/MJ**	**40.8**	**96.2**
Total fuel yield	**GGE/ton algae (AFDW)**	**121.3**	**37.5**
Total fuel production	MM GGE/year	14.3	5.5
Fuel breakdown:			
Diesel	%	27%	26%
SAF	**%**	**63%**	**60%**
Naphtha	%	10%	14%
Minimum biomass selling price	$/ton AFDW	691	688
Biomass feed rate (seasonal average)	ton/day AFDW	357	445
Total capital investment	MM $	$541	$483
Cultivation	MM $	$335	$342
Conversion	MM $	$206	$141
Variable operating costs	MM $/yr	$134	$157
Cultivation [b]	MM $/yr	$27 ($21)	$46 ($32)
Conversion	MM $/yr	$113	$125
Fixed operating costs	MM $/yr	$22	$17
Cultivation	MM $/yr	$11	$12
Conversion	MM $/yr	$11	$6
Average fuel, coproduct, and policy revenue [a]	MM $/yr	$161	$102
Revenue breakdown: [a]			
Fuels	%	19.6%	12.0%
Solid coproduct [c]	%	0.2%	79.4%
PU	%	54.3%	0.0%
Electricity	%	1.4%	4.7%
Policy credits	%	24.6%	3.8%

[a] Fuels are valued at market value for calculation of IRR and revenue values (see Table 19).

[b] First value represents gross cost of nutrients and CO_2; value in parentheses represents net costs after nutrient and CO_2 recycle.

[c] Includes revenue from land application of anaerobic digestate in HL case.

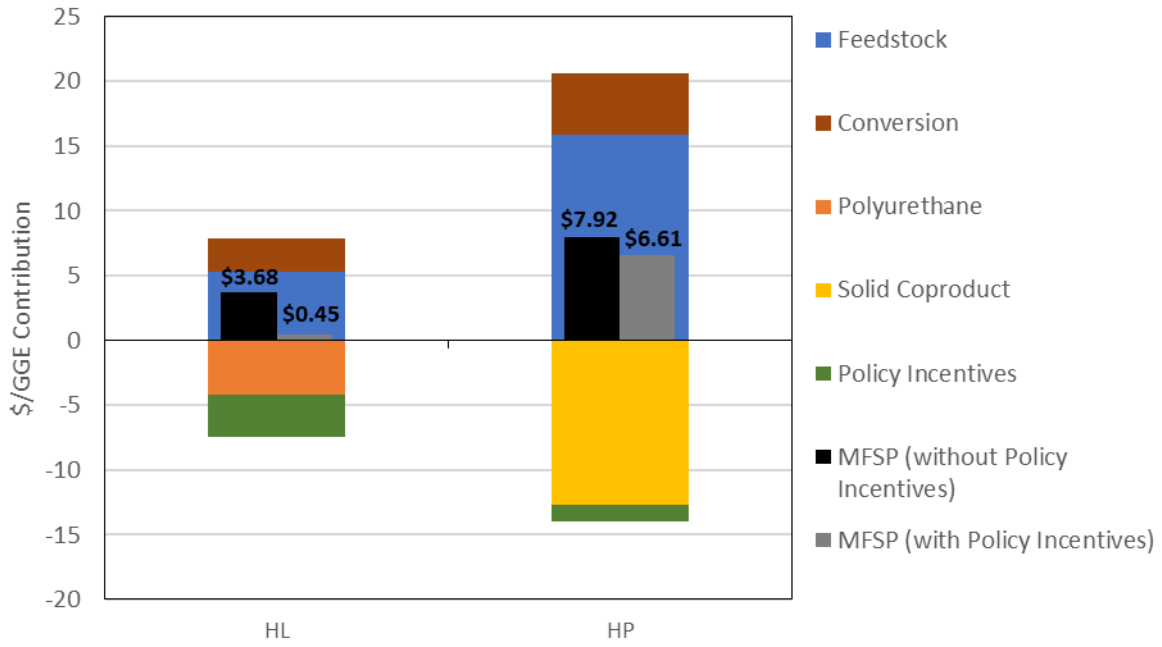

Figure 12. Cost breakdown of the MFSP for each case.

Black bars represent MFSP without policy incentives; gray bars represent MFSP inclusive of revenues generated from policy incentives, including LCFS, RINs, 45Q, and the Clean Fuel Production Credit. "Conversion" excludes costs and revenues specifically related to coproducts or policy incentives.

The TEA results for both cases improve upon inclusion of policy incentives, particularly in the HL case. When including applicable policy incentives based on GHG reductions from petroleum benchmarks as described in Section 5.2.2, the MFSP for the HL case reduces by an additional $3.23/GGE, reaching a net MFSP of $0.45/GGE. Alternatively, as shown in Table 22, this translates to a 26% biorefinery IRR when selling all fuels and coproducts at market values upon the inclusion of coproduct incentives, with the majority of revenue (54%) stemming from the NIPU coproduct, followed by policy credits (25%) and then fuels (20%). Figure 13 shows that policy credits for the HL scenario are driven primarily by LCFS and RIN credits. These policy credits are based on the displacement method for LCA coproduct handling, which reflects among the lowest GHG intensities for the fuel product in the HL case. However, MFSP results are relatively similar when using alternative LCA methodologies, including mass allocation ($0.85/GGE, with policy incentives contributing −$2.83/GGE), market allocation ($0.44/GGE, with policy incentives contributing −$3.24/GGE), and energy allocation ($0.90/GGE, with policy incentives contributing −$2.78/GGE).

In contrast, policy incentives earned by the HP feedstock case are lower, reducing the MFSP by $1.31/GGE to a value of $6.61/GGE (based on the mass allocation LCA method, though results are consistent for all allocation methods considered). This is because the fuel CI in the HP case fails to generate policy incentives, which are contingent on demonstrating a 50% reduction compared to petroleum fuels. The only policy incentives generated are 45Q credits, which are based purely on capturing and utilizing industrial CO_2 and are earned irrespective of process CI. As shown in Figure 13, the 45Q credits earned in the HP case exceed those in the HL case on a

$/GGE basis; however, this is purely an artifact of lower fuel yields, and the total revenue generated from 45Q credits is similar in both cases.

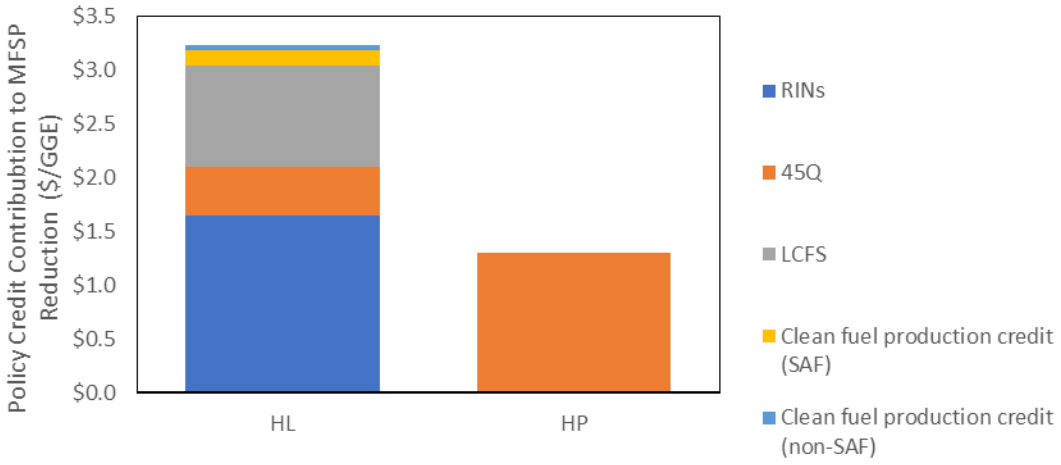

Figure 13. Policy credits contribution to the MFSP reductions for each case, broken down by policy incentive.

Policy incentive qualification is calculated based on the displacement method for the HL scenario and the mass allocation method for the HP scenario. MFSP contribution is calculated based on average annual revenue from each incentive for the life of the plant, adjusted to 2020 dollars using a 10% discount rate.

6.1.3 Marginal Cost of GHG Abatement

The marginal abatement cost (MAC) provides a means of quantitatively combining the added cost from producing low-GHG fuels and products (represented here by the difference between the MFSP and a reference cost) with the corresponding GHG reductions. The MAC can be calculated numerous ways depending on the key outputs of the TEA and LCA, with each yielding the same result for a given scenario. Here, we calculate the MAC based on the incremental *increase* in the cost of biofuel (i.e., the difference between the MFSP and market value, translated from $/GGE to $/MJ based on a standard lower heating value of 122.5 MJ/GGE) divided by the incremental *reduction* in the GHG emissions enabled by the overall biorefinery (normalized to a fuel basis), to quantify the incremental cost of reducing GHG emissions as supported by adoption of the modeled technology over the incumbent baseline ($/tonne CO_2e):

$$GHG\ emissions\ reduction, fuel\ basis\ \left({}^{g\ CO_2e}/_{MJ}\right) = \frac{biorefinery\text{-}level\ GHG\ reduction\ \left({}^{g\ CO_2e}/_{tonne\ biomass\ AFDW}\right)}{fuel\ yield\ \left({}^{MJ}/_{tonne\ biomass\ AFDW}\right)}$$

$$Marginal\ GHG\ abatement\ cost = \frac{cost\ of\ biofuel\ \left({}^{\$}/_{MJ}\right) - cost\ of\ reference\ fuel\ \left({}^{\$}/_{MJ}\right)}{GHG\ emissions\ reduction, fuel\ basis\ \left({}^{g\ CO_2e}/_{MJ}\right)}$$

Particularly when prioritizing maximum decarbonization potential, MAC provides useful information to understand the cost of achieving such decarbonization as may be compared to

other technologies. Direct air capture of atmospheric CO_2 is one basis often used as a comparator in this context, with a current benchmark MAC of approximately \$600–\$1,000/tonne CO_2e as a reference case focused strictly on ambient CO_2 drawdown and sequestration [71]. Improvements in direct air capture are projected to reduce the MAC cost projections to a range of \$100–\$600/tonne CO_2e by 2050 [71–73], though further out-year values for 2100 may extend to significantly higher values in the range of \$1,000–\$5,000/tonne CO_2e for deeper emissions reductions [72]. A SAF/biofuel conversion pathway that could meet or improve on the MAC relative to direct air capture would reflect a preferential strategy for GHG abatement, as it would simultaneously provide a useful service to support aviation and other transportation fuel needs alongside bio-derived chemical products.

Table 23 provides MAC metrics corresponding to both biomass compositional scenarios, reflecting biomass MFSPs exclusive of policy incentives. The MAC for the HL case (\$176/tonne CO_2e) provides a comparatively lower GHG abatement cost given the lower MFSP and thus lower incremental cost difference relative to incumbent fuels and products compared to the HP case (\$221/tonne CO_2e), but both are shown to achieve favorable MACs based on biorefinery-level GHG reductions compared to the current direct air capture cost range of \$600–\$1,000/tonne, as well as the 2050 cost range of \$100–\$600/tonne CO_2e.

Table 23. Marginal Cost of GHG Abatement Results.

Average fuel market selling price is calculated as a weighted average of the market prices for all fuels produced, calculated on an energy basis (values provided in Table 3).

	HL	HP	Units
MFSP without policy incentives	\$3.68	\$7.92	\$/GGE
Average fuel market selling price	\$2.23	\$2.26	\$/GGE
Incremental cost of fuel	\$1.45	\$5.66	\$/GGE
Translation at 122.5 MJ/GGE	\$0.0119	\$0.0462	\$/MJ
Biorefinery-level GHG reduction	1,106	1,057	kg CO_2e/tonne biomass (AFDW)
Translation to fuel basis	67.6	209.0	g CO_2e/MJ
Marginal Cost of GHG Abatement	**\$176**	**\$221**	**\$/tonne CO_2e**

6.2 Alternative Case Results

6.2.1 Fuel-Focused HL Scenario

In light of the encouraging results presented above for the HL biomass case inclusive of NIPU coproduction, an alternative case was also evaluated to investigate trade-offs on MFSP and GHG emissions assuming all lipids are routed to fuel upgrading alone. Results are presented in Table 24, with MFSP cost breakouts shown in Figure 14. In summary, given the high market values for PU under the NIPU base case, the removal of this coproduct would increase the MFSP by approximately 80% to \$6.60/GGE excluding policy credits. This represents an MFSP increase of \$2.92/GGE relative to the base case, although this is lower than the \$4.23/GGE net MFSP reduction brought about by the NIPU coproduct discussed above given that the lipids previously diverted to NIPU would now be utilized to produce additional fuel. This results in a roughly 15% increase in fuel yield, up to 140 GGE/ton AFDW (at a similar 63% selectivity to SAF), corresponding to the same 15% lipid diversion to NIPU assumed in the base case. While this represents a nontrivial penalty on MFSP, it would still exceed 50% GHG reduction relative to

petroleum fuels and thus qualify for policy incentives, which in turn could bring the MFSP down to a net $3.90/GGE. This would also be more favorable in reducing the overall complexity of the system, thereby supporting near-term deployment prospects—including a nearly 50% reduction in total capital investment—as well as a 10% and 50% reduction in variable and fixed operating costs, respectively, for the conversion biorefinery compared to the base case including the NIPU coproduct train.

Table 24. Primary Results for the Fuel-Focused HL Scenario.

Results for the base case HL scenario, which includes NIPU production, are also presented for comparison.

	Units	HL (Fuel Only)	HL (Base Case With NIPU)
MFSP (no policy incentives)	**$/GGE**	**$6.60**	**$3.68**
MFSP (with policy incentives)	**$/GGE**	**$3.90**	**$0.45**
IRR (with policy incentives) [a]	%	N/A	26.0%
Fuel CI			
Displacement	**g CO_2e/MJ**	**41.2**	**21.9**
Mass	**g CO_2e/MJ**	**41.2**	**38.6**
Market	**g CO_2e/MJ**	**41.2**	**21.6**
Energy	**g CO_2e/MJ**	**41.2**	**40.8**
Total fuel yield	**GGE/ton algae (AFDW)**	**140.1**	**121.3**
Total fuel production	MM GGE/year	16.5	14.3
Fuel breakdown:			
Diesel	%	27%	27%
SAF	**%**	**63%**	**63%**
Naphtha	%	10%	10%
Minimum biomass selling price	$/ton AFDW	691	691
Biomass feed rate (seasonal average)	ton/day AFDW	357	357
Total capital investment	MM $	$444	$541
Cultivation	MM $	$335	$335
Conversion	MM $	$109	$206
Variable operating costs	MM $/yr	$120	$134
Cultivation [b]	MM $/yr	$27 ($22)	$27 ($21)
Conversion	MM $/yr	$98	$113
Fixed operating costs	MM $/yr	$17	$22
Cultivation	MM $/yr	$11	$11
Conversion	MM $/yr	$5	$11
Average fuel, coproduct, and policy revenue [a]	MM $/yr	$78	$161
Revenue breakdown: [a]			
Fuels	%	47.0%	19.6%
Solid coproduct [c]	%	0.4%	0.2%
PU	%	0.0%	54.3%
Electricity	%	2.4%	1.4%
Policy credits	%	50.2%	24.6%

[a] Fuels valued at market value for calculation of IRR and revenue values (see Table 19).

[b] First value represents gross cost of nutrients and CO_2; value in parentheses represents net costs after nutrient and CO_2 recycle.

[c] Includes revenue from land application of anaerobic digestate.

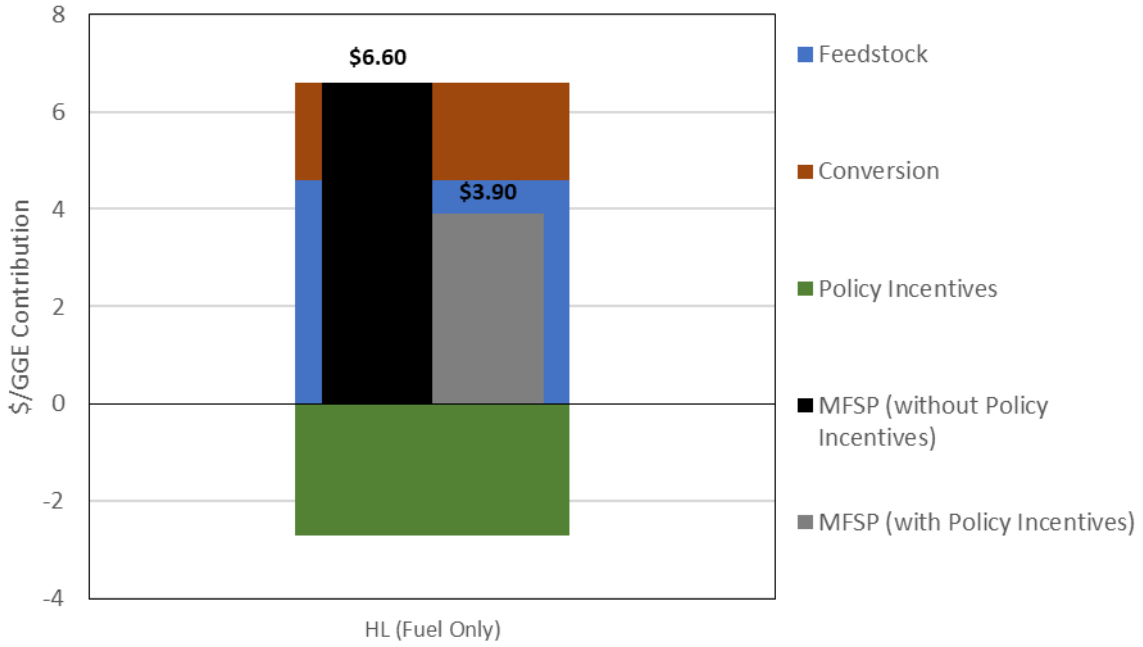

Figure 14. MFSP cost breakdowns for alternative fuel-focused HL scenario (removing NIPU coproduction)

6.2.2 NIPU Sensitivity Analysis

The results discussed above highlight the profound impact that the NIPU coproduct has on process economics and sustainability. While the NIPU coproduction section is modeled rigorously based on experimental results and inputs from an engineering subcontractor, there is still significant uncertainty associated with some of the key assumptions that cannot be eliminated. For one, there is uncertainty related to the assertion of producing a satisfactory NIPU foam coproduct at scale from algal lipids generated from biomass grown outdoors year-round in open ponds, which has been demonstrated with promising results at limited scale [21,30–32], but is still not at a commercialization-ready stage of technology maturity. Outside of this qualitative assumption, however, there are a few key variables that can be investigated quantitatively in detail: the NIPU selling price, the percentage of algal lipids used for NIPU coproduction, and the average number of double bonds per FAME in the NIPU lipid feedstock. Figure 15 shows the economic implications of varying the NIPU price and the percentage of lipids converted to NIPUs, both of which incur significant impacts on process economics. The average number of double bonds in the feedstock had a less significant impact, though it is understood that this parameter will have a significant impact on NIPU product properties (and potentially in turn the selling price) [32]. The economic impact of the number of double bonds in the feedstock, assuming a saleable product in all cases, is shown in Figure 16 along with the percentage of lipids used for NIPU coproduction.

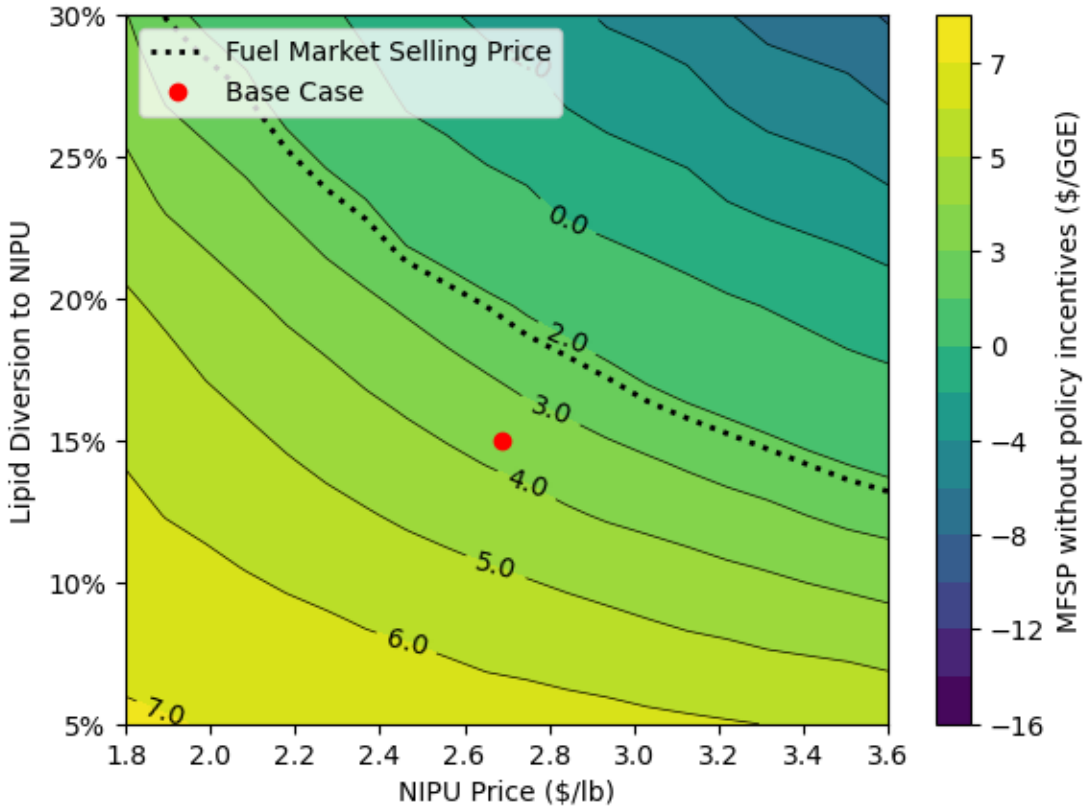

Figure 15. MFSP without policy incentives as a function of NIPU selling price (x-axis) and percentage of lipids used for NIPU production (y-axis).

The average number of double bonds for lipids sent to NIPUs is 3, consistent with the base case. Fuel market selling price is assumed to be $2.23/GGE for the HL scenario, represented by a dotted line.

For the sensitivity scan depicted in Figure 15, lipid diversion to NIPUs was altered over a range of 5%–30% (representing a nominal range of PUFA content that could be produced by HL microalgae at scale), while NIPU price was varied over a range of $1.80/lb to $3.60/lb (representing the approximate range of selling prices for conventional PU foams from 2016 to 2021, adjusted to 2020 dollars). Relatively small variations in each parameter were shown to have a significant impact on the MFSP. For example, at the base case assumption of 15% lipid diversion to NIPUs, an increase of $0.10/lb in NIPU price would decrease the minimum selling price by approximately $0.25/GGE. At 15% lipid diversion, within the range of NIPU prices considered, this means that the MFSP could vary from less than $2/GGE to nearly $6/GGE. This suggests that the economic feasibility of the process is highly dependent on market conditions, including the normal fluctuations of the overall PU market and the market demand for a sustainable rigid foam made without toxic isocyanates. If the regulatory environment changed to more strictly limit the use of isocyanates, or if sufficient consumer demand signaled for a shift to NIPUs, it is possible that the NIPU selling price could exceed that of conventional PU, which would lead to the possibility of even more favorable economics.

In contrast to NIPU selling price, which is dependent on external market conditions (assuming satisfactory product performance and quality), lipid diversion to NIPUs is dependent on (1) the capability of the selected microalgae strain to produce enough PUFAs with a sufficient amount

of double bonds per fatty acid while meeting all other targeted parameters (e.g., biomass productivity and total lipid content), and (2) the capability to isolate those PUFAs from fatty acids with lower unsaturation via low-temperature crystallization of FAME lipids. The base case assumes 100% recovery of PUFAs during low-temperature crystallization, so any reduction in this parameter would result in an equivalent reduction in PUFAs diverted to NIPUs (e.g., an 80% recovery of the 15% PUFA lipids in the base case would result in 12% of PUFAs diverted to NIPUs). At the base case NIPU selling price of $2.69/lb, a 5% increase in lipids diverted to NIPUs results in a corresponding MFSP decrease ranging from $1.48/GGE (moving from 5% to 10% lipid diversion) to $2.20 (moving from 25% to 30% lipid diversion). This sensitivity to lipid diversion (as a proxy for PUFA production and isolation) highlights the fact that PUFA production and recovery is a key component of the modeled HL process.

Experimental results thus far have demonstrated that satisfactory NIPU products made from a FAME feedstock require at least 3 double bonds per fatty acid [32]; however, there is more research to be done to determine the optimal feedstock for a rigid NIPU foam, and in fact, it is likely that the optimal feedstock and formulation varies depending on the desired product properties. Higher functionality will result in a higher degree of cross-linking during polymerization, leading to a more rigid product (and potentially brittle, if too much cross-linking occurs [32]). Despite the potential for too much cross-linking, though, a higher average number of double bonds in the lipid feedstock is preferable, because in this case the conversion in the epoxidation and carbonation reactions may be purposefully reduced to tune product properties [21,32]. For example, an 18:3 FAME feedstock at 100% conversion of double bonds to carbonates may exhibit similar product properties to an 18:4 FAME feedstock at 75% conversion (though recognizing that this is likely an oversimplification).

As the functionality of the lipid feedstock changes, the chemical loadings in each step also change, which impacts economics. To quantify the impacts on MFSP, we retained the conversion assumptions in the base case (100% conversion across all steps) and considered a functionality ranging from 3 to 6 double bonds per FAME, while otherwise assuming a fixed NIPU selling price. Figure 16 shows that the impact of the feedstock functionality on process economics is significant, but less impactful than lipid diversion and NIPU selling price. For example, at the base case level of 15% lipid diversion to NIPUs, moving to a feedstock with 4 double bonds per FAME results in an MFSP decrease of $0.73/GGE. This reduction is driven by increased conversion of cheaper raw material inputs (H_2O_2, CO_2, and ethylene diamine) into NIPUs, increasing the overall mass yield per FAME feedstock. This impact increases at higher double bond numbers ($2.30/GGE reduction for 6 versus 3 double bonds at 15% lipid diversion) and at higher lipid diversion to NIPUs.

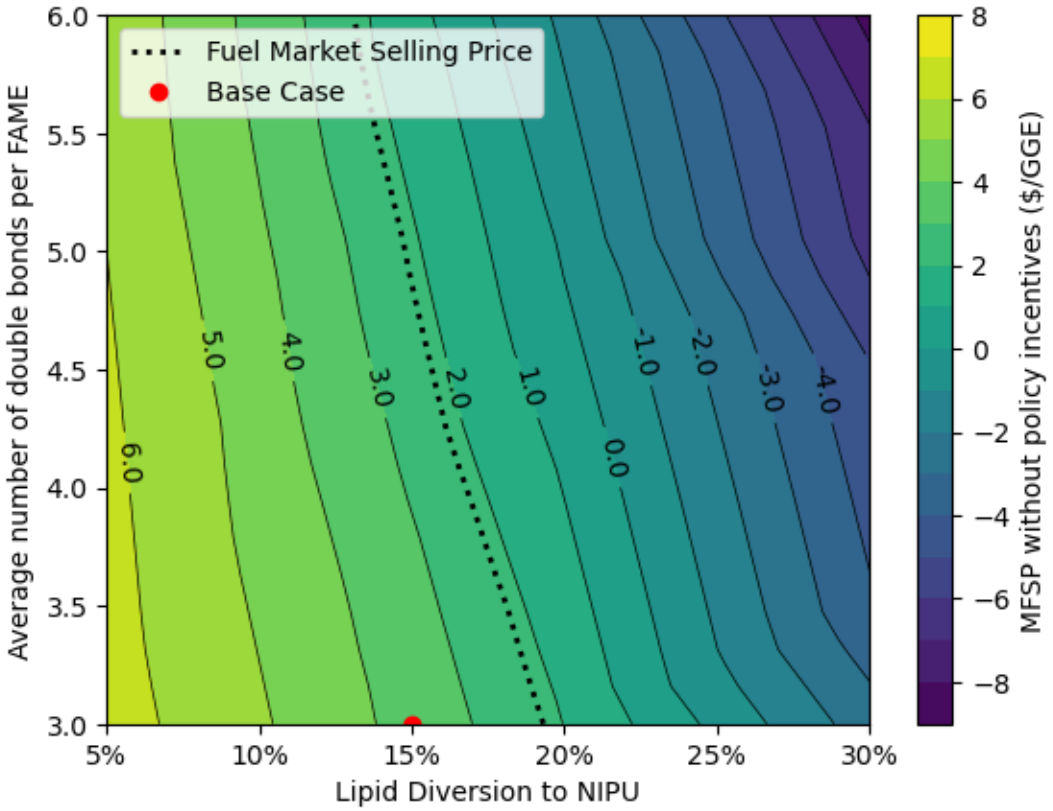

Figure 16. MFSP without policy incentives as a function of lipids diverted to NIPUs and the average number of double bonds per FAME in the NIPU lipid feedstock.

Fuel market selling price is assumed to be $2.23/GGE for the HL scenario, represented by a dotted line. NIPU selling price is fixed at the base case value of $2.69/lb.

6.2.3 Biorefinery-Level Policy Incentives for the HP Scenario

The LCA results presented for the HP scenario indicated that the reduction in biorefinery-level GHG emissions was less than the HL scenario on a basis of relative reduction compared to conventional products (24% for the HP case versus 54% for the HL case), but that the overall reduction was similar in magnitude (1,057 kg CO_2e/tonne AFDW biomass for the HP case versus 1,106 kg CO_2e/tonne AFDW biomass for the HL case). This is driven by higher GHG emissions for the incumbent products in the HP scenario (specifically, conventional EVA; see Figure 11(c)), leading to a lower relative reduction despite a similar magnitude. Additionally, because of higher biomass productivity in upstream cultivation assumed for the HP case, the total GHG reduction rate for the biorefinery is higher for the HP case (470 tonnes CO_2e/day versus 395 tonnes CO_2e/day for the HL case). However, despite these promising GHG reductions at the overall biorefinery level, fuel-specific CI results did not reflect a reduction compared to petroleum fuels, and thus any policy incentives based on fuel CI reduction would not be earned.

To assess hypothetical economic implications of administering policy incentives based on the *overall* GHG reduction achieved (i.e., at the biorefinery level), we considered an alternative scenario that applied the same policy incentives as were applied for the HL scenario (on the basis

of credit value dollars per tonne CO_2e reduction). The value from the HL scenario, representing the sum total of all policy incentives earned (translating to $391 per tonne CO_2e reduction), was applied equally to the HP scenario to assess the economic potential if similar policy incentives were in place that could apply to the whole HP biorefinery concept (i.e., GHG reductions earned primarily by displacing petroleum-based thermoplastics with lower-CI bioplastics). This scenario indicated that the MFSP with policy incentives could be reduced by $10.00/GGE (reaching a value of *negative* $2.05/GGE), or alternatively demonstrate an IRR of 27.9% when selling all fuels and products at market value. These economic results are comparable to the results for the HL scenario with policy incentives (MFSP = $0.45/GGE, IRR = 26.0%), though they rely on a higher portion of revenues from policy incentives (36% for this theoretical HP scenario, compared to 25% for the HL scenario). It is important to note that this scenario is entirely hypothetical at present, given that the current landscape of GHG-based policy incentives in the United States is structured around transportation fuels rather than plastics or other products. However, from the perspective of technology-agnostic GHG reduction, this scenario highlights advantages of the HP scenario that are not immediately apparent from the base case results.

6.2.4 Algae Farm Size and Productivity

Next, recognizing that CAP conversion economics are inextricably linked to the algae farm co-located as a single integrated system, key parameters were explored relating to algae farm outputs for resultant sensitivity on conversion MFSPs. Namely, the primary drivers on minimum biomass selling price (equal to the CAP conversion biomass feedstock cost) have been previously highlighted to be the cultivation productivity ($g/m^2/day$) and algae farm size (based on production pond area) [15,20]. In addition to being key cost drivers, there is significant variability observed in these parameters between site locations, with productivity largely dependent on the local climate and farm size limited by the area available at each site. Notably, the base case farm size of 3,900 acres was chosen based on the average facility size modeled in the 2022 harmonization study [15], but is somewhat skewed by a number of very large facilities and is thus significantly higher than the median size of 2,145 acres. Accordingly, both parameters were varied in the algae farm TEA model between 10 and 35 $g/m^2/day$ productivity and 500–5,000 acre farm size, relative to the base case at 20–25 $g/m^2/day$ (bridging HL and versus HP biomass, respectively) and 3,900 acres. The results are shown as contour plots in Figure 17 and Figure 18, reflecting MFSPs excluding policy incentives.

For HL biomass processing, both the farm size and productivity exhibit similarly strong impacts on MFSP, reflective of the diagonal contour lines covering most of the plot—although farm size becomes a more dominant factor at smaller cultivation areas below roughly 1,500 acres (contour lines begin to flatten out). While algae farm size has a nontrivial impact on cultivation minimum biomass selling price, this trend is a stronger reflection on economy-of-scale dependencies in the CAP conversion biorefinery, which are more pronounced in the HL case particularly for NIPU processing (i.e., a larger farm size equates to a larger biomass feedstock rate to be processed through the CAP facility). In contrast, the HP case shows more independence of feedstock scale/algae farm size over most of the range considered. In other words, MFSP is more strongly a function of cultivation productivity alone (reflecting more vertical contour lines toward the top of the plot), until reaching an inflection again at smaller farm sizes around 1,000–1,500 acres, at which point farm size factors more prominently into MFSP sensitivities. This is a reflection of (1) lower economy-of-scale dependencies in general for the HP biorefinery (although this may be somewhat artificial given that capital costs are not accounted for in downstream solid residual

coproduct conversion to bioplastics in the HP case like NIPU costs are in the HL case), and (2) a lower fuel yield achieved in the HP case, which magnifies the sensitivity to biomass feedstock cost (which in turn is comparatively more sensitive to cultivation productivity than to algae farm size). Notably, Figure 17 for HL conversion also highlights algae farm parameters that could ultimately achieve MFSP market parity without policy incentives ($2.23/GGE as defined in Table 22), which could be achieved over various combinations of productivity over 27 g/m^2/day and algae farm size greater than 2,500 acres. Such market parity cannot be achieved in the HP case.

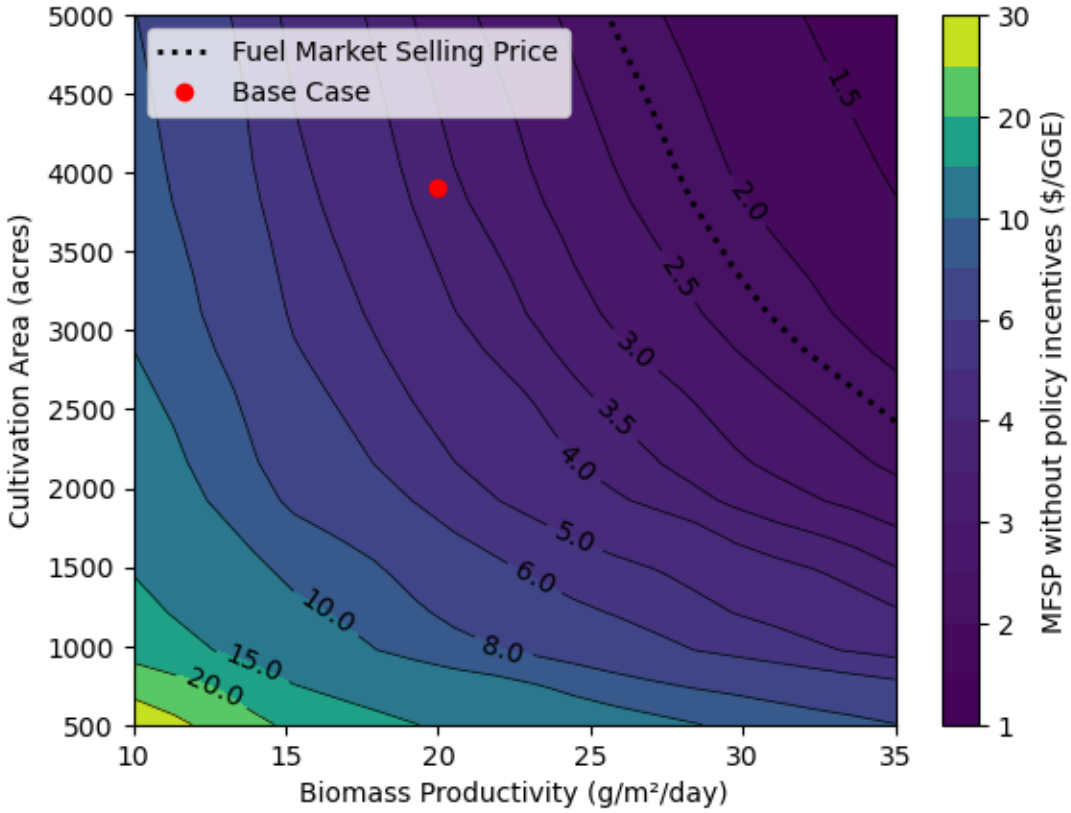

Figure 17. MFSP without policy incentives as a function of biomass productivity (x-axis) and cultivation area (y-axis) for the HL case.

Result for the HL base case ($3.68/GGE) is represented by the red marker. Fuel market selling price is assumed to be $2.23/GGE for the HL case, represented by a dotted line.

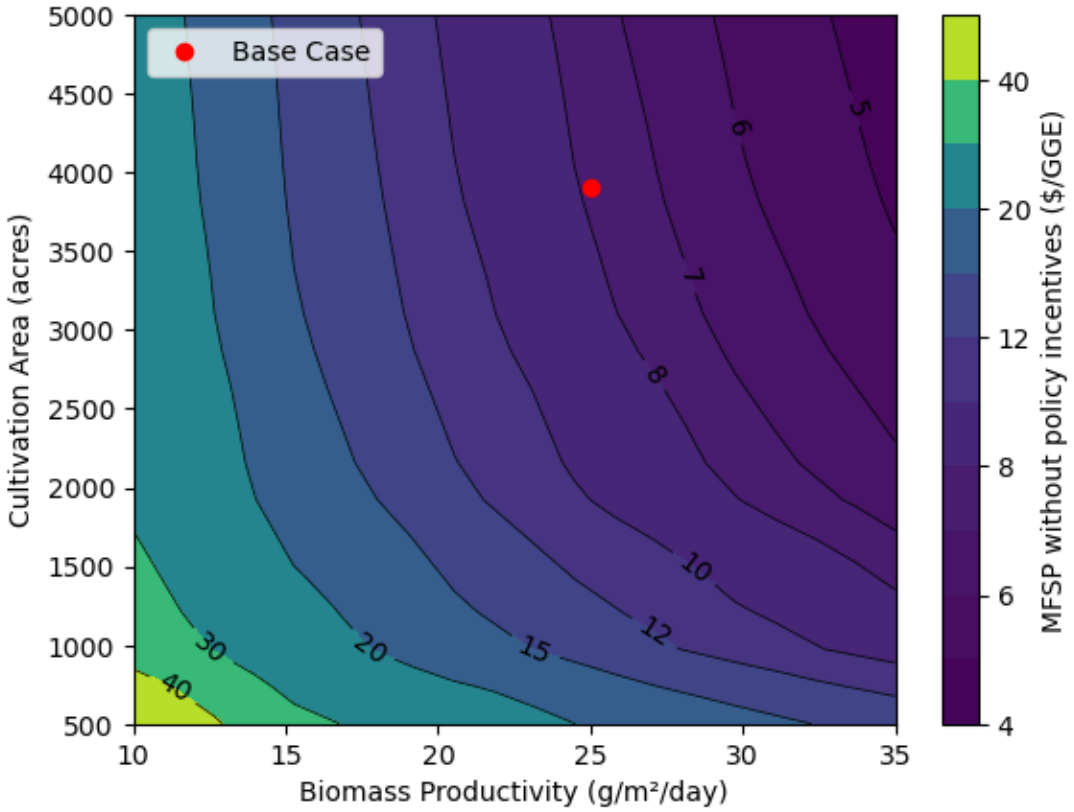

Figure 18. MFSP without policy incentives as a function of biomass productivity (x-axis) and cultivation area (y-axis) for the HP case.

Result for the HP base case ($7.92/GGE) is represented by the red marker. Fuel market selling price ($2.26/GGE for the HP case) does not appear within parameter ranges considered, so is omitted.

6.3 Single-Point Sensitivity Analysis

Beyond the targeted sensitivity cases presented above, a comprehensive TEA sensitivity analysis for the integrated CAP biorefineries was conducted to highlight drivers on MFSPs via tornado plots based on varying individual parameters over reasonable respective ranges as could plausibly be observed for these systems. Selected parameters and their varied ranges are defined in Table 25, spanning economic and policy-related factors, as well as key process considerations for upstream algae cultivation, lipid extraction and fuel upgrading, and coproduct drivers (NIPU for HL biomass, residual solids for HP biomass). Associated MFSP results with and without policy incentives are presented in Figure 19 and Figure 20. An overall discussion on key points is provided below, though most parameters are self-explanatory and not discussed individually.

Table 25. Assumptions Varied in the Single-Point Sensitivity Analysis

Variable	Unit	Base Value	Minimum MFSP	Maximum MFSP
Algae Farm Parameters				
CO_2 utilization efficiency	%	75%	90%	50%
Algae farm average annual productivity	$g/m^2/day$	20 (HL) 25 (HP)	+25%	−25%
Algae farm cultivation area	acres	3,900	5,000	1,000
Minimum biomass selling price (CAP biomass feedstock cost)	$/ton AFDW	$691 (HL) $688 (HP)	−25%	+25%
Biomass lipid concentration	wt %	47.4% (HL) 8.0% (HP)	+20%	−50%
LCA & Policy Incentives				
LCFS credit value	$/tonne CO_2e	$132.00	+50%	-50%
RIN credit value	$/gal ethanol	$1.08	+50%	-50%
Duration of Clean Fuel Production Credit	years	5	30	2
Hydrogen source	Gray vs. blue hydrogen	$1.69/kg, 11.0 kg CO_2e/kg	-	$3.00/kg, 4.0 kg CO_2e/kg
Hydrogen source	Gray vs. green hydrogen	$1.69/kg, 11.0 kg CO_2e/kg	-	$4.50/kg, 1.8 kg CO_2e/kg
Lipid Extraction, Cleanup, and Fuel Upgrading				
Lipid extraction yield	%	96%	99%	80%
Lipid cleanup requirement		Base	No cleanup required	2× capital and operating expenses
Esterification/trans-esterification conversion	%	92% (HL) 99% (HP)	100%	75%
Yield to liquid hydrocarbons from HDO feed	wt % of oil feed	76% (HL) 80% (HP)	85%	60%
Hydrogen consumption in HDO/HI	wt % of oil feed	3.1%	−25%	+25%
HDO/HI capital expenses		Base	−50%	+50%
NIPUs				
Lipid diversion to NIPUs	%	15%	20%	10%
Average number of double bonds in NIPU lipid feed	double bonds/mol	3	4.5	-
Diamine used		Ethylene diamine	Hexane diamine	Bio-based pentane diamine
NIPU selling price	$/lb	$2.69	+25%	-25%
NIPU foam production cost factor		5	1	10
Residual Solid Coproduct				
Residual solid selling price	$/dry ton	$818	+25%	-25%
Economics				
Total capital investment	$MM	$182 (HL) $141 (HP)	-25%	+25%
Discount rate	%	10%	5%	20%

Of all sensitivity parameters evaluated, the strongest drivers on MFSP for either biomass scenario are largely related to biomass feedstock and to parameters directly influencing coproduct yields/revenues, in keeping with the same primary TEA drivers as highlighted in Section 6.1. Namely, within the top third of the tornado plots, both compositional scenarios share algae feedstock cost and cultivation productivity (in turn the strongest driver on biomass cost [20]) as common MFSP drivers, as well as feedstock processing scale [tied to upstream algae farm size, though primarily reflecting economy-of-scale impacts on CAP biorefinery costs]). Algae farm/feedstock scale is a particularly strong driver if it were to be reduced from 3,900 acres to 1,000 acres for algae farm pond size, incurring MFSP penalties on the order of roughly $5/GGE in either compositional case, though only marginally reducing MFSP moving to a larger farm scale up to 5,000 acres. Alternatively, at a farm size of 2,145 acres (reflecting the median farm size in the 2022 harmonization study), MFSPs increase by approximately $1.5/GGE compared to the base case scenarios ($5.12/GGE for the HL case and $9.55/GGE for the HP case). Biomass feedstock costs and related cultivation productivity incur a stronger MFSP impact for the HP case (increasing MFSP by approximately $4/GGE for a 25% detrimental change in either parameter) compared to the HL case (increasing MFSP by roughly $1.5/GGE for a similar 25% change in biomass cost/productivity), due to lower fuel yields in the $/GGE denominator magnifying such sensitivities for HP biomass.

Additionally, for the HL case, parameters most strongly influencing NIPU coproduct revenues also fall in the top third of the HL tornado plot, including biomass lipid composition (adding roughly $7/GGE if lipid content were reduced by half), lipid diversion to NIPUs (adding nearly $2/GGE if this were reduced from 15% to 10%), and NIPU selling price (impacting MFSPs by more than $1.5/GGE for a 25% variation in NIPU coproduct value). MFSP could also be reduced by more than $1/GGE if lipid content could be increased by an additional 20%, also a nontrivial impact, recognizing it would become more difficult to increase lipids any further than that given the high starting baseline in the HL case (for either case, all other non-ash species were adjusted proportionately to maintain compositional closure when varying this parameter). Likewise, for the HP case, a 25% variation in residual solids value for bioplastics upgrading would incur a nearly $4/GGE MFSP impact. Finally, the TEA discount rate (IRR when solving for MFSP) is a strong driver in both cases, particularly if increased from 10% to 20%, adding more than $1/GGE to the MFSP in the HL case and more than $2/GGE in the HP case, again exhibiting stronger sensitivity in the HP case due to lower fuel yields.

Other TEA sensitivities are more specific to the compositional scenario. For example, policy-related metrics have no impact on the HP scenario due to the high fuel CI, which does not qualify for policy incentives. In the HL case, policy-related metrics are moderate drivers of MFSP; for example, increasing or decreasing RIN and LCFS credit value by 50% results in respective MFSP changes of $0.80/GGE and $0.50/GGE. In terms of additional process parameters, the HL case is more sensitive to lipid extraction efficiency than hydrotreating fuel yield from HDO feed lipids given the dual relevance for the former to NIPU coproduction as well. The HP case is more sensitive to hydrotreating yields given the larger range considered for this parameter (and thus larger impact on fuel yield variability) than the range considered for extraction efficiency. The choice of diamine used as a co-reactant in NIPU upgrading was also shown to incur moderate MFSP sensitivity. For this parameter, hexamethylene diamine was assumed to be sourced from a fossil-based route at a CI of 5.65 kg CO_2e/kg [74] and a price of $1.67/kg [44]. Pentane diamine was assumed to be sourced from a bio-based route at a CI of 1.36

kg CO_2e/kg [75]; no price data were available, so a conservative price point of $10/kg was assumed. A bio-based diamine in particular is anticipated to achieve substantial further CI reductions for NIPU upgrading given its high consumption in NIPU synthesis.

Finally, also worth highlighting are parameters that do *not* carry significant MFSP sensitivities. In both cases, parameters such as lipid cleanup costs (whether doubled or removed entirely) translated to trivial impacts on MFSP, as did hydrogen sourcing/consumption inputs for fuel upgrading. Namely, relative to base case hydrogen sourcing assumed to be from natural gas steam methane reforming (gray hydrogen), modifying hydrogen costs to reflect either steam methane reforming with sequestration of evolved CO_2 (blue hydrogen) or water electrolysis using renewable power (green hydrogen) added less than $0.35/GGE to MFSPs, indicating these options may be worthwhile given potentially larger GHG benefits for their use. Moreover, this cost premium could be nearly entirely offset in the HL scenario if green hydrogen costs could be reduced from $4.50/kg assumed here (reflecting near-term estimates [76,77]) to $2.00/kg as may represent longer-term cost potential for green hydrogen [77,78]. In fuel upgrading, hydrogen consumption is based on experimental conversion data (originally based on lipids extracted from *Scenedesmus* sp.), rather than calculated based on a specified fatty acid profile. Accordingly, we considered the economic sensitivity to increased consumption due to the presence of PUFAs (especially in the HP case, where they are not specifically removed prior to fuel upgrading). Hydrogen consumption was increased by 25%, which would correlate to the presence of approximately 21% docosahexaenoic acid (C22:6) content in the lipid profile. This degree of variance, or alternatively a similar 25% reduction in hydrogen consumption, again was shown to incur minimal impacts on overall MFSP.

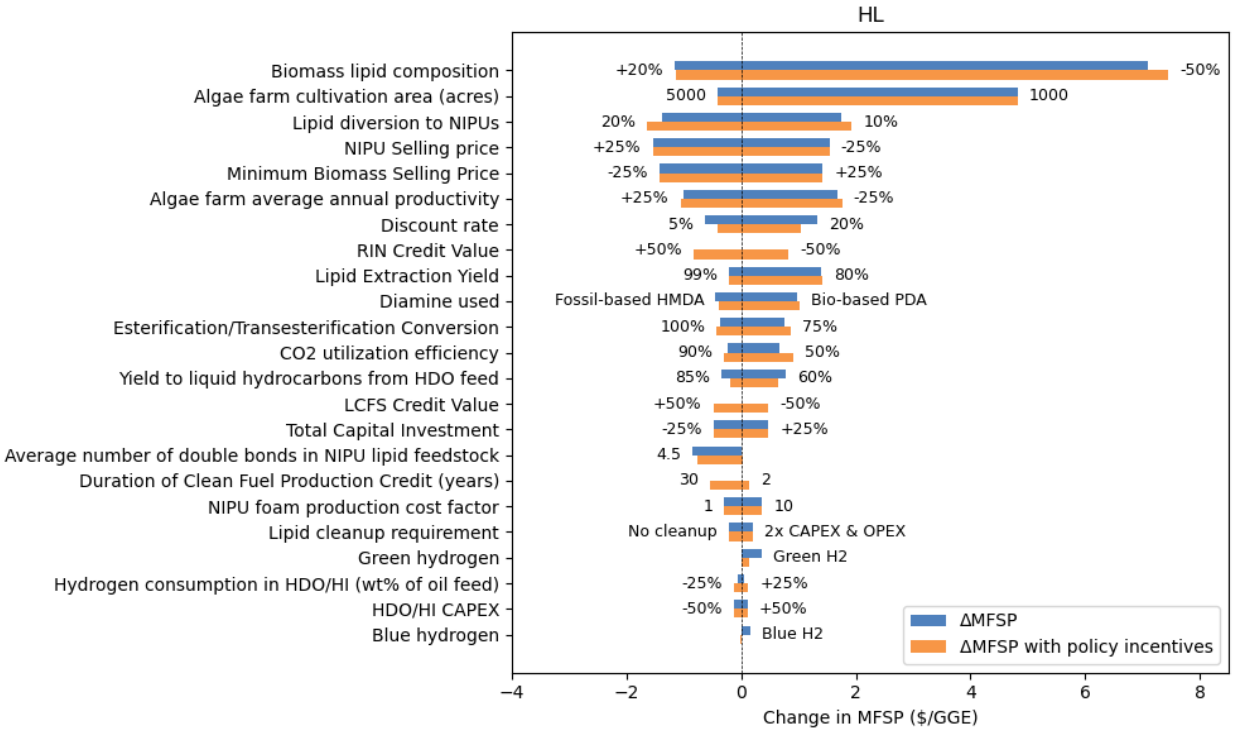

Figure 19. Tornado plot depicting the sensitivity of the HL scenario MFSP to key parameter variances (see Table 25 for additional details)

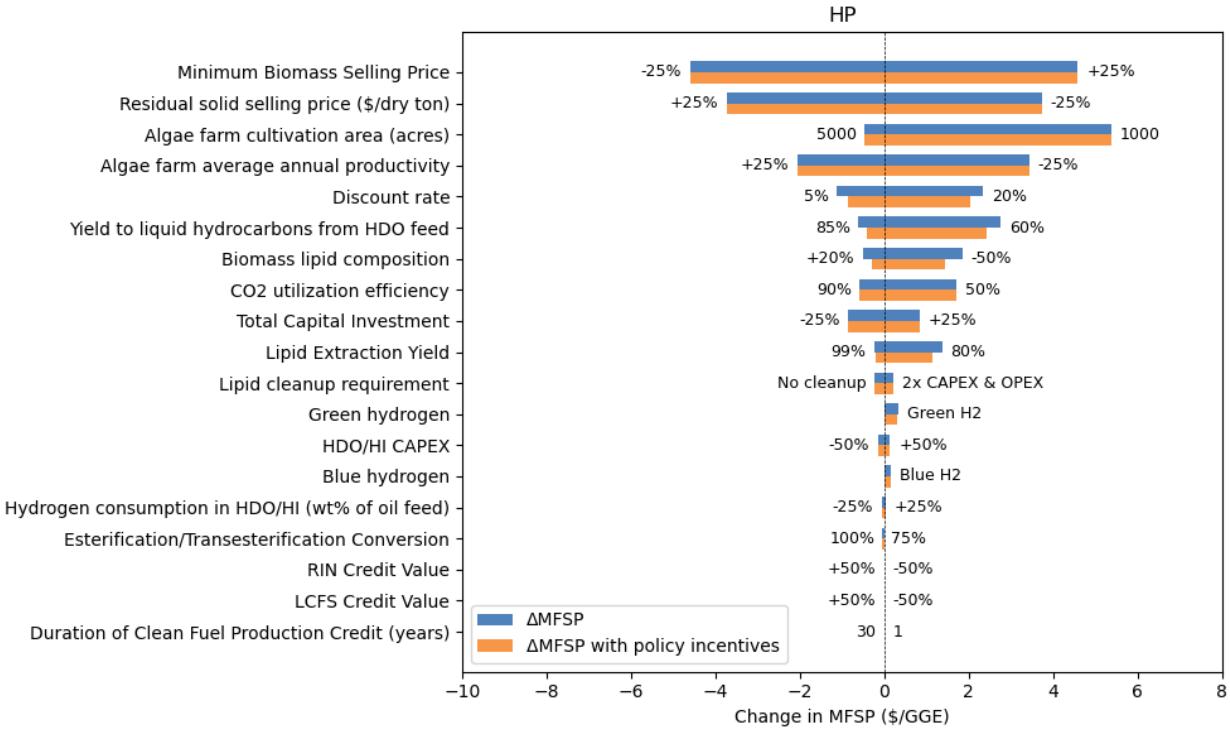

Figure 20. Tornado plot depicting the sensitivity of the HP scenario MFSP to key parameter variances (see Table 25 for additional details)

6.4 Lipid Coprocessing

The base case process design concepts assume that lipids are catalytically upgraded at the biorefinery. However, existing petroleum refinery infrastructure presents an enticing opportunity to simplify the lipid upgrading approach by coprocessing it alongside petroleum fuels. We consider this approach in a stand-alone scenario relevant for lipids produced in the HL case, which is described below.

6.4.1 Methods

An existing refinery optimization framework, developed using AspenTech's Process Industry Modeling System (PIMS) software, was employed to evaluate the economic potential of various streams produced from the CAP process [79,80]. The objective of the PIMS optimizer is to maximize the refinery model's gross margin subject to constraints on crude availability, limitations on process unit capacities and operating conditions, and specifications on finished fuels. The refinery model used for this analysis represented a large, high-conversion refinery with a 400,000-bbl/day capacity located in the U.S. Gulf Coast, based on the models established in the same prior studies [79,80].

Multiple integration strategies were explored, including co-hydroprocessing the lipid biointermediate stream alongside fossil-based feedstocks [81], as well as blending the finished naphtha, jet, and diesel bioblendstocks directly into the refinery's finished product pools. Although co-hydroprocessing can occur in various refinery units such as the diesel hydrotreater or hydrocracker, the kerosene hydrotreater was selected to align with the standalone

hydroprocessing reaction conditions implemented in the design case (375 °C, 435 psig) and to maximize SAF yield. It was assumed that one CAP biorefinery producing 1,152 bbl/day of lipid biointermediate would co-feed the kerosene hydrotreater modeled with a capacity of 31,300 bbl/day, implying a co-processing level of 3.7%. Co-hydroprocessing in hydrotreaters is relatively common, typically to produce renewable diesel, and requires minimal process modifications at levels below 5% except for catalyst modifications. More specifically for a kerosene hydrotreater, a dewaxing catalyst layer would be required after hydro-desulfurization/deoxygenation to isomerize the biogenic n-paraffins to meet cold flow property specifications [82].

The critical properties of each stream were predicted using the Aspen Plus process model and programmed into the PIMS model so that refinery operations were optimized such that final gasoline, jet, and diesel products adhered to ASTM D4814, D1655, and D975 specifications, respectively. Although most predicted blending properties fell within ASTM specifications, the freeze point of the finished jet bioblendstock was reduced from 8°C to −50°C to resemble the jet blendstock produced from upgrading fats, oils, and greases through the hydroprocessed esters and fatty acids pathway. This modification was justified because isomerization reactions were not rigorously modeled in the Aspen Plus hydroprocessing reactor, which resulted in an inaccurately high freeze point. Moreover, lipid biointermediate co-hydrocracking yields were assumed to equal those calculated in the Aspen Plus hydroprocessing reactor (8 wt %, 48 wt %, and 20 wt % for naphtha, jet, and diesel respectively).

Break-even value (BEV), referring to the maximum cost a refiner would pay for a given quantity of blendstock to maintain the gross margin achieved while operating under identical conditions without the blendstock purchase, was chosen as a valuation metric as in similar studies [79,80]. BEV analysis is commonly used in the refining industry using linear programming optimization models when assessing new feedstocks [83]. Moreover, BEVs were calculated across changing input variables, including (1) benchmark oil price and (2) product demands, to reflect different economic scenarios. First, a library of historical crude and petroleum product to benchmark West Texas Intermediate (WTI) oil price correlations were used to price all input/output streams given WTI prices of $20, $40, $60, $80, and $100 per barrel, as shown in prior analysis [79]. Second, refinery product demand projections, spanning 2025 to 2050 in 5-year increments, sourced from the U.S. Energy Information Administration's Annual Energy Outlook, were imposed in the optimizer as volumetric inequality constraints. However, gasoline demand projections from the Annual Energy Outlook were interchanged with projections from the Automotive Deployment Options Projection Tool (ADOPT), which predicts a higher degree of light-duty vehicle electrification and, consequently, lower gasoline demands [84]. In total, 30 optimization scenarios were assessed, which allowed BEV trends under various price and demand conditions to be analyzed.

6.4.2 Results

After optimizing both the baseline and CAP integration model configurations across the 30 scenarios considered, the calculated BEVs were averaged over WTI prices and plotted across time, corresponding to evolving refinery product demand projections (Figure 21). The relationship between benchmark WTI prices and BEVs was approximately linear, as expected, so BEV variations across WTI price assumptions are simply captured as whiskers. This simple

relationship arises from the pricing model's linear structure, where higher WTI prices proportionally increase all input costs. As a result, the marginal cost of fossil feedstocks rises, which allows alternative feedstocks, such as the CAP outputs, to also command higher prices, which is directly reflected in the BEVs. The lower and upper bounds of the whiskers in Figure 21 correspond to the $20/bbl and $100/bbl WTI price scenarios, respectively, providing a clear indication of the sensitivity of BEVs to fluctuations in WTI prices.

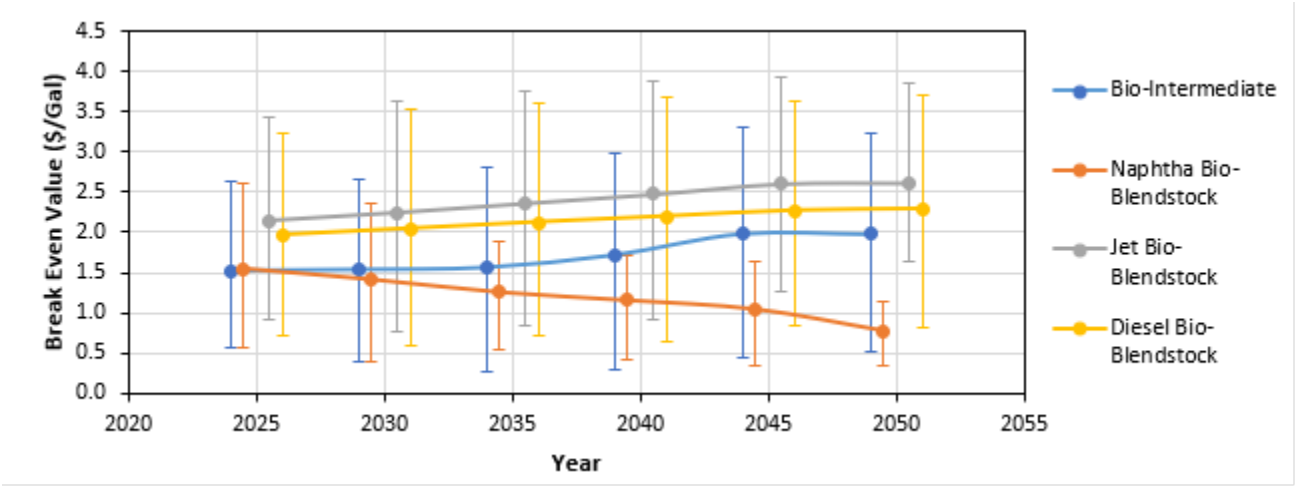

Figure 21. BEVs calculated for CAP lipid-oil biointermediate and naphtha, jet, and diesel finished bioblendstock integration scenarios

BEVs are calculated using benchmark WTI price assumptions of $20, $40, $60, $80, and $100 per barrel and product demand constraints corresponding to years from 2025 to 2050. BEV variations across WTI prices are displayed as whiskers. Data points correspond to years in increments of 5 and are offset for legibility.

Both jet and diesel bioblendstock values displayed a consistent upward trend over time, which can be directly attributed to increasing demands for these products in the Annual Energy Outlook projections imposed as constraints in the model. Conversely, the value of the CAP-derived naphtha blendstock trends downward over time. This decline is largely driven by the anticipated halving of gasoline demand, as projected by the ADOPT model, which accounts for a projected high degree of light-duty vehicle electrification [79,84]. Given these evolving transportation fuel demands, maximizing the production of jet and diesel fuels from CAP feedstocks would further differentiate their value, reinforcing the economic benefits of CAP in a future where gasoline demand is shifted to jet and diesel products. However, even without further improvements, the modeled CAP yields for jet and diesel are proportionally higher than those of traditional fossil-based hydrocrackers, which tend to produce more naphtha. As a result, CAP yields more closely align with evolving fuel demands, thereby increasing the process's economic viability over time.

Similarly, co-hydroprocessing the lipid biointermediate over time showed the same yield advantage, reflected in its upward BEV trend. While operational risks and required process modifications would be minimized at the modeled 3.7% co-processing level, several challenges could remain. Chief among them is the difficulty of biogenic carbon tracking, which is traditionally accomplished using Carbon-14 analysis [85,86]. At low co-processing levels, the concentration of biogenic carbon in the hydrotreater's product streams may fall below detection

limits, which are typically around 1 wt %. This constraint could hinder a refiner's ability to claim low-carbon fuel credits and, in turn, limit their financial return on investments into renewable fuel production. Even if future advances in biogenic carbon detection enable accurate tracking at low concentrations, the emissions reduction potential at 3.7% co-processing would remain modest. To overcome these challenges, increasing co-processing levels may be necessary by scaling up individual algae facilities or utilizing multiple production sites to supply a centralized refinery. Such strategies would require a higher capital investment but would become more practical as the technology matures and adoption accelerates.

7 Concluding Remarks

This report summarizes the prospects for converting purpose-grown microalgae biomass into sustainable and economical fuels and products. Two base scenarios are considered, with each reflecting a tailored conversion approach appropriate for the relevant biomass composition. The HL scenario focuses on utilizing a preferred biomass composition and produces fuels and a NIPU coproduct from the abundance of lipids, while the HP scenario produces fuels and a bioplastic coproduct from an algae feedstock enriched in protein (a more challenging feedstock in the context of fuels). An alternative scenario where HL biomass is converted to fuels only is also considered, and the sensitivity of process economics and sustainability to key process parameters is presented.

The HL scenario highlighted the possibility of highly promising economics even before the consideration of policy incentives, with an MFSP of $3.68/GGE and a fuel CI of 21.6–40.8 g CO_2e/MJ depending on the LCA allocation method used (representing a 54%–76% reduction compared to petroleum fuels). These results are largely enabled by the inclusion of a high-value NIPU coproduct produced from a fraction of lipids containing high levels of unsaturation. However, despite diverting a fraction of lipids to NIPU production, high fuel yields are also projected at approximately 121 GGE/ton AFDW, 63% of which is SAF. Extending the HL scenario to estimate a national potential indicates significant fuel volumes of 14.1 billion GGE/year or 8.3 billion gallons of SAF per year. When present-day policy incentives (including RINs, 45Q, 45Z, and LCFS credits) are considered, economics can improve even further, with the potential to lower the MFSP to less than $1/GGE or alternatively demonstrate an IRR of 26% if fuels are instead sold at market values. A fuel-focused HL scenario also indicated that positive economics and significant fuel CI reduction may be demonstrated even without the NIPU coproduct, exceeding a 50% GHG reduction compared to petroleum fuels and indicating MFSP values approaching fuel market prices ($6.60/GGE, or $3.90/GGE with the inclusion of policy incentives).

The HP scenario indicated more challenging economics, as is typical of algae compositions lacking high levels of lipids or carbohydrates, given fewer options for converting protein. An MFSP of $7.92/GGE is estimated, with fuel yields roughly one-third of those shown in the HL case. Biorefinery-level LCA of the HP scenario indicated an overall GHG reduction of 24% compared to conventional products, though this reflects a *magnitude* of GHG reduction similar to that estimated in the HL scenario. However, in contrast to the HL case, the LCA reflecting a process-level allocation method indicates that fuel CI could *increase* compared to petroleum fuels, highlighting the dependence of the overall process on the bioplastic coproduct. Accordingly, the HP scenario does not appear to readily qualify for policy incentives requiring a minimum GHG reduction threshold, though could be reduced to a value of $6.61/GGE after accounting for credits associated with sequestering industrial carbon emissions. A theoretical scenario considering policy incentives calculated based on biorefinery-level emissions reductions, rather than reductions attributed to transportation fuels alone, could enable the HP case to reach similar economics as the HL case; however, these assumptions are not reflective of current-day policy structures. Without considering incentives currently in place, either compositional case could achieve favorable metrics for marginal GHG abatement costs at $176–$221/tonne CO_2e for HL versus HP biomass, respectively, well below current or near-future

benchmarks for decarbonization technologies such as direct air capture, though these values are strongly dependent on coproduct TEA/LCA benefits (particularly so in the HP case).

Additional sensitivity analyses shed light on key cost drivers. Parameters related to algae cultivation (i.e., biomass productivity and algae farm size) had profound impacts on economics in both cases, as have been highlighted previously. The HL case showed the potential for reaching market parity with petroleum fuels without policy incentives at various combinations of productivity exceeding 27 $g/m^2/day$ and algae farm size greater than 2,500 acres; however, the same could not be achieved for the HP case. Other key cost drivers were illuminated in a single-point sensitivity analysis, including biomass composition, yields related to lipid extraction and fuel/coproduct production, and prices of coproducts and policy incentive credits. Further sensitivity analysis on key NIPU process parameters for the HL case also provided more granular economic sensitivity to key NIPU assumptions such as the percentage of lipids used for NIPU production, the NIPU selling price, and the number of double bonds in the NIPU lipid feedstock.

The comprehensive analysis conducted here highlights important areas to focus on for making microalgae-based fuels and products a reality. Coproducts have repeatedly been shown to be an enabling factor for economic and sustainable algal biofuels in order to offset higher biomass costs compared to terrestrial feedstocks, and this has been reinforced here. However, recent improvements in lipid productivity as reflected in recent NREL SOT reports based on industry data also point to a plausible scenario for sustainability and economic feasibility *without coproducts.* In either case, though, success hinges on producing biomass with sufficient lipid content (and, in the HL base case with NIPU, sufficient PUFA content) while maintaining high biomass productivity. Additionally, the contrast between the HL and HP scenarios reinforces a paradigm that has become increasingly clear: fuel production from purpose-grown HP biomass is a challenging endeavor, regardless of the conversion method. Procuring HP biomass from low-cost sources with secondary applications such as wastewater treatment may be a more feasible option. However, from the perspective of a commercial biorefinery, success in producing fuels from HP biomass would primarily rely on achieving GHG reductions and producing satisfactory revenues from a source other than fuels (i.e., products, policy incentives, and/or a secondary provided service), with fuel production viewed as a secondary priority or possibly even forgoing fuel production entirely.

References

[1] Davis R, Kinchin C, Markham J, Tan E, Laurens L, Sexton D, et al. Process Design and Economics for the Conversion of Algal Biomass to Biofuels: Algal Biomass Fractionation to Lipid- and Carbohydrate-Derived Fuel Products. National Renewable Energy Lab., Golden, CO; 2014.

[2] Humbird D, Davis R, Tao L, Kinchin C, Hsu D, Aden A, et al. Process Design and Economics for Biochemical Conversion of Lignocellulosic Biomass to Ethanol: Dilute-Acid Pretreatment and Enzymatic Hydrolysis of Corn Stover. National Renewable Energy Lab., Golden, CO; 2011.

[3] Davis RE, Grundl NJ, Tao L, Biddy MJ, Tan EC, Beckham GT, et al. Process Design and Economics for the Conversion of Lignocellulosic Biomass to Hydrocarbon Fuels and Coproducts: 2018 Biochemical Design Case Update; Biochemical Deconstruction and Conversion of Biomass to Fuels and Products via Integrated Biorefinery Pathways. National Renewable Energy Lab. (NREL), Golden, CO (United States); 2018.

[4] Wiatrowski M, Davis R. Algal Biomass Conversion to Fuels via Combined Algae Processing (CAP): 2020 State of Technology and Future Research. National Renewable Energy Lab, Golden, CO; 2021.

[5] Wiatrowski M, Davis R, Kruger J. Algal Biomass Conversion to Fuels via Combined Algae Processing (CAP): 2021 State of Technology and Future Research. National Renewable Energy Laboratory, Golden, CO; 2022.

[6] Wiatrowski M, Davis R. Algal Biomass Conversion to Fuels via Combined Algae Processing (CAP): 2022 State of Technology and Future Research. Golden, CO: National Renewable Energy Laboratory; 2023.

[7] Davis R, Markham JN, Kinchin CM, Canter C, Han J, Li Q, et al. 2017 Algae Harmonization Study: Evaluating the Potential for Future Algal Biofuel Costs, Sustainability, and Resource Assessment from Harmonized Modeling. 2018. https://doi.org/10.2172/1468333.

[8] Kruger JS, Wiatrowski M, Davis RE, Dong T, Knoshaug EP, Nagle NJ, et al. Enabling Production of Algal Biofuels by Techno-Economic Optimization of Co-Product Suites. Frontiers in Chemical Engineering 2022;3.

[9] Wiatrowski M, Klein BC, Davis RW, Quiroz-Arita C, Tan ECD, Hunt RW, et al. Techno-Economic Assessment for the Production of Algal Fuels and Value-Added Products: Opportunities for High-Protein Microalgae Conversion. Biotechnology for Biofuels and Bioproducts 2022;15:8. https://doi.org/10.1186/s13068-021-02098-3.

[10] Davis R, Wiatrowski M, Kinchin C, Humbird D. Conceptual Basis and Techno-Economic Modeling for Integrated Algal Biorefinery Conversion of Microalgae to Fuels and Products. 2019 NREL TEA Update: Highlighting Paths to Future Cost Goals via a New Pathway for Combined Algal Processing. National Renewable Energy Lab., Golden, CO; 2020. https://doi.org/10.2172/1665822.

[11] Wiatrowski M, Klein B, Kinchin C, Huang Z, Davis R. Opportunities for Utilization of Low-Cost Algae Resources: Techno-Economic Analysis Screening for Near-Term Deployment. Golden, CO: National Renewable Energy Laboratory; 2022.

[12] Bioenergy Technologies Office Multi-Year Program Plan. Bioenergy Technologies Office: 2023.

[13] Sustainable Aviation Fuel Grand Challenge. EnergyGov n.d. https://www.energy.gov/eere/bioenergy/sustainable-aviation-fuel-grand-challenge (accessed September 21, 2022).
[14] Davis R, Clippinger J. Algae Production via Open Pond Cultivation: NREL Algae Farm Model (Excel TEA Tool). Golden, CO: National Renewable Energy Laboratory; 2018.
[15] National Renewable Energy Laboratory (NREL), Argonne National Laboratory (ANL), Pacific Northwest National Laboratory (PNNL). Economic, Greenhouse Gas, and Resource Assessment for Fuel and Protein Production from Microalgae: 2022 Algae Harmonization Update. Golden, CO: National Renewable Energy Laboratory; 2024.
[16] Klein B, Davis R. Algal Biomass Production via Open Pond Algae Farm Cultivation: 2021 State of Technology and Future Research. National Renewable Energy Lab. (NREL), Golden, CO (United States); 2022.
[17] Davis R, Klein B. Algal Biomass Production via Open Pond Algae Farm Cultivation: 2020 State of Technology and Future Research. National Renewable Energy Lab. (NREL), Golden, CO (United States); 2021. https://doi.org/10.2172/1784890.
[18] Klein B, Davis R, Wiatrowski M. Algal Biomass Production via Open Pond Algae Farm Cultivation: 2023 State of Technology and Future Research. Golden, CO: National Renewable Energy Laboratory; 2024.
[19] Klein B, Davis R. Algal Biomass Production via Open Pond Algae Farm Cultivation: 2022 State of Technology and Future Research. National Renewable Energy Lab. (NREL), Golden, CO (United States); 2023.
[20] Davis R, Markham J, Kinchin C, Grundl N, Tan ECD, Humbird D. Process Design and Economics for the Production of Algal Biomass: Algal Biomass Production in Open Pond Systems and Processing Through Dewatering for Downstream Conversion. 2016. https://doi.org/10.2172/1239893.
[21] Dong T, Dheressa E, Wiatrowski M, Pereira AP, Zeller A, Laurens LM, et al. Assessment of Plant and Microalgal Oil-Derived Nonisocyanate Polyurethane Products for Potential Commercialization. ACS Sustainable Chemistry & Engineering 2021;9:12858–69.
[22] Klein BC, Chagas MF, Davis RE, Watanabe MDB, Wiatrowski MR, Morais ER, et al. A systematic multicriteria-based approach to support product portfolio selection in microalgae biorefineries. Chemical Engineering Journal 2024;481:148462. https://doi.org/10.1016/j.cej.2023.148462.
[23] Klein BC, Davis RE, Laurens LML. Quantifying the intrinsic value of algal biomass based on a multi-product biorefining strategy. Algal Research 2023;72:103094. https://doi.org/10.1016/j.algal.2023.103094.
[24] Rowland SM, Van Wychen S, Dong T, Leach R, Laurens LML. High-Resolution Lipidomics Reveals Influence of Biomass and Pretreatment Process on the Composition of Extracted Algae Oils As Feedstock for Sustainable Aviation Fuels. Energy Fuels 2024;38:6547–52. https://doi.org/10.1021/acs.energyfuels.3c04857.
[25] Cooke T, Pomeroy RS. Chapter 11 - The bioplastics market: History, commercialization trends, and the new eco-consumer. In: Pomeroy RS, editor. Rethinking Polyester Polyurethanes, Elsevier; 2023, p. 261–80. https://doi.org/10.1016/B978-0-323-99982-3.00003-1.
[26] Pomeroy RS. Rethinking Polyester Polyurethanes: Algae Based Renewable, Sustainable, Biodegradable and Recyclable Materials. 2023.

[27] Isocyanates - Overview | Occupational Safety and Health Administration n.d. https://www.osha.gov/isocyanates (accessed September 30, 2024).
[28] Cornille A, Auvergne R, Figovsky O, Boutevin B, Caillol S. A perspective approach to sustainable routes for non-isocyanate polyurethanes. European Polymer Journal 2017;87:535–52. https://doi.org/10.1016/j.eurpolymj.2016.11.027.
[29] REACH Restriction on diisocyanates | ISOPA 2022. https://www.isopa.org/reach-restriction-on-diisocyanates/ (accessed September 30, 2024).
[30] Dong T, Laurens LM, Pienkos PT, Spinelli PF. Renewable polymers and resins and methods of making the same. US Patent 11,104,763, 2021.
[31] Dong T, Pienkos PT. Non-isocyanate polyurethane products and methods of making the same. US Patent App. 18/484,160, 2024.
[32] Dong T, Schutter S, Zhang C, Kruger J. Non-isocyanate Polyurethane from Vegetable and Microalgal Oils 2023. https://doi.org/10.1039/BK9781837671595-00092.
[33] García Martín JF, Carrión Ruiz J, Torres García M, Feng C-H, Álvarez Mateos P. Esterification of Free Fatty Acids with Glycerol within the Biodiesel Production Framework. Processes 2019;7:832. https://doi.org/10.3390/pr7110832.
[34] Laurens LML. Whole algal biomass *in situ* transesterification to fatty acid methyl esters as biofuel feedstocks. In: Dahiya A, editor. Bioenergy (Second Edition), Academic Press; 2020, p. 525–37. https://doi.org/10.1016/B978-0-12-815497-7.00025-7.
[35] Maltsev Y, Maltseva K. Fatty acids of microalgae: diversity and applications. Reviews in Environmental Science and Bio/Technology 2021;20:515–47. https://doi.org/10.1007/s11157-021-09571-3.
[36] Laurens LML, Van Wychen S, Pienkos PT, Harmon VL, McGowen J. Harmonization of experimental approach and data collection to streamline analysis of biomass composition from algae in an inter-laboratory setting. Algal Research 2017;25:549–57. https://doi.org/10.1016/j.algal.2017.03.029.
[37] Laurens LML, Van Wychen S, McAllister JP, Arrowsmith S, Dempster TA, McGowen J, et al. Strain, biochemistry, and cultivation-dependent measurement variability of algal biomass composition. Analytical Biochemistry 2014;452:86–95. https://doi.org/10.1016/j.ab.2014.02.009.
[38] Qin JG. Lipid-Containing Secondary Metabolites from Algae, n.d. https://doi.org/10.1007/978-3-540-77587-4_225.
[39] Commercial scale algal EPA due by year end, says Qualitas Health. NutraIngredientsCom 2013. https://www.nutraingredients.com/Article/2013/07/16/Commercial-scale-algal-EPA-due-by-year-end-says-Qualitas-Health/ (accessed December 16, 2024).
[40] Kruger JS, Schutter S, Knoshaug EP, Panczak B, Alt H, Sowell A, et al. De-risking Pretreatment of Microalgae To Produce Fuels and Chemical Co-products. Energy & Fuels 2024;38:8804–16.
[41] Wendt LM, Kinchin C, Wahlen BD, Davis R, Dempster TA, Gerken H. Assessing the stability and techno-economic implications for wet storage of harvested microalgae to manage seasonal variability. Biotechnology for Biofuels 2019;12:80. https://doi.org/10.1186/s13068-019-1420-0.
[42] Dalheim L, Svenning JB, Eilertsen HC, Vasskog T, Olsen RL. Stability of lipids during wet storage of the marine diatom Porosira glacialis under semi-preserved conditions at 4 and 20 °C. Journal of Applied Phycology 2020;33:385–95. https://doi.org/10.1007/s10811-020-02292-0.

[43] Shokravi Z, Shokravi H, Atabani AE, Lau WJ, Chyuan OH, Ismail AF. Impacts of the harvesting process on microalgae fatty acid profiles and lipid yields: Implications for biodiesel production. Renewable and Sustainable Energy Reviews 2022;161:112410. https://doi.org/10.1016/j.rser.2022.112410.
[44] Dong T, Knoshaug EP, Davis R, Laurens LML, Van Wychen S, Pienkos PT, et al. Combined algal processing: A novel integrated biorefinery process to produce algal biofuels and bioproducts. Algal Research 2016;19:316–23. https://doi.org/10.1016/j.algal.2015.12.021.
[45] Haas MJ, Bloomer S, Scott K. Simple, high-efficiency synthesis of fatty acid methyl esters from soapstock. Journal of the American Oil Chemists' Society 2000;77:373–9. https://doi.org/10.1007/s11746-000-0061-1.
[46] Park J-Y, Wang Z-M, Kim D-K, Lee J-S. Effects of water on the esterification of free fatty acids by acid catalysts. Renewable Energy 2010;35:614–8. https://doi.org/10.1016/j.renene.2009.08.007.
[47] Haas MJ, Michalski PJ, Runyon S, Nunez A, Scott KM. Production of FAME from acid oil, a by-product of vegetable oil refining. Journal of the American Oil Chemists' Society 2003;80:97–102. https://doi.org/10.1007/s11746-003-0658-4.
[48] van Dyk S, Su J, Mcmillan JD, Saddler J (John). Potential synergies of drop-in biofuel production with further co-processing at oil refineries. Biofuels, Bioproducts and Biorefining 2019;13:760–75. https://doi.org/10.1002/bbb.1974.
[49] Marker TL. Opportunities for Biorenewables in Oil Refineries. UOP LLC, Des Plaines, IL (United States); 2005. https://doi.org/10.2172/861458.
[50] Hossain ABMS, (Hossain A, Nasrulhaq Boyce A, (Boyce A, A N, Salleh, et al. Biodiesel production from waste soybean oil biomass as renewable energy and environmental recycled process. AFRICAN JOURNAL OF BIOTECHNOLOGY 2010;9:4233.
[51] Duan E, Li Z, Liu J, Liu Y, Song Y, Guan J, et al. Anaerobic biodegradability and toxicity of caprolactam -tetrabutyl ammonium bromide ionic liquid to methanogenic gas production 2013. https://doi.org/10.1039/C3RA42638F.
[52] Xue K, Yang C, He Y. A review of technologies for bromide and iodide removal from water. Environmental Technology Reviews 2023;12:129–48. https://doi.org/10.1080/21622515.2023.2184275.
[53] Atnoorkar S, Wiatrowski M, Newes E, Davis R, Peterson S. Algae to HEFA: Economics and potential deployment in the United States. Biofuels, Bioproducts and Biorefining 2024;18:1121–36. https://doi.org/10.1002/bbb.2623.
[54] Bryant HL, Gogichaishvili I, Anderson D, Richardson JW, Sawyer J, Wickersham T, et al. The value of post-extracted algae residue. Algal Research 2012;1:185–93. https://doi.org/10.1016/j.algal.2012.06.001.
[55] Maisashvili A, Bryant H, Richardson J, Anderson D, Wickersham T, Drewery M. The values of whole algae and lipid extracted algae meal for aquaculture. Algal Research 2015;9:133–42. https://doi.org/10.1016/j.algal.2015.03.006.
[56] R&D GREET Model. n.d.
[57] IPCC. Climate Change 2023: Synthesis Report. Contribution of Working Groups I, II and III to the Sixth Assessment Report of the Intergovernmental Panel on Climate Change. IPCC, Geneva, Switzerland: 2023.
[58] Cai H, Han J, Wang M, Davis R, Biddy M, Tan E. Life-cycle analysis of integrated biorefineries with co-production of biofuels and bio-based chemicals: co-product handling

methods and implications. Biofuels, Bioproducts and Biorefining 2018;12:815–33. https://doi.org/10.1002/bbb.1893.
[59] Petroleum & Other Liquids Data - U.S. Energy Information Administration (EIA) n.d. https://www.eia.gov/petroleum/data.php (accessed September 21, 2022).
[60] Hasanzadeh R, Mojaver P, Khalilarya S, Azdast T, Chitsaz A, Mojaver M. Polyurethane Foam Waste Upcycling into an Efficient and Low Pollutant Gasification Syngas. Polymers 2022;14:4938. https://doi.org/10.3390/polym14224938.
[61] Farrell C, Osman A, Zhang X, Murphy A, Doherty R, Morgan K, et al. Assessment of the energy recovery potential of waste Photovoltaic (PV) modules. Scientific Reports 2019;9. https://doi.org/10.1038/s41598-019-41762-5.
[62] Cai H, Ou L, Wang M, Davis R, Dutta A, Harris K, et al. Supply Chain Sustainability Analysis of Renewable Hydrocarbon Fuels via Indirect Liquefaction, Ex Situ Catalytic Fast Pyrolysis, Hydrothermal Liquefaction, Combined Algal Processing, and Biochemical Conversion: Update of the 2020 State-of-Technology Cases. Argonne National Lab.(ANL), Argonne, IL (United States); National Renewable …; 2021.
[63] California Air Resources Board. California Code of Regulations, title 17, section 95484. 2024.
[64] U.S. Environmental Protection Agency. Lifecycle Greenhouse Gas Results 2024. https://www.epa.gov/fuels-registration-reporting-and-compliance-help/lifecycle-greenhouse-gas-results.
[65] Wang M, Elgowainy A, Lee U, Baek KH, Balchandani S, Benavides PT, et al. Summary of Expansions and Updates in R&D GREET® 2023. 2023.
[66] U.S. Bureau of Labor Statistics. Producer price index (PPI) industry sub-sector data for Chemical mfg, not seasonally adjusted (Series ID: PCU325---325---). Bureau of Labor Statistics 2024. https://data.bls.gov/cgi-bin/srgate (accessed October 2, 2024).
[67] U.S. Bureau of Labor Statistics. Average hourly earnings of production and nonsupervisory employees, chemical manufacturing, not seasonally adjusted (Series ID: CEU3232500008) 2024. https://data.bls.gov/cgi-bin/srgate (accessed October 2, 2024).
[68] Chemical Engineering Magazine. The Chemical Engineering Plant Cost Index (CEPCI) 2024. https://www.chemengonline.com/pci-home (accessed October 2, 2024).
[69] ICAO. CORSIA Supporting Document: CORSIA Eligible Fuels—Life Cycle Assessment Methodology 2022.
[70] Jones SB, Zhu Y, Anderson DB, Hallen RT, Elliott DC, Schmidt AJ, et al. Process design and economics for the conversion of algal biomass to hydrocarbons: whole algae hydrothermal liquefaction and upgrading. Pacific Northwest National Lab.(PNNL), Richland, WA (United States); 2014.
[71] Webb D. Achieving net zero: Why costs of direct air capture need to drop for large-scale adoption. World Economic Forum 2023. https://www.weforum.org/agenda/2023/08/how-to-get-direct-air-capture-under-150-per-ton-to-meet-net-zero-goals/ (accessed September 30, 2024).
[72] Akimoto K, Sano F, Oda J, Kanaboshi H, Nakano Y. Climate change mitigation measures for global net-zero emissions and the roles of CO2 capture and utilization and direct air capture. Energy and Climate Change 2021;2:100057. https://doi.org/10.1016/j.egycc.2021.100057.
[73] Young J, McQueen N, Charalambous C, Foteinis S, Hawrot O, Ojeda M, et al. The cost of direct air capture and storage can be reduced via strategic deployment but is unlikely to fall

below stated cost targets. One Earth 2023;6:899–917. https://doi.org/10.1016/j.oneear.2023.06.004.
[74] Dros AB, Larue O, Reimond A, Campo FD, Pera-Titus M. Hexamethylenediamine (HMDA) from fossil- vs. bio-based routes: an economic and life cycle assessment comparative study. Green Chem 2015;17:4760–72. https://doi.org/10.1039/C5GC01549A.
[75] Cathay Biotech Inc. with Donghua University. Project 2: The Complete sets of technology development for bio-based polyamide 56 industrial chain. International Textile Manufacturing Federation; n.d.
[76] Dees J, Goldstein H, Grim G, Harris K, Huang Z, Lee U, et al. US DRIVE Net-Zero Carbon Fuels Technical Team Analysis Summary Report 2020 2021.
[77] KPMG. The Hydrogen Trajectory. KPMG 2023. https://kpmg.com/be/en/home/insights/2021/03/eng-the-hydrogen-trajectory.html (accessed September 29, 2024).
[78] US Department of Energy. US National Clean Hydrogen Strategy and Roadmap 2023.
[79] Carlson NA, Singh A, Talmadge MS, Jiang Y, Zaimes GG, Li S, et al. Economic analysis of the benefits to petroleum refiners for low carbon boosted spark ignition biofuels. Fuel 2023;334:126183. https://doi.org/10.1016/j.fuel.2022.126183.
[80] Jiang Y, Zaimes GG, Li S, Hawkins TR, Singh A, Carlson N, et al. Economic and environmental analysis to evaluate the potential value of co-optima diesel bioblendstocks to petroleum refiners. Fuel 2023;333:126233. https://doi.org/10.1016/j.fuel.2022.126233.
[81] Song M, Zhang X, Chen Y, Zhang Q, Chen L, Liu J, et al. Hydroprocessing of lipids: An effective production process for sustainable aviation fuel. Energy 2023;283:129107. https://doi.org/10.1016/j.energy.2023.129107.
[82] Perez MJL, Nygaard GT, Verdier S. SAF production via co-processing in the kerosene hydrotreater. Digital Refining 2024.
[83] Göthe-Lundgren M, T. Lundgren J, A. Persson J. An optimization model for refinery production scheduling. International Journal of Production Economics 2002;78:255–70. https://doi.org/10.1016/S0925-5273(00)00162-6.
[84] Brooker A, Gonder J, Lopp S, Ward J. ADOPT: A historically validated light duty vehicle consumer choice model. SAE Technical Paper; 2015.
[85] Haverly MR, Fenwick SR, Patterson FPK, Slade DA. Biobased carbon content quantification through AMS radiocarbon analysis of liquid fuels. Fuel 2019;237:1108–11. https://doi.org/10.1016/j.fuel.2018.10.081.
[86] Doll CG, Plymale AE, Thompson CJ, O'Hara MJ, Olarte MV. Determination of Biogenic Content by 14C in fuels using Liquid Scintillation Analysis Laboratory Analytical Procedure (LAP). Pacific Northwest National Laboratory (PNNL), Richland, WA (United States); 2022.

Appendix

Table A-1. Mass and Carbon Balance for the HL Scenario.

Carbon balance is reported on a component basis (resulting from the specific elemental composition of the components modeled in Aspen Plus) and differs slightly from the reported carbon content of the biomass.

Inputs	Mass Flow (kg/h)	Component Carbon Flow (kg/h)
Feedstock		
Raw algae biomass (AFDW)	13,502	9,089
Raw ash	4,219	0
Raw water	54,008	0
Stored algae biomass (AFDW)	1,833	1,336
Stored ash	573	0
Stored water	9,657	0
Stored acetic acid	7	3
Stored lactic	125	67
Stored succinic	89	36
Stored propionic acid	14	7
Pretreatment		
Sulfuric acid	594	0
Ammonia	192	0
Lipid Extraction and Cleanup		
Hexane	146	122
Ethanol	166	86
Caustic (saponification)	538	0
Phosphoric acid (lipid neutralization)	0	0
Sulfuric acid (transesterification)	512	0
Methanol	1,614	605
Product Upgrading		
Hydrogen	228	0
Combined Heat and Power		
Supplemental natural gas	558	418
Combustion air in	154,508	0
Utilities & Storage		
Process water	33,103	0
Cooling tower air in	810,774	0
Polyurethane Production		
Toluene	127	115
Acetic acid	335	134
H_2O_2	569	0
Ion-exchange resin	27	25
CO_2 (carbonation)	540	147
Tetrabutylammonium bromide catalyst	54	32
Toluene	63	58
CO_2 (foaming)	50	14

Inputs	Mass Flow (kg/h)	Component Carbon Flow (kg/h)
Ethylene diamine	168	67
Triazabicyclodecene	5	3
Surfactant	8	4
Total	**1,088,906**	**12,368**
Outputs		
Products		
Diesel	1,346	1,137
SAF	3,175	2,685
Naphtha	508	421
AD sludge	31,446	2,862
PU	1,914	1,056
Recycle Streams		
CO_2 recycle	161,243	2,756
Nutrient recycle	34,327	57
Emissions		
Cooling tower air out	84,4358	0
Ammonia loss in AD	15	0
Steam blowdown	127	0
Biomass Storage and Degradation		
Biomass diverted to storage (AFDW)	2,111	1,421
Diverted ash	660	0
Diverted water	8,442	0
Total	**1,089,672**	**1,2395**
Balance	**−766**	**−27**
Error	−0.07%	−0.22%

Table A-2. Mass and Carbon Balance for the HP Scenario.

Carbon balance is reported on a component basis (resulting from the specific elemental composition of the components modeled in Aspen Plus) and differs slightly from the reported carbon content of the biomass.

Inputs	Mass Flow (kg/h)	Component Carbon Flow (kg/h)
Feedstock		
Raw algae biomass (AFDW)	16,805	9,450
Raw ash	3,855	0
Raw water	67,222	0
Stored algae biomass (AFDW)	2,281	1,398
Stored ash	523	0
Stored water	12,020	0
Stored acetic acid	8	3
Stored lactic	146	78
Stored succinic	104	42
Stored propionic acid	17	8
Pretreatment		
Sulfuric acid	739	0
Ammonia	239	0
Lipid Extraction and Cleanup		
Hexane	151	126
Ethanol	198	103
Caustic (saponification)	106	0
Phosphoric acid (lipid neutralization)	0	0
Sulfuric acid (transesterification)	354	0
Methanol	607	228
Product Upgrading		
Hydrogen	81	0
Combined Heat and Power		
Supplemental natural gas	4,341	3,250
Combustion air in	250,834	0
Utilities & Storage		
Process water	85,898	0
Cooling tower air in	739,099	0
Total	**1,185,628**	**14,686**
Outputs		
Products		
Diesel	496	419
SAF	1,169	989
Naphtha	268	222
Biomass to solid coproduct	12,145	4,130
Recycle Streams		
CO_2 recycle	256,253	3,573
Nutrient recycle	132,336	3,741
Emissions		
Cooling tower air out	769,714	0

Outputs		
Ammonia loss in AD	0	0
Steam blowdown	107	0
Biomass Storage and Degradation		
Biomass diverted to storage (AFDW)	2,625	1,477
Diverted ash	602	0
Diverted water	10,498	0
Total	**1,186,213**	**14,551**
Balance	**−585**	**135**
Error	−0.05%	0.92%

Table A-3. Energy Balance Data for the HL Case.

Heat duties are reported in MMkcal/h; work is reported in kW. Energy supply and demand are broken down by energy source (biomass refers to energy recovered from process off-gas and biogas from AD; natural gas refers to externally sourced natural gas) and area (A100 = Pretreatment; A300 = Lipid Extraction and Cleanup; A400 = Fuel Upgrading; A500 = Protein/Residual Processing; A600 = Combined Heat and Power; A700 = Utilities and Storage; A800 = Polyurethane Production). Heat transfer losses are included under waste. P2P refers to process-to-process heat exchange; LP = low-pressure stream; HP = high-pressure steam; CW = cooling water; CH = chilled water; AC = air cooling.

	Heat (MMkcal/h)													Work (kW)	
	Net	Supply			Demand									Supply	Demand
Area	Net Heat	Fuel	P2P	Total Supply	LP	HP	Furnace	P2P	Gross Heat Demand	Net Heat Demand	CW	CH	AC	Work	Work
A100	−4.1	—	—	—	—	−3.9	—	−0.2	−4.1	−4.1	5.0	—	—	—	1,199
A300	−9.6	—	0.2	0.2	−9.1	−0.7	—	—	−9.8	−9.6	7.7	0.3	—	—	592
A400	−1.2	—	—	—	−0.0	−0.8	−0.4	—	−1.2	−1.2	2.7	—	1.1	—	656
A500	−2.6	—	—	—	−2.6	—	—	—	−2.6	−2.6	2.1	—	—	—	1,154
A600	—	—	—	—	—	—	—	—	—	—	—	—	—	−9,076	35
A700	—	—	—	—	—	—	—	—	—	—	—	—	—	—	511
A800	−1.2	—	—	—	−0.1	−1.1	—	—	−1.2	−1.2	1.5	—	—	—	73
Biomass	17.4	17.4	—	17.4	—	—	—	—	—	—	—	—	—	—	—
Natural gas	4.0	4.0	—	4.0	—	—	—	—	—	—	—	—	—	—	—
Waste	−2.6	—	—	—	−2.1	−0.5	—	—	−2.6	−3.0	—	—	—	—	—
Total	**0.1**	**21.4**	**0.2**	**21.6**	**−13.9**	**−7.0**	**−0.4**	**−0.2**	**−21.5**	**−21.7**	**18.9**	**0.3**	**1.1**	**−9,076**	**4,220**

Table A-4. Energy Balance Data for the HP Case.

Heat duties are reported in MMkcal/h; work is reported in kW. Energy supply and demand are broken down by energy source (biomass refers to energy recovered from process off-gas; natural gas refers to externally sourced natural gas) and area (A100 = Pretreatment; A300 = Lipid Extraction and Cleanup; A400 = Fuel Upgrading; A500 = Protein/Residual Processing; A600 = Combined Heat and Power; A700 = Utilities and Storage; A800 = Polyurethane Production). Heat transfer losses are included under waste. P2P refers to process-to-process heat exchange; LP = low-pressure stream; HP = high-pressure steam; CW = cooling water; CH = chilled water; AC = air cooling.

	Heat (MMkcal/h)													Work (kW)	
	Net	Supply			Demand									Supply	Demand
Area	Net Heat	Fuel	P2P	Total Supply	LP	HP	Furnace	P2P	Gross Heat Demand	Net Heat Demand	CW	CH	AC	Work	Work
A100	−5.2	—	—	—	—	−5.2	—	−0.1	−5.2	−5.2	5.9	—	—	—	1,395
A300	−10.9	—	0.1	0.1	−10.7	−0.3	—	—	−10.9	−10.9	8.9	0.1	—	—	652
A400	−0.5	—	—	—	−0.0	−0.3	−0.1	—	−0.5	−0.5	0.3	—	0.4	—	230
A500	−12.7	—	—	—	−12.7	—	—	—	−12.7	−12.7	2.3	—	—	—	1,127
A600	—	—	—	—	—	—	—	—	—	—	—	—	—	−14,538	23
A700	—	—	—	—	—	—	—	—	—	—	—	—	—	—	422
A800	−0.0	—	—	—	−0.0	—	—	—	−0.0	−0.0	—	—	—	—	—
Biomass	2.6	2.6	—	2.6	—	—	—	—	—	—	—	—	—	—	—
Natural gas	31.1	31.1	—	31.1	—	—	—	—	—	—	—	—	—	—	—
Waste	−4.3	—	—	—	−4.2	−0.1	—	—	−4.3	−4.4	—	—	—	—	—
Total	**0.2**	**33.7**	**0.1**	**33.8**	**−27.6**	**−5.8**	**−0.1**	**−0.1**	**−33.6**	**−33.6**	**17.4**	**0.1**	**0.4**	**−14,538**	**3,851**